

# UNIVERSITY OF TORINO



Department of Oncological Sciences

Bioindustry Park “Silvano Fumero” – LIMA Unit  
Molecular and Cell Biology laboratory

PhD Programme  
“Complexity in post-genomic biology”  
XXIII cycle

## **“Biological activity and signalling pathways activated by AIMP1 in endothelial cells and identification of new cellular interactors”**

CANDIDATE:  
Valentina Jackson

ACADEMIC TUTOR:  
Prof. Federico Bussolino

COMPANY TUTOR:  
Barbara Canepa, Ph.D

CYCLE COORDINATOR:  
Prof. Michele Caselle

Academic years 2008-2010

Scientific sector: BIO-11

# INDEX

page

<b>1. Introduction</b>	<b>5</b>
1.1 Introduction and aim of the thesis	5
1.2 Multifunctionality of proteins	6
1.3 Moonlighting functions of ARS proteins	7
1.4 Mammalian multiaminoacyl-ARS complex (MARS)	9
1.5 Physical structure of the multi-ARS complex	11
1.6 AIMP1 gene structure	12
1.7 AIMP1 protein structure	13
1.8 Discovery of the non-canonical functions of AIMP	17
1.9 Biological functions of AIMP1 and EMAP II	19
1.9.1 <i>Functional domains</i>	21
1.9.2 <i>Antitumour and anti-angiogenic properties</i>	23
1.9.3 <i>Apoptosis and inflammation</i>	24
1.9.4 <i>Injury, development and metabolism</i>	25
1.10 From AIMP1 to EMAP II	26
1.11 Receptors mediating AIMP1/EMAP II cytokine activities on endothelial cells	27
<b>2. Materials and methods</b>	<b>29</b>
2.1 Materials	29
2.2 Cell cultures	29
2.3 Production and purification of human recombinant AIMP1	30
2.4 Circular Dichroism spectrometry	31
2.5 AIMP1 stability in conditioned cell culture medium	32
2.6 Western blotting analysis	32
2.7 Biological assays	32
2.7.1 <i>Cell viability assay</i>	32

2.7.2	<i>Cell Proliferation Assay</i>	33
2.7.3	<i>Tubulogenesis assay</i>	34
2.7.4	<i>Migration assay</i>	34
2.7.5	<i>Adhesion assay</i>	35
2.8	Immunofluorescence	35
2.9	Analysis of AKT, ERK and JNK activation through phosphorylation	36
2.10	Subcellular fractionation	36
2.11	Affinity purification of AIMP1-binding proteins	37
2.12	Protein identification by mass spectrometry (MS)	37
2.13	Pull-down assay	38
2.14	Co-immunoprecipitation	38
2.15	Cell treatment, protein extraction and sample preparation for 2-D electrophoresis	39
2.16	2-D electrophoresis	39
2.17	Image analysis	40
2.18	Cell treatment, RNA extraction and retrotranscription for Real Time PCR analysis	41
<b>3.</b>	<b>Results</b>	<b>43</b>
3.1	Production and purification of recombinant AIMP1	43
3.2	AIMP1 stability in conditioned cell culture medium	46
3.3	Biological assays	47
3.3.1	<i>AIMP1 has a dose-dependent role on ECs proliferation</i>	47
3.3.2	<i>AIMP1 inhibits ECV tubulogenesis in matrigel</i>	50
3.3.3	<i>AIMP1 stimulates macrophages migration</i>	51
3.4	AIMP1 inhibitory effect on PAEC viability is reverted by pre-treatment with anti- $\alpha 5\beta 1$ integrin antibody	53
3.5	AIMP1 inhibits cell adhesion on fibronectin	54
3.6	Subcellular localization of exogenous AIMP1 in PAEC	55

3.7	AIMP1 treatment of PAEC activates ERK and JNK, but not AKT	57
3.8	Affinity purification of AIMP1-binding molecules	60
3.9	Validation of putative AIMP1-interacting proteins through pull-down and co-immunoprecipitation	62
3.10	AIMP1 co-localizes with cingulin and filamin-A in endothelial cells	64
3.11	AIMP1 treatment induces phosphorylation of $\alpha$ -tubulin, EF-1 $\delta$ and RPLP2	65
3.12	AIMP1 treatment regulates gene expression in PAEC	68
<b>4.</b>	<b>Discussion</b>	<b>71</b>
4.1	Production, purification, conformation and stability of recombinant AIMP1	71
4.2	AIMP1 biological activities	72
4.3	AIMP1 has an $\alpha$ 5 $\beta$ 1 integrin-dependent inhibitory effect on PAEC viability and inhibits PAEC adhesion	74
4.4	Subcellular localization of exogenous AIMP1 in PAEC	75
4.5	Proteins activated upon AIMP1 treatment of PAEC	76
4.6	AIMP1 new interactors in endothelial cells	79
4.7	Transcriptional gene regulation upon AIMP1 stimulation of PAEC	80
<b>5.</b>	<b>Conclusions</b>	<b>82</b>
	Acknowledgements	85
<b>6.</b>	<b>References</b>	<b>86</b>

# 1. Introduction

## 1.1 Introduction and aim of the thesis

AIMP1 (ARS-Interacting Multifunctional Protein 1) is a cofactor of the Aminoacyl-tRNA Synthetase (ARS) complex, which is composed of nine different enzymes and three non-enzymatic factors, including AIMP1 (Quevillon *et al.*, 1996). AIMP1 is also the precursor of EMAP II (Endothelial Monocyte-Activating Polypeptide II) (Quevillon *et al.*, 1997; Shalak *et al.*, 2001), which possesses a wide range of activities toward endothelial cells (ECs), neutrophils and monocyte/macrophages *in vitro* (Kao *et al.*, 1994a; Kao *et al.*, 1994b). Interestingly, AIMP1 itself shows cytokine properties and secreted AIMP1 works on different target cells such as monocyte/macrophages (Ko *et al.*, 2001; Park *et al.*, 2002a; Park *et al.*, 2002b), endothelial cells (Chang *et al.*, 2002; Park *et al.*, 2002c), and fibroblasts (Park *et al.*, 2005b). It activates monocytes/macrophages to induce various pro-inflammatory cytokines, such as tumour necrosis factor (TNF)- $\alpha$ , interleukin-8 (IL-8), macrophage chemotactic protein-1 (MCP-1), macrophage inflammatory protein-1 $\alpha$  (MIP-1 $\alpha$ ), and IL-1 $\beta$  (Ko *et al.*, 2001) and controls angiogenesis by a dual mechanism involving the migration and death of endothelial cells (Park *et al.*, 2002c; Hou, 2006). Furthermore, AIMP1, as well as EMAP II, have been reported to suppress *in vivo* tumour growth (Schwarz *et al.*, 1999b; Lee *et al.*, 2006).

The aim of this thesis is to elucidate both existing and new biological functions of AIMP1, to find new cellular interactors for exogenous AIMP1 and to unravel the molecular pathways involved, providing more information on this molecule that shows surprising pleiotropic effects. To accomplish this goal an endothelial cell line model was used (immortalized Porcine Aortic Endothelial Cells – PAEC) and a set of *in vitro* techniques has been applied in order to investigate the signalling pathways activated by exogenous AIMP1 in endothelial cells.

## **1.2 Multifunctionality of proteins**

Although multicellular organisms have a very complex organization, the size of their genomes is relatively small in comparison with unicellular species (Lander *et al.*, 2001). One explanation of such discrepancy is the availability of mechanisms that allow synthesis of several proteins from one gene (for example, through alternative splicing). But even these mechanisms could not explain functional variability of proteomes. The recently discovered concept of multifunctional proteins is a special characteristic of mammalian cells that can significantly expand the number of encoded functions. The three dimensional structure of a protein can contain motifs that allow it to perform different functions with very small structural changes. It is becoming clear that the functions of a protein could vary greatly depending on its posttranslational modifications, its intracellular localization and on the general physiologic state of the cell (Jeffery, 1999). Mammalian systems appear to take advantage of subcellular compartments, in which the same protein can be placed in a different physical environment or combined with a different repertoire of proteins. Perhaps higher organisms have evolved to maximize the safety and flexibility of genetic information by having extra DNA, yet economizing by using one protein for many different purposes (Lee *et al.*, 2004). Obviously, both alternative splicing and post-translational mechanisms responsible for protein variability are not exclusive and functional variability of most vertebrate protein is regulated by both mechanisms (Jeffery, 2003).

In this line of work, proteins that can have multiple distinct functions represent a particularly interesting challenge. In this regard, the mammalian ARSs and their associated factors provide a fascinating example of such multi-functionality.

### **1.3 Moonlighting functions of ARS proteins**

One family of these moonlighting proteins displaying multi-functionality is represented by some aminoacyl-tRNA synthetases and cofactors of the aminoacylation reaction. The major housekeeping function of aminoacyl-tRNA synthetases is attachment of amino acids to their cognate tRNAs during translation. In mammalian, additional cofactors – firstly known as protein p43, p38 and p18, then renamed as AIMP1, AIMP2 and AIMP3, respectively – form the core of multiaminoacyl-tRNA synthetase complex (MARS), which has a scaffold function in aminoacylation. However, two synthetases in mammals, tyrosyl-tRNA synthetase (TyrRS) and tryptophanyl-tRNA synthetase (TrpRS) and cofactor AIMP1 (Fig 1.1), upon release in the extracellular space gain additional activities and begin to act as cytokines, regulating migration, division, differentiation and apoptosis of various cells of the immune system, endothelial cells and fibroblasts.

Translation is one of the most complex biological processes, involving diverse protein factors and enzymes as well as messenger and transfer RNAs. As this process is required for the basic operation of cells, many translational factors and enzymes are considered to be housekeeping proteins. Aminoacyl-tRNA synthetases (ARSs) catalyze the ligation of specific amino acids to their cognate tRNAs, which is the initial step in protein synthesis. The aminoacylation reaction proceeds in two stages. First, ARSs activate their substrate amino acids forming aminoacyl-adenylates. Second, the enzyme-bound reaction intermediates are transferred to the 3' acceptor end of the tRNAs docking onto their active sites. Because tRNAs cannot distinguish amino acids conjugated to their ends, the correct recognition of amino acids and tRNAs by these enzymes is a crucial determinant to maintain the fidelity of protein synthesis.

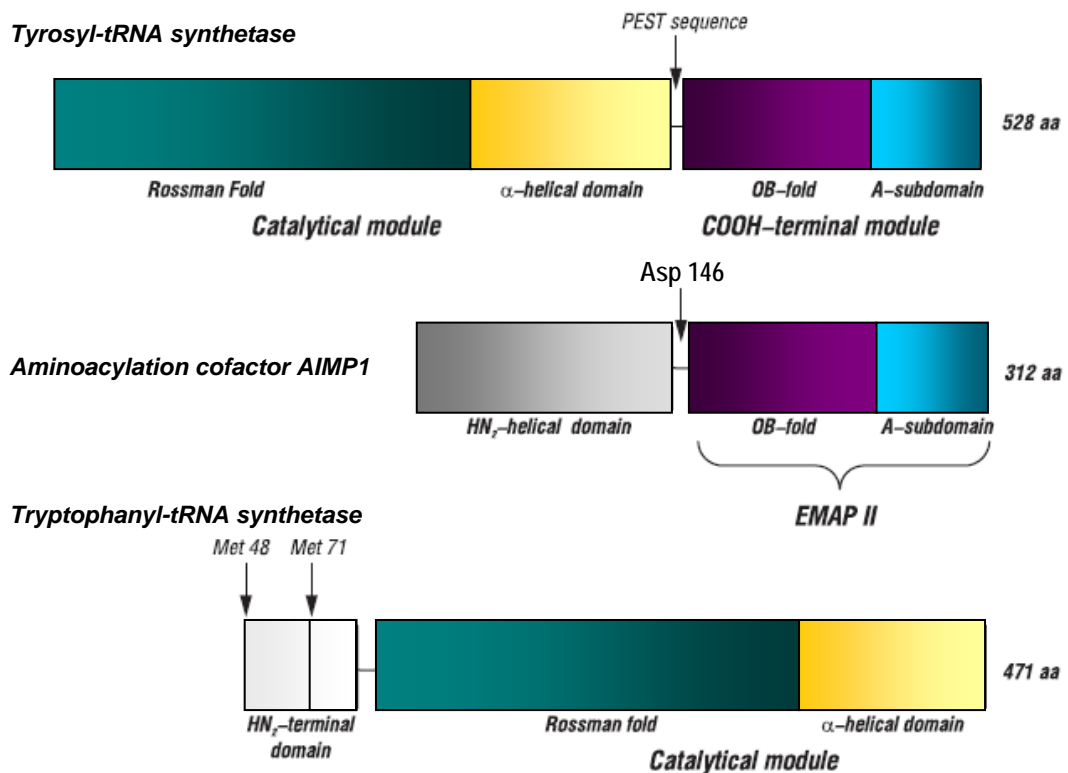


Fig. 1.1. Domain organization of tyrosyl-tRNA synthetase, aminoacylation cofactor AIMP1 and tryptophanyl-tRNA synthetase. (Modified from Ivakhno & Kornelyuk, 2004).

Since ARSs play a crucial part in the flow of genetic information from nucleic acids to proteins, they are thought to have emerged early in evolution and to be structurally highly tailored to specifically recognize substrate amino acids and tRNAs. Although the catalytic activities of these enzymes represent their essential role in maintenance of cell viability, accumulating evidence demonstrates that they actually are versatile, multi-functional proteins regulated by a diverse set of control mechanisms. This functional flexibility appears to be extended through physical interactions with each other, as well as with additional cofactors, to areas not directly related to protein synthesis. These include RNA processing and trafficking, apoptosis, rRNA synthesis, angiogenesis and inflammation (Martinis *et al.*, 1999; Ibba & Soll, 2001; Ko *et al.*, 2002) (Table 1.1).

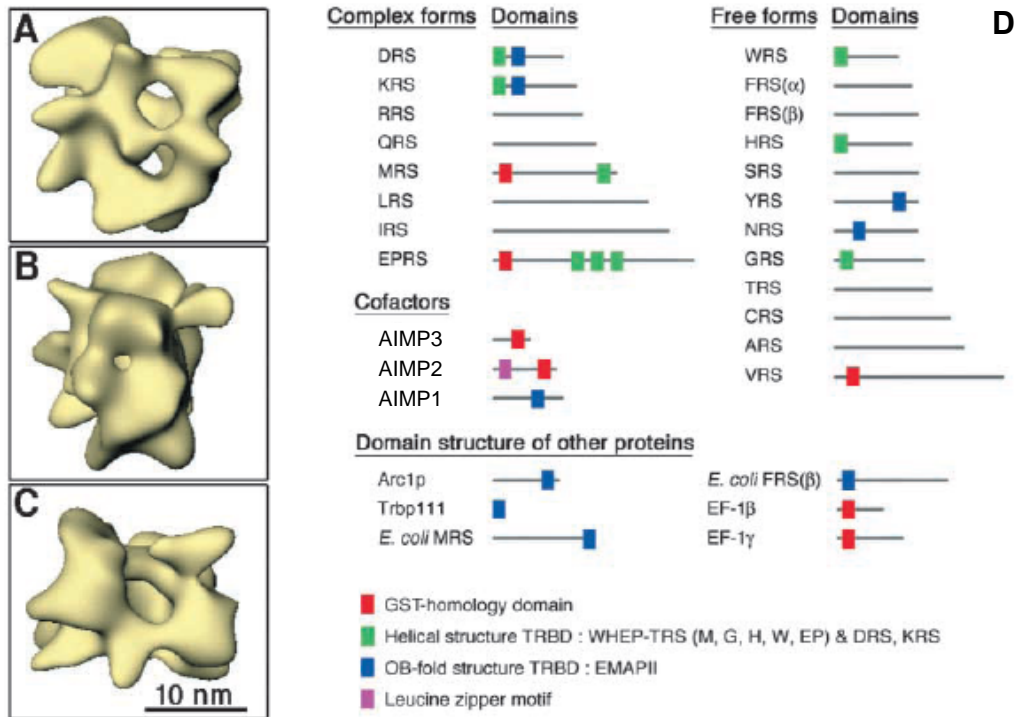
Species	ARSs (classes)	Location	Target	Activities
<i>Homo sapiens</i>	YRS (I)	Extracellular	Endothelial cell	Angiogenic cytokine
<i>H. sapiens</i>	WRS (I)	Extracellular	Endothelial cell	Angiostatic cytokine
<i>H. sapiens</i>	KRS (II)	Extracellular	Macrophage	Inflammatory cytokine
<i>H. sapiens</i>	KRS (II)	Plasma membrane	HIV Gag	Viral assembly
<i>H. sapiens</i>	EPRS (I, II)	Cytoplasmic	3' UTR	Translational silencing
<i>H. sapiens</i>	ORS (I)	Cytoplasmic	ASK1	Anti-apoptosis
<i>H. sapiens</i>	KRS (II)	Nuclear	MITF	Transcriptional control
<i>H. sapiens</i>	MRS (I)	Nuclear	Nucleoli	rRNA transcription
<i>N. crassa</i>	YRS (I)	Mitochondrial	Group I intron	Splicing
<i>Saccharomyces cerevisiae</i>	LRS (I)	Mitochondrial	Group I intron	Splicing
<i>E. coli</i>	TRS (II)	Bacterial	5'UTR	Translational control

Table 1.1. Non-canonical activities of ARSs. (From Park *et al.*, 2005)

## 1.4 Mammalian multiaminoacyl-ARS complex (MARS)

Several lines of evidence have suggested that the translational apparatus in mammalian cells is highly organized. In particular, association of translational components such as tRNA, ARSs and elongation factors with the cytoskeletal framework (Dang *et al.*, 1983; Mirande *et al.*, 1985; Sanders *et al.*, 1996) and co-localization of these components have been described (Barbarese *et al.*, 1995). ARSs can be classified into two groups based on their structural features (Eriani *et al.*, 1990; Cusack *et al.*, 1991; Burbaum & Schimmel, 1991). Class I ARSs each possess a Rossman fold in their catalytic domains, whereas class II enzymes contain three homologous motifs with degenerate sequence similarity. ARSs can also be grouped on the basis of their ability to form complexes with each other and with non-enzymatic factors. Among the complexes formed by ARSs, the mammalian ARS complex is the most intriguing (Robinson *et al.*, 2000; Ko *et al.*, 2002; Kim *et al.*, 2002b; Han *et al.*, 2003). This complex is distinctive compared with other macromolecular protein complexes in that its components are enzymes that carry out similar catalytic reactions simultaneously, and only a subset of ARSs are involved. Although there is still some ambiguity about the stoichiometry and total number of components, at least nine different ARSs, including both class I and class II enzymes, have been consistently found in the mammalian complex: EPRS, IRS, LRS, MRS, QRS, RRS, KRS, and DRS. Among these, IRS, LRS, MRS, QRS and RRS are monomers, whereas KRS and DRS are dimers. The largest component – EPRS – harbours two catalytic activities in a single polypeptide. The complex also contains three auxiliary factors: AIMP1, AIMP2 and AIMP3 (Quevillon & Mirande, 1996; Quevillon *et al.*, 1997; Quevillon *et al.*, 1999) (Fig. 1.2D).

The gross morphology of the complex has been explored by electron microscopy (Norcum, 1989; Norcum & Boisset, 2002; Wolfe *et al.*, 2003)(Fig. 1.2A-C), and the nearest neighbours among the component parts have been determined by chemical cross-linking (Norcum, 1989) and genetic approaches (Rho *et al.*, 1996; Quevillon *et al.*, 1999).



**Fig. 1.2. Three-dimensional structure of the human multi-synthetase complex and functional domains in ARSs and ARS-related factors.** **A:** ‘Front’ view. **B:** ‘Side’ view created by  $-90^\circ$  rotation about the vertical axis. **C:** ‘Top’ view created by  $-90^\circ$  rotation about the horizontal axis. **D:** Functional domains in ARSs and ARS-related factors. The domains homologous to glutathione  $S$ -transferase (GST; red boxes) are shown in the N-terminal regions of MRS, EPRS and VRS, as well as in the C-terminal regions of AIMP3 and AIMP2. AIMP2 also contains a leucine zipper motif (violet box) and is involved in macromolecular assembly of ARSs (Quevillon *et al.*, 1999). The sequence similarity between the helical tRNA-binding domain (green boxes) of MRS, GRS, HRS, WRS and the three repeated domains of EPRS was revealed by sequence alignment (Kaminska *et al.*, 2001b). Interestingly, these motifs are also involved in protein-protein interactions (Rho *et al.*, 1996b; Rho *et al.*, 1998). DRS and KRS also contain helical tRNA-binding domains (TRBD; blue boxes), although they are not related to the motif mentioned above (Frugier *et al.*, 2000; Francin *et al.*, 2002). By contrast, the oligonucleotide-binding (OB) fold domains (blue boxes) in AIMP1 and YRS are related (Renault *et al.*, 2001). Similar RNA-binding OB folds can also be detected in some ARSs (human DRS, KRS and NRS; *Escherichia coli* MRS and FRS b-subunit) and other proteins (Arc1p, Trbp111, EF-1 $\beta$  and EF-1 $\gamma$ ). (Modified from Lee *et al.*, 2004)

## 1.5 Physical structure of the multi-ARS complex

Kaminska *et al.* (Kaminska *et al.*, 2001) performed *in vivo* silencing, using stable small interfering RNA, to assess the conformation of the multi-ARS complex. On the basis of their exploration the following scheme of multi-ARS assembly can be proposed (Fig. 1.3). Two subcomplexes could be isolated in the absence of the scaffold protein AIMP2 and thus are likely to be able to assemble *in vivo* in the absence of AIMP2; subcomplex I contains MetRS, AIMP3, GluProRS, IleRS, and LeuRS, and subcomplex II is composed of AIMP1, GlnRS, and ArgRS. Association of either LysRS or AspRS to these complexes requires AIMP2. While AIMP3 and AIMP1 depletion causes a partial disaggregation of the ARS-complex, AIMP2 depletion completely disintegrates the whole complex (Robinson *et al.*, 2000; Norcum & Warrington, 2000; Kim *et al.*, 2002).

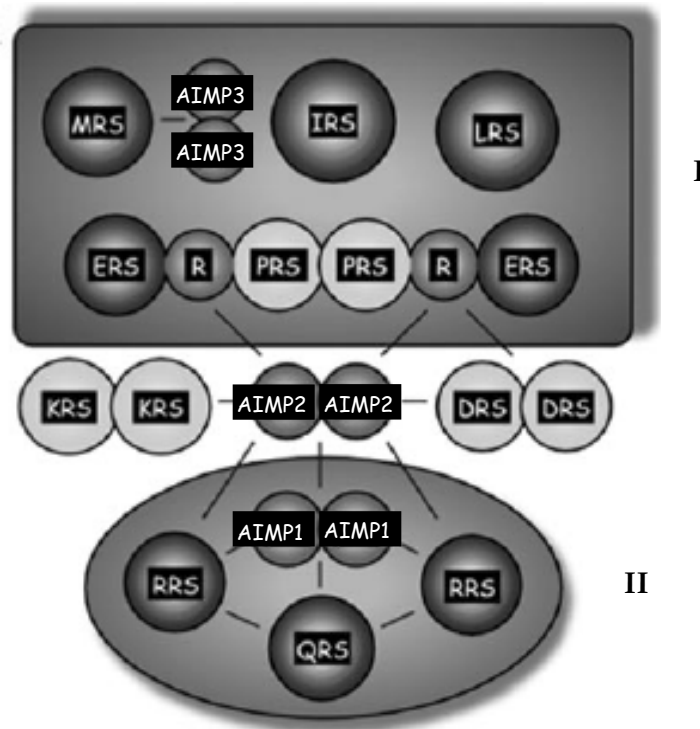


**Fig. 1.3. Connectivity map of the MARS complex.** Class I aminoacyl-tRNA synthetases are indicated in *dark gray*, and Class II aminoacyl-tRNA synthetases are shown in *light gray*. The three auxiliary proteins AIMP3, AIMP2, and AIMP1, as well as the linker domain of multifunctional GluProRS (R), are shown in *white*. The two subcomplexes I and II that may form *in vivo* in the absence of AIMP2 are indicated on a *gray background*. Connectivities identified previously by a two-hybrid analysis (Quevillon *et al.*, 1999) are shown by *black lines*. The stoichiometries of the components are from (Mirande *et al.*, 1982) and (Johnson & Yang, 1981). (Modified from Kaminska *et al.*, 2009).

## 1.6 AIMP1 gene structure

AIMP1 is known in literature by several synonyms: SCYE1, small inducible cytokine subfamily E member 1; p43, multisynthetase complex auxiliary component p43; MCA1, multisynthetase complex auxiliary component 1; EMAP II, endothelial monocyte activating polypeptide II.

The human AIMP1 gene is located on chromosome 4q24 and spans approximately 31.2 kb. The AIMP1 gene contains seven exons and the ATG start site is located in the second exon. Gene transcription results in a 1057 bp mRNA transcript of which 118 bp are untranslated divided between 5' and 3' into 49 and 69 bp, respectively. The human AIMP1 gene structure and the mRNA sequence are depicted in Fig. 1.4.

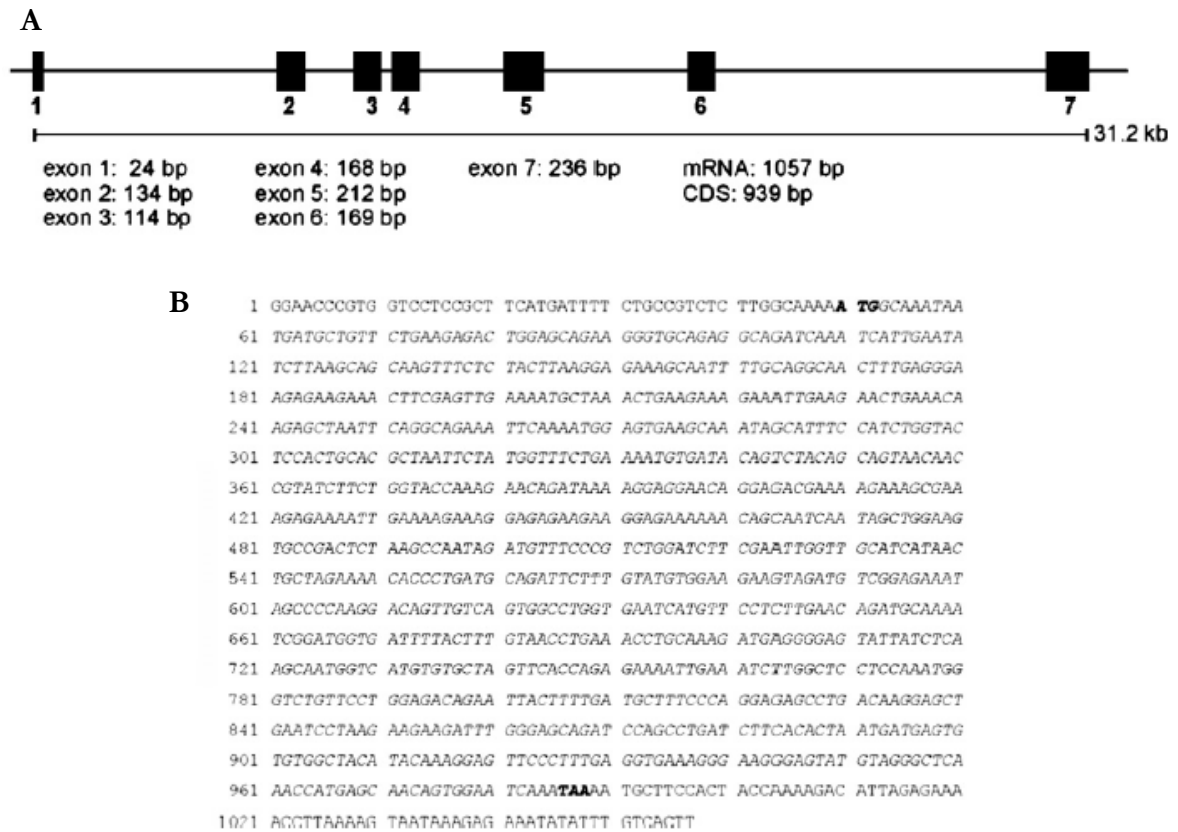


**Fig. 1.4. Structure of the human AIMP1 gene.** **A:** Schematic representation of the human AIMP1 gene. Transcription of the AIMP1 gene results in a 1057 bp mRNA (Accession number U10117) and the coding sequence (CDS) is 939 bp. The human AIMP1 gene contains seven exons spanning approximately 31.2 kb on chromosome 4q24. For gene structure information GENATLAS was used. **B:** mRNA sequence of AIMP1 transcript. The CDS is depicted in italic and the start and stop codon are depicted in **bold italic**. (Modified from van Horssen *et al.*, 2006a).

Because of its function as auxiliary protein within the ARS complex, AIMP1 is expressed in virtually all tissues and can be considered as a housekeeping gene and marker for protein synthesis (Knies *et al.*, 1998; Lee *et al.*, 2004). Although AIMP1 is universally expressed, the level of expression varies and is abundant at sites of apoptosis and tissue remodelling (Tas & Murray, 1996; Knies *et al.*, 1998).

## 1.7 AIMP1 protein structure

Human AIMP1 is a 34 kDa protein constituted by 312 amino acids. AIMP1 protein can be considered subdivided in a N-terminal portion (aa 1-146 in the human protein) and a C-terminal domain (aa 147-312 in the human protein), which is also known as EMAP II and will be further described below (Fig. 1.5).

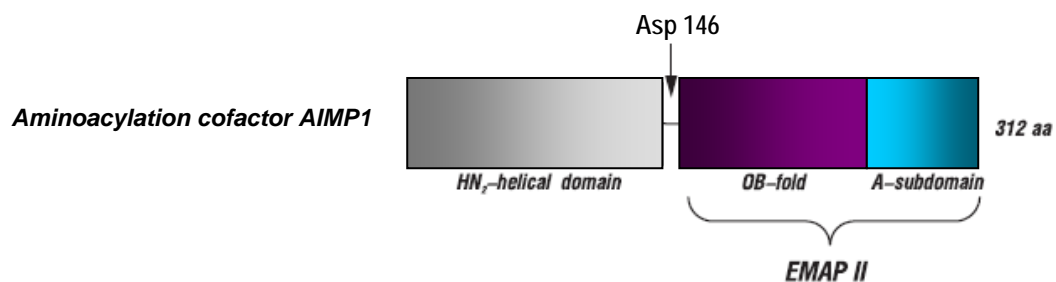


Fig. 1.5. Domain organization of aminoacylation cofactor AIMP1. (Modified from Ivakhno & Kornelyuk, 2004).

Physicochemical properties of full-chain AIMP1 protein and its parts are quite illustrative. It can be seen from the data of Table 1.2 that the N-module of AIMP1 expressed in bacteria has a 10 hour long half-time life, which provides stability to AIMP1. Separate EMAP II cytokine is less stable. Having higher hydrophobicity, the N-module plays an anchor role, determining the localization of AIMP1 in the multisynthetase complex structure (Deineko, 2006).

Parameters	N-module	C-module	Full-chain AIMP1
Number of amino acids	147	165	312
Molecular weight	16239.5	18131.0	34352.6
Isoelectric point, pI	9.14	7.00	8.61
Average hydropathy	-0.824	-0.242	-0.516
Half-life time in <i>E. coli</i> cells	10 hours	3 minutes	10 hours
Stability index	48.84	36.89	42.55

Tab. 1.2. Predicted physical and chemical properties of full-chain AIMP1 protein and its modules. (From Deineko, 2006).

Currently, AIMP1 proteins have been identified in a broad set of organisms. Fig 1.6 shows AIMP1 protein sequence and alignment of a selection of species. Homology is the highest among vertebrates and, in particular, among mammals. Similarity between the human protein and the porcine, bovine and murine proteins is, respectively, 95, 93 and 90% (as calculated by UniProtKB). As to be expected, domains showing high homology overlap, in part, with the functional domains, which are discussed below.

```

Sus scrofa           MIFCRFFTKMATSDAVLKRLEQKGAEADQII EYLKQQVA ILKEKAVLQAT
Bos taurus        MIFCRLLAKMATGDAVLKRLEQKGAEADQII EYLKQQVALLKEKAILQAT
Homo sapiens      -----MANNDAVLKRLEQKGAEADQII EYLKQQVSL LKEKAILQAT
Rattus norvegicus MIFCRFWGKMATNDAVLKRLEQKGAEADQII EYLKQQVALLKEKAILQAT
Mus musculus     MFLCRFWGKMATNDAVLKRLEQKGAEADQII EYLKQQVALLKEKAILQAT
Xenopus laevis   -----MATSNPVLNRLDQRAAEADQII EYLKQQVALLKEKAILQAS
Danio rerio      MFLVRSLFKMSGHTPSLMRLEQKAAEAEQII EYLKQQVQLLKEKAI VQAT

Sus scrofa           LREEKKLRVENAKLKKEIEELKQELIKAEIQNGVKQI PFP SGTALQADSM
Bos taurus        LREEKKLRVENAKLKKEIEGLKQELIKAEIQNGVKQI PFP SDTPLKTDST
Homo sapiens      LREEKKLRVENAKLKKEIEELKQELIQAEIQNGVKQI PFP SGTPLHANSM
Rattus norvegicus LREEKKLQVENAKLKKEIEELKQELIQAEIHNGVKQV PVP SSSSLETHCS
Mus musculus     MREEKKLRVENAKLKKEIEELKQELILAEIHNGVEQVR VRLSTPLQTNCT
Xenopus laevis   VREEKKLRVENAKLKKEIEVLKEQIVTTEIKNGVKQI S IPTST SADSSVS
Danio rerio      LKEEKKLMVENAKLKKDIEELKKQLLDKEKMRGV I DVP ---STEFVQC-

Sus scrofa           VSENVIQSTPVT TILSEAKEQIKEE-GEE--KVK EKV EKKGEKKEKKQQ
Bos taurus        VSENEIQSIPIT AISSGAKEQVKG G-GEEEEKMK KEA EKKGEKKEKKQQ
Homo sapiens      VSENVIQSTAVT TVSSGTKEQIKGGTGDE--KKA KEK I EKKGEKKEKKQQ
Rattus norvegicus VSESVTRSASV TTTTMTG----GG-GEE--KVK EKT EKKGEKKEKKQQ
Mus musculus     ASESVVQSPSVATTAS PATKEQIKA-GEE--KVK EKT EKKGEKKEK-QQ
Xenopus laevis   APVSAPQPAPV KSSPPAPKS-----GEE--K K K KEA EKKGEKKEK--
Danio rerio      VSKPTSADPPV SASPSAASTKTPSAKNND--EAKMK KEA EKKGEKKEK--

Sus scrofa           SVAGSADSKPVDVSR LDLRIGCIT TARKHPDADSLYVEEVDVGE TAPRTV
Bos taurus        PVAGSADSKPVDVSR LDLRIGCIT TARKHPDADSLYVEEVDVGE TAPRTV
Homo sapiens      SIAGSADSKPIDVSR LDLRIGCIT TARKHPDADSLYVEEVDVGE IAPRTV
Rattus norvegicus SAAASADSKPVDVSR LDLRIGCIVT AKKHPDADSLYVEEVDVGE AAPRTV
Mus musculus     SAAASTDSKPIDASRLDLRIGCIVT AKKHPDADSLYVEEVDVGE AAPRTV
Xenopus laevis   PPASEDELKAVDVSRLDLR VGCIT TARKHPDADSLYVEEVDVGE ATPRTV
Danio rerio      AAAPPQEDAKVDVSR LDLRVGRI I SAEKHPDADSLYVEQVDVGE AAPRTV

```

<i>Sus scrofa</i>	VSGLVNHVPLEQMQRNVLLCNLKPAMRGVVSQAMVMCASSPEKVEIL
<i>Bos taurus</i>	VSGLVNHVPLEQMQRNVLLCNLKPAMRGVVSQAMVMCASSPEKVEIL
<i>Homo sapiens</i>	VSGLVNHVPLEQMQRNVLLCNLKPAMRGVLSQAMVMCASSPEKIEIL
<i>Rattus norvegicus</i>	VSGLVNHVPLEQMQRNVLLCNLKPAMRGVLSQAMVMCASSPEKVEIL
<i>Mus musculus</i>	VSGLVNHVPLEQMQRNVLLCNLKPAMRGVLSQAMVMCASSPEKVEIL
<i>Xenopus laevis</i>	VSGLVKHIPLQMQNRMAVLLCNLKPAMRGILSQAMVMCASSPEKVEIL
<i>Danio rerio</i>	VSGLVKHIPLDQMQNRMAVLLCNLKPAMRGVLSQAMVMCASSPEKVEIL
<i>Sus scrofa</i>	APPHGSVPGDRVTFDAFPGEKELNPKKKIWEQIQPDLYTNDDEVATYK
<i>Bos taurus</i>	APPNGSVPGDRITFDAFPGEKELNPKKKIWEQIQPDLYTNDVCVATYK
<i>Homo sapiens</i>	APPNGSVPGDRITFDAFPGEKELNPKKKIWEQIQPDLYTNDDEVATYK
<i>Rattus norvegicus</i>	APPNGSVPGDRITFDAFPGEKELNPKKKIWEQIQPDLYTNDDEVATYK
<i>Mus musculus</i>	APPNGSVPGDRITFDAFPGEKELNPKKKIWEQIQPDLYTNDDEVATYK
<i>Xenopus laevis</i>	DPPSGAVPGDRITFQGFPEKELNPKKKTWEQIQPDLLTNDKCVATYK
<i>Danio rerio</i>	DPPSGAAGDRITFQGFPEKELNPKKKVWEQIQPDLLTDDQCVATYK
<i>Sus scrofa</i>	GAPFEVKGKGVCRQAQTMANSGIK 320aa
<i>Bos taurus</i>	GAPFEVKGKGVCRQAQTMANSGIK 320aa
<i>Homo sapiens</i>	GVPFEVKGKGVCRQAQTMANSGIK 312aa
<i>Rattus norvegicus</i>	GAPFEVKGKGVCRQAQTMANSGIK 315aa
<i>Mus musculus</i>	GAPFEVKGKGVCRQAQTMANSGIK 319aa
<i>Xenopus laevis</i>	GAPFEVQKGCARLRP----- 297aa
<i>Danio rerio</i>	GVAFEVTGKGVCKAQTMSKSGIK 315aa

**Fig. 1.6. Homology of AIMP1 protein sequence between different species.** Alignment of protein sequence of a selection of species in which AIMP1 protein is found using ClustalW software. Amino acids present in all the species are indicated in light blue, conservation of strong groups is indicated in green, conservation of weak groups is indicated in dark blue, amino acids present in at least four species are indicated in violet. Accession numbers of the protein sequences are: *Sus scrofa* (gi\_166796059), *Bos taurus* (gi\_87080799), *Homo sapiens* (gi\_85700432), *Rattus norvegicus* (gi\_75832035), *Mus musculus* (gi\_126012517), *Xenopus laevis* (gi\_148236241), *Danio rerio* (gi\_113951751).

The C-terminal module structure has been revealed by crystallography (Renault *et al.*, 2001), while the N-terminus has not been crystallized and its structure has been modelled with bioinformatics tools (Deineko, 2006). Figure 1.7 reports a bioinformatic model of full-chain AIMP1 three-dimensional structure.

**N-terminus structure:** According to analysis data performed by Deineko (Deineko, 2006), one globular domain and three disordered loops exist in the structure of N-module of AIMP1. The globular domain that borrows approximately 80 residues seems to have a coil-coiled nature, because of the presence of lysine residues. Interactions between coil-coiled sections play an important role in the formation of tertiary protein structure and domain appearance. The disordered residues from amino acids 139 till 147 respond to the exhibited region which treats the enzyme action. Secondary structure prediction of the human AIMP1 N-module revealed the presence of an alpha helix region in the amino-terminal end starting from the fourth to the seventy-fourth residue.

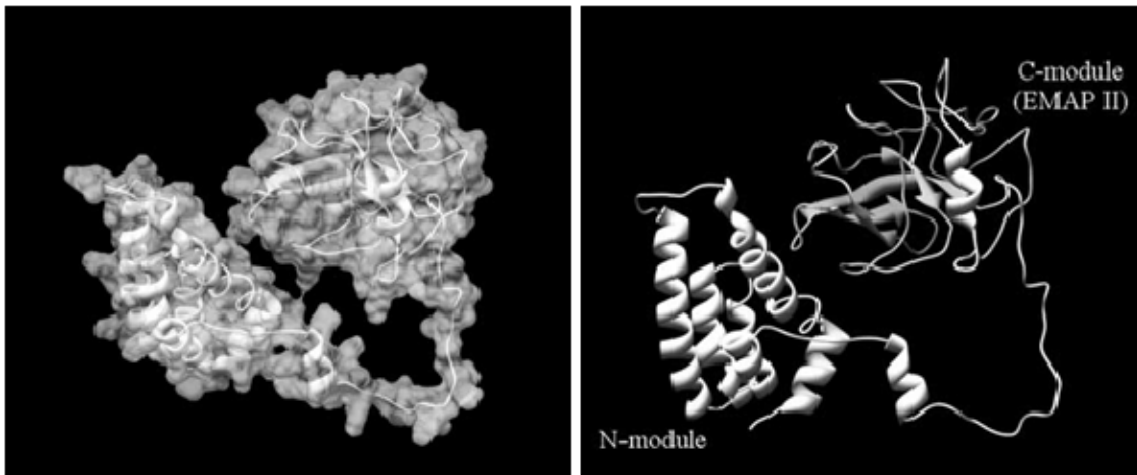


**Fig. 1.7. Three-dimensional structure of full-chain AIMP1.** Left – a surface view of protein; right – a conformation of backbone with elements of secondary structure;  $\alpha$ -helix is designated by a spire and  $\beta$ -sheet is designated by an arrow. This structure agrees both with the majority of secondary structure predictions and with experimental results. (From Deineko, 2006).

This region was also found conserved in many species (spanning from *Homo* to *Drosophila*), suggesting similarity at the structural level as well. The high degree of sequence homology and conservation of functional sites among the sequences suggest a specialized function for N-module of human multisynthetase auxiliary component AIMP1. Relation of secondary structure types is:  $\alpha$ -helix – 59,86%;  $\beta$ -sheet – 7,48%; loops – 32,65% (Deineko, 2006).

**C-terminus structure (EMAP II):** EMAP II forms a compact globule composed of two domains of 100 and 66 amino acids tightly associated through the interdomain interface. The larger domain at NH<sub>2</sub>-terminus (aa 148-252 in AIMP1) forms the open  $\beta$ -barrel-distinguishing feature of OB-folds (oligonucleotide-binding) present in many RNA binding domains (Ivakhno & Kornelyuk, 2004). The OB fold displays two  $\beta$ -sheets,  $\beta$ 1- $\beta$ 2- $\beta$ 3 and  $\beta$ 1- $\beta$ 4  $\beta$ 5, which share the twisted  $\beta$ 1 strand and interact at almost a right angle with each other. Whereas the OB-fold is common in RNA-binding proteins and in a number of other proteins unrelated to oligonucleotide binding (Murzin, 1993; Draper & Reynaldo, 1999), no protein with a significant similarity score to the C-terminal domain (A-subdomain, residues 253-312) was detected (Renault *et al.*, 2001).

The OB-fold domain of EMAP II has 30% sequence identity with a recently characterized family of bacterial tRNA-binding proteins, which includes Trbp111 (Morales *et al.*, 1999) and CsaA (Stover *et al.*, 2000).

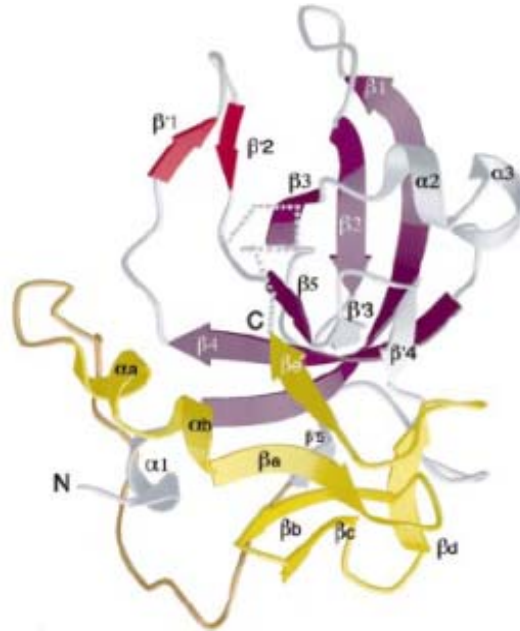


**Fig. 1.8. Structure of the C-terminal module of AIMP1, EMAP II.** The five  $\beta$ -strands of the OB-fold are in violet, the linker region in orange and the C-terminal domain in yellow (From Renault *et al.*, 2001).

## 1.8 Discovery of the non-canonical functions of AIMP1

The discovery of AIMP1 non-canonical functions began in 1992, with the isolation of a 22 kDa polypeptide from the conditioned medium of methylcholanthrene A (Meth A) fibrosarcoma cells (Kao *et al.*, 1992). This factor had a unique amino-terminal sequence, induced tissue factor (TF) expression to modulate coagulant responses, was chemotactic for monocytes and granulocytes and induced inflammation upon injection (Kao *et al.*, 1992). Based on its properties, this factor was named EMAP II (Endothelial Monocyte-Activating Polypeptide II) and was suggested to manipulate the tumour microenvironment, especially the vasculature. Two years later EMAP II was reported to activate EC and monocytes *in vitro* and to induce thrombo-hemorrhagic effects and tumour regression when injected intratumourally in Meth A sarcomas (Kao *et al.*, 1994b).

Leukocyte migration was shown to be directed by EMAP II and, in addition, an increase in intracellular calcium levels was found to be involved in this cellular activation (Kao *et al.*, 1994b). These activities towards monocytes and EC were analyzed in more detail to point out the molecular players involved. In EC, EMAP II induces E- and P-selectin expression, release of von Willebrand factor and TNF production by monocytes (Kao *et al.*, 1994a). Given the 22 kDa molecular weight of EMAP II, cDNA of the cloned gene suggested the existence of a 34 kDa EMAP II precursor (pro-EMAP II) (Kao *et al.*, 1994). It was three years later, in 1997, that Quevillon *et al.* proposed AIMP1 as the precursor of EMAP II (Quevillon *et al.*, 1997). Despite so many cytokine activities, the protein sequence of AIMP1 has no signalling peptide for secretion into the endoplasmic reticulum or amino acids residues for attachment of PI3 anchors, which would explain how AIMP1 or EMAP II may be transported to the plasma membrane.

Studying the mechanisms of EMAP II processing and transport to intercellular space, Knies *et al.* (Knies *et al.*, 1998) have proposed a model for EMAP II proteolysis that involves apoptosis pathways. Immuno-cytochemical analysis and mRNA in situ hybridization of early mouse embryos showed that EMAP II is transported to regions that undergo a lot of restructuring and have many apoptotic cells (Knies *et al.*, 1998). In addition, western blotting proved that apoptosis, but not necrosis, induced intracellular release of 22 kDa form of EMAP II and some other products of proteolysis (Shalak *et al.*, 2001). Knies *et al.* (Knies *et al.*, 1998) proposed a model in which, during apoptosis, AIMP1 could be cleaved through a caspase dependent mechanism, accelerating cell death by breaking the aminoacyl-tRNA synthetase complex and, in addition, upon release in extracellular space, attracting monocytes to the sites with apoptotic cells to clear tissues from cell debris (Knies *et al.*, 1998). This model explained EMAP II and AIMP1 localization and expression during development, but recent researches have shown that these proteins have much broader functions, that AIMP1 itself acts as a pleiotropic cytokine and, furthermore, the cleavage of AIMP1 by a caspase dependent mechanism has been confuted and the proteolytic mechanism is still under debate.

There is growing evidence that AIMP1 has higher cytokine activities than EMAP II and it is possible that AIMP1 is the major protein form in angiogenesis and other processes,

revealing its multifunctional nature. Different data support this hypothesis. EMAP II is not observed at early stages of apoptosis and is passively secreted with other cellular proteins (such as p18 and tubulin) from cells that are already destroyed by apoptosis, suggesting that EMAP II could not be an active cytokine responsible for recruiting monocytes in the early stage of apoptosis (Ko *et al.*, 2001). AIMP1 is constitutively secreted in methylcholanthrene fibrosarcoma cells, 32D myeloid precursor cells, and human prostatic adenocarcinoma cells even in the absence of apoptotic stimulus (Knies *et al.*, 1998 ;Barnett *et al.*, 2000). AIMP1 induces endothelial cells apoptosis at lower doses respect to EMAP II (Park *et al.*, 2002c) and has higher cytokine activities on immune and endothelial cells than EMAP II (Park *et al.*, 2002a; Park *et al.*, 2002b). Furthermore, EMAP II is rarely secreted whereas AIMP1 is highly secreted from Raw264.7 cells stimulated by tumour necrosis factor (Park *et al.*, 2002a). Finally, EMAP II has a weaker binding activity to endothelial cell surface than AIMP1 (Yi *et al.*, 2005). All these data suggest that AIMP1 is specifically secreted from intact mammalian cells, while EMAP II is released only when the cells are disrupted; therefore AIMP1 has shown to be a real cytokine for activating immune cells and endothelial cells.

## 1.9 Biological functions of AIMP1 and EMAP II

As mentioned above, AIMP1 (as its cleavage product EMAP II) exhibits a broad spectrum of biological activities. Both for EMAP II and for its precursor AIMP1 multiple functions have been described in literature. Table 1.3 summarizes thus far identified activities and shows whether the activity has been documented for EMAP II, AIMP1 or both.

Biological function, feature	AIMP1	EMAP II	Refs
Manipulation of EC coagulation properties		X	(Kao <i>et al.</i> , 1992)
Upregulation of TF expression		X	(Kao <i>et al.</i> , 1992)
Monocyte/macrophage, granulocyte chemotaxis		X	(Kao <i>et al.</i> , 1992)
Proinflammatory response (footpad)		X	(Kao <i>et al.</i> , 1992)
Directed leukocyte migration		X	(Kao <i>et al.</i> , 1994b)
Increase of intracellular calcium levels		X	(Kao <i>et al.</i> , 1994b)

Biological function, feature	AIMP1	EMAP II	Refs
Release of von Willebrand factor by EC		X	(Kao <i>et al.</i> , 1994)
Upregulation of E- and P-selectin by EC		X	(Kao <i>et al.</i> , 1994)
Induction of TNF production by monocytes		X	(Kao <i>et al.</i> , 1994)
Thrombo-hemorrhage in Meth A (i.t.)		X	(Kao <i>et al.</i> , 1994)
Induction of TNF-sensitivity (i.v.) of mammary carcinoma (i.t.)		X	(Kao <i>et al.</i> , 1994)
Induction of TNF-sensitivity (i.v.) of B16, HT-1080 (i.t.)		X	(Marvin <i>et al.</i> , 1996)
Auxiliary component of multi ARS complex	X		(Quevillon <i>et al.</i> , 1997)
Induction of TNF-sensitivity (i.v.) of TAV in human melanoma (EMAP-gene transfer)	X	X	(Wu <i>et al.</i> , 1999; Gnant <i>et al.</i> , 1999)
Association with (autoimmune) brain diseases, injury	X	X	(Schluesener <i>et al.</i> , 1997; Mueller <i>et al.</i> , 2003)
Neovascularization during lung development	X	X	(Schwarz <i>et al.</i> , 1999a; Warburton <i>et al.</i> , 2000)
High serum levels during pregnancy	X	X	(Wellings <i>et al.</i> , 1999)
Inhibition of primary and metastatic tumour growth	X	X	(Schwarz <i>et al.</i> , 1999a; Schwarz & Schwarz, 2004; Lee <i>et al.</i> , 2006)
Anti-angiogenic, apoptosis of growing EC	X	X	(Schwarz <i>et al.</i> , 1999b; Berger <i>et al.</i> , 2000; Park <i>et al.</i> , 2002c)
Association with apoptosis-induced influx of leucocytes into reperfused kidneys		X	(Daemen <i>et al.</i> , 1999b)
Apoptosis of corneal EC after transplantation		X	(Liu & Gottsch, 1999)
Position in multi RS complex near midpoint	X		(Norcum & Warrington, 2000)
Upregulation of TNF-R1 mRNA in EC		X	(Berger <i>et al.</i> , 2000)
Improvement of photodynamic therapy effects		X	(Ferrario <i>et al.</i> , 2000)
Induction of pro-inflammatory genes (like TNF)	X		(Ko <i>et al.</i> , 2001; Park <i>et al.</i> , 2002a)
Highly expressed in the foam cells of atherosclerosis lesions	X		(Ko <i>et al.</i> , 2001)
Reduction of keratitis via anti-angiogenesis		X	(Zheng <i>et al.</i> , 2001)
Binding to $\alpha$ ATP synthase on tumour cells	X	X	(Chang <i>et al.</i> , 2002)
Expression negatively regulated by PGE(2)	X		(Battersby <i>et al.</i> , 2002)
Dose-dependent role in angiogenesis	X		(Park <i>et al.</i> , 2002c)
Induction of TNF-sensitivity (ILP) of BN175 (EMAP-gene transfer)	X	X	(Lans <i>et al.</i> , 2002; Lans <i>et al.</i> , 2004)
Marker for microglial cells in brain		X	(Mueller <i>et al.</i> , 2003)
Association with macrophages in uveal melanoma		X	(Clarijs <i>et al.</i> , 2003)
Affects EC actin cytoskeleton (at high dose)		X	(Keezer <i>et al.</i> , 2003)
Induction of lymphocyte apoptosis in solid tumours		X	(Murray <i>et al.</i> , 2004a; Murray <i>et al.</i> , 2004b)
Involved in rapamycin decreased inflammation		X	(Zohlhofer <i>et al.</i> , 2004; Nuhrenberg <i>et al.</i> , 2005)
Induction of vasodilatation via NOS		X	(Tsai <i>et al.</i> , 2004)
Induction of fibroblast proliferation, wound repair	X		(Park <i>et al.</i> , 2005)
Binds to heparan sulphate at low pH		X	(Chang <i>et al.</i> , 2005)
Induction of DOC1 gene expression in EC		X	(Tandle <i>et al.</i> , 2005)
Binding to $\alpha$ 5 $\beta$ 1 integrin, blocks adhesion of EC to FN		X	(Schwarz <i>et al.</i> , 2005)
TNF-R1 and TRADD mobilization in EC		X	(van Horssen <i>et al.</i> , 2006c)
Controls glucose homeostasis	X		(Park <i>et al.</i> , 2006)

Biological function, feature	AIMP1	EMAP II	Refs
Correlation with response of melanoma patients to TNF-based ILP		X	(van Horssen <i>et al.</i> , 2006b)
Interacts with CXCR3 receptor, induces EPC migration	X		(Hou <i>et al.</i> , 2006)
Cleaved by MMP-9, elastase and cathepsin L	X		(Liu & Schwarz, 2006)
Controls endoplasmic reticulum retention of heat shock protein gp96	X		(Han <i>et al.</i> , 2007)
Secretion modulated by proteasome and RARS	X	X	(Bottoni <i>et al.</i> , 2007)
Expression increased in acute lung inflammation	X	X	(Journey <i>et al.</i> , 2007)
Down-regulation of TGF- $\beta$ signalling via stabilization of smurf2	X		(Lee <i>et al.</i> , 2008)
Required for axonal development in motor neurons	X		(Zhu <i>et al.</i> , 2009)
Binding to VEGFR1 and VEGFR2, interferes with VEGF-induced pro-angiogenic signalling		X	(Awasthi <i>et al.</i> , 2009)
Regulation of HIF-1 $\alpha$ activity, inhibits angiogenic cord formation in ECs		X	(Tandle <i>et al.</i> , 2009)

**Tab. 1.3. Summary of reported biological functions and features of AIMP1 and EMAP II.** All published features from AIMP1 and EMAP II isolation till now are listed and the table indicates whether activity has been described for AIMP1, EMAP II or both and their corresponding references are given. Abbreviations: EC, endothelial cells; TF, tissue factor; TNF, tumour necrosis factor- $\alpha$ ; RS, tRNA synthetase; TAV, tumour-associated vasculature; i.v., intravenous; i.t., intratumoural, PGE(2), prostaglandin E(2); ILP, isolated limb perfusion; NOS, nitric oxide synthase; DOC1, downregulated in ovarian cancer 1; FN, fibronectin; TRADD, TNFR associated death domain; HIF, hypoxia-inducible factor; VEGF, vascular endothelial growth factor; CXCR3, chemokine (C-X-C motif) receptor 3; EPC, endothelial progenitor cells; MMP-9, matrix metalloproteinase; TGF, transforming growth factor; RARS, arginyl- aminoacyl tRNA synthetase. (Modified from van Horssen *et al.*, 2006).

### 1.9.1 Functional domains

By peptide-sequence analysis and deletion fragment studies within the AIMP1 sequence, several functional domains have been identified (Han *et al.*, 2006). Figure 1.9 summarizes the different motifs and domains found. The division of AIMP1 and EMAP II (being the C-terminal part, residues 147–312 based on cleavage after Asp<sub>146</sub>) is also depicted in Fig. 1.9. The first functional domain, the peptide responsible for induction of monocyte and leukocyte migration, inflammatory response and binding to a monocyte-derived protein, was identified as the N-terminal region of EMAP II protein (Kao *et al.*, 1994b). This peptide corresponds to amino acids 152–166 within the AIMP1 protein. Interestingly, this peptide contains a so-called RIGRIIT motif, also present in tyrosyl-RS and corresponding to residues 158–164, that was later identified as being responsible for monocyte and leukocyte migration (Wakasugi & Schimmel, 1999). The tRNA binding domain is the most prominent domain within the protein and is mapped to the EMAP II part of the

protein (Quevillon *et al.*, 1997; Kim *et al.*, 2000b). This domain encompasses amino acids 151–252 of the AIMP1 protein.

Three other functional domains were described recently using deletion fragments of AIMP1 (Wang *et al.*, 2006). Both the regions which regulate fibroblast proliferation and EC apoptosis are located in the AIMP1 part of the protein, corresponding with observations that several cell types secrete AIMP1 (Barnett *et al.*, 2000; Ko *et al.*, 2001).

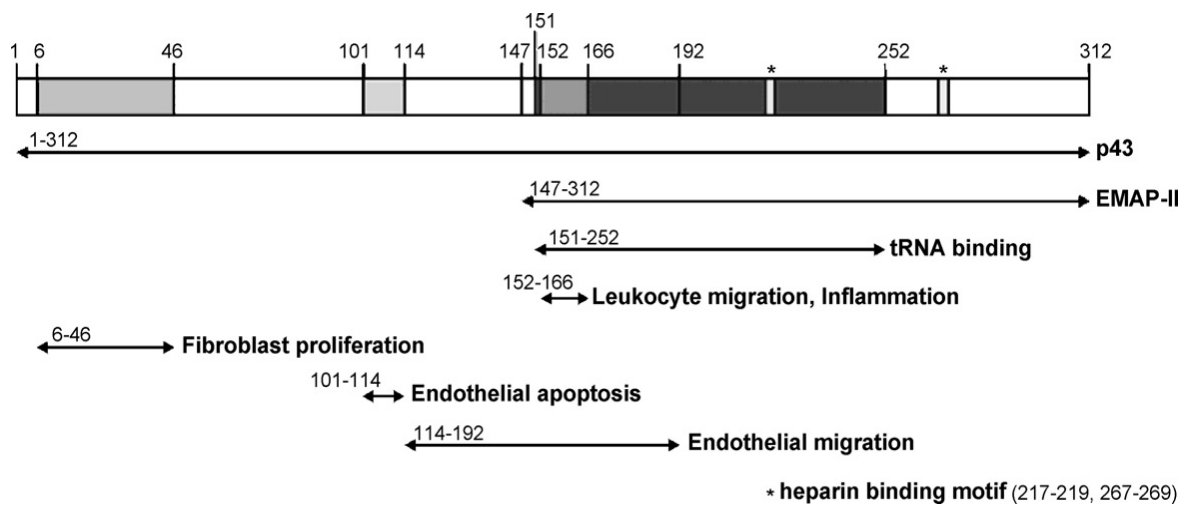


**Fig. 1.9. Functional domains within AIMP1 protein.** Different domains identified in literature as functional domains are depicted. Numbers refer to the amino acid sequence of human AIMP1. In this figure Asp146 is proposed as cleavage-site to process AIMP1 into mature EMAP II. Different domains and motifs are derived from different studies using different experimental setups. (From van Horsen *et al.*, 2006).

The fibroblast proliferation region corresponds with amino acids 6–46 and the EC apoptosis region with amino acids 101–114 (Wang *et al.*, 2006). A relatively large region of the protein appeared to have a function in EC migration (residues 114–192). This region overlaps the peptide involved in leukocyte migration and thus also contains the RIGRIIT motif. Finally, EMAP II contains two heparin-binding motifs, both located in the C-terminal portion of the protein (residues 217–219 and 267–269). These motifs were shown to be involved in the anti-angiogenic activities of EMAP II at acidic pH (Chang *et al.*, 2005).

### ***1.9.2 Antitumour and anti-angiogenic properties***

When injected intra-tumourally into Meth A fibrosarcoma-bearing mice, EMAP II was shown to induce a TNF-like thrombo-hemorrhage and for the mammary carcinoma cells MC-2 the same treatment induced sensitivity to systemic TNF treatment (Kao *et al.*, 1994). Similar observations were made for mouse melanoma (B16) and human fibrosarcoma (HT-1080) (Marvin *et al.*, 1996). EMAP II was shown to inhibit primary and metastatic tumour growth of lung carcinoma (LLC) and mammary tumours (MDA-MB-468) in mice (Schwarz *et al.*, 1999) and primary tumour growth of glioma in rats (Schwarz & Schwarz, 2004). TNF-resistant human melanomas (Pmel) were rendered sensitive to systemic TNF therapy when the tumour cells were transfected to increase AIMP1 and EMAP II protein expression (Wu *et al.*, 1999; Gnant *et al.*, 1999). AIMP1 was shown to have an anti-tumour activity in mouse xenograft models: in Meth A-bearing Balb/c mice AIMP1 treatment reduced tumour volume, in mice xenografted with human lung cancer AIMP1 has a cooperative effect with paclitaxel (Lee *et al.*, 2006).

These anti-tumour effects were suggested to be angiogenesis-mediated because EMAP II showed anti-angiogenic activities and was capable of inducing apoptosis in growing EC (Schwarz *et al.*, 1999b; Berger *et al.*, 2000). Also for AIMP1 a role in angiogenesis has been described. This role turned out to be biphasic and dose-dependent; low concentrations are pro-angiogenic and induce endothelial cell migration (Park *et al.*, 2002c; Hou *et al.*, 2006) while high concentrations are anti-angiogenic and induce endothelial cell death (Park *et al.*, 2002c). Further experiments have demonstrated that different concentrations of AIMP1 activated different intracellular pathways. Low doses of AIMP1 activated ERK kinase that controls expression of matrix metalloproteinase 9. The later hydrolysed collagen and thus promotes endothelial cell migration. On the other hand, higher doses of AIMP1 stimulated pro-apoptotic kinase JNK and this can be one of the mechanisms for AIMP1-induced apoptosis of endothelial cells (Park *et al.*, 2002c; Hou *et al.*, 2006). These properties are very similar to other cytokines, like TNF (Fajardo *et al.*, 1992).

The anti-angiogenic activity of AIMP1 plays an important role in the impaired neovascularization associated with the pathologic presentation of bronchopulmonary

displasia (BPD). In fact, AIMP1 is highly expressed in BPD affected lungs and its inhibition increases both neovascularization and alveolar development (Schwarz *et al.*, 2000; Quintos-Alagheband *et al.*, 2004).

In a search for proteins involved in corneal transplant rejection, AIMP1 was found in serum and appeared capable of inducing corneal EC apoptosis, which was suggested to be involved in corneal decompensation after transplantation (Mai *et al.*, 1999).

In slides of glioblastoma tumours from patients treated with a mutated form of TNF (TNF-SAM2, which has higher tumour killing activity than TNF- $\alpha$  and fewer side effects) and chemotherapy, high AIMP1 mRNA expression correlated with longer progression free survival (Yamamoto *et al.*, 2000).

### ***1.9.3 Apoptosis and inflammation***

The initially described function of EMAP II as chemo-attractant for leukocytes and macrophages has been translated to a set of disease settings. In areas of apoptosis in ischemia-reperfused kidneys, high EMAP II expression correlated with sites of leukocytes-infiltrated inflamed tissue. When apoptosis was inhibited, inflammation was also declined (Daemen *et al.*, 1999). In primary uveal melanoma, areas of high EMAP II expression correlate with tumour-associated macrophages accumulation (Clarijs *et al.*, 2003). Comparable correlation was found in experiments with melanoma biopsies of ILP (isolated limb perfusion) treated patients (van Horssen *et al.*, 2006b). A more detailed function of EMAP II in solid tumours has been described recently, showing that EMAP II expressing tumour cells can induce apoptosis of lymphocytes in solid tumours. This function in the tumour microenvironment suggests an immunosuppressive role of EMAP II in growing solid tumours (Murray *et al.*, 2004a; Murray *et al.*, 2004b).

The pro-inflammatory role of EMAP II, as observed during protein characterization right after EMAP II identification (Kao *et al.*, 1992), has also been further investigated. For AIMP1 a pro-inflammatory role has been described, in line with the initial finding for EMAP II, resulting in upregulation of pro-inflammatory genes like TNF (Ko *et al.*, 2001; Park *et al.*, 2002b). EMAP II downregulation is reported to contribute to the beneficial

effects of rapamycin, both after injury and neointima formation (Zohlhofer *et al.*, 2004; Nuhrenberg *et al.*, 2005; Nuhrenberg *et al.*, 2008). Furthermore, AIMP1 is highly expressed by the foam cells of atherosclerosis lesions, implying that it could be a major contributor of inflammation in the atherosclerosis development (Ko *et al.*, 2001). AIMP1 and EMAP II expression is also increased in acute lung inflammation and intra-tracheal instillation of EMAP II induces recruitment of monocytes/macrophages and granulocytes into the lungs (Journey *et al.*, 2007).

#### ***1.9.4 Injury, development and metabolism***

Beside anti-tumour activities, EMAP II is also reported to be involved in a broad set of brain diseases and injury. More specific, EMAP II is associated with macrophages in several autoimmune inflammatory lesions, spinal cord injury, virus induced inflammation of the nervous system, hippocampal brain damage, and traumatic brain injury (Schluesener *et al.*, 1997; Wege *et al.*, 1998; Brabeck *et al.*, 2002; Mueller *et al.*, 2003). Based on these findings, during brain damage, injury and inflammation EMAP II is considered to be a marker for microglial cells in these lesions (Mueller *et al.*, 2003). Recently, Zhu *et al.* (Zhu *et al.*, 2009) demonstrated that AIMP1 is essential for neurofilaments assembly and axon maintenance in motor neurons.

During embryogenesis, a role for AIMP1 and EMAP II has been found in lung development. This function is linked to the effect on neovascularisation by AIMP1 and EMAP II during embryonic development (Schwarz *et al.*, 1999a; Warburton *et al.*, 2000). Interestingly, also during pregnancy AIMP1 and EMAP II serum levels are increased. Next to pregnancy, also during the menstrual cycle a temporal AIMP1 and EMAP II expression pattern is observed. The RNA coding for the AIMP1 protein, is negatively regulated by prostaglandin E2 (Battersby *et al.*, 2002).

AIMP1 expression has been demonstrated to rapidly increase after skin injury and to facilitate wound repair through direct stimulation of fibroblasts proliferation and collagen production (Park *et al.*, 2005b). Furthermore, AIMP1 has been demonstrated to be secreted from the pancreas upon glucose starvation and, moreover, exogenous infusion

of AIMP1 increased plasma levels of glucose, glucagon and fatty acid (Park *et al.*, 2006). Lee *et al.* (Lee *et al.*, 2008) reported a further activity of AIMP1 as a component of the negative feedback loop of TFG- $\beta$  signalling, mediated by Smurf2, in MEF cells.

Unexpectedly, given the many functions of AIMP1 and EMAP II, including the presence as a component of the ARS complex, AIMP1 knock-out mice survive (Park *et al.*, 2005b). Apparently, due to the crucial importance of protein translation, there is a kind of rescue by other (unknown) proteins and mechanisms. The major defect reported in these knockouts is a retarded wound closure due to a decrease in fibroblast proliferation (Park *et al.*, 2005b).

### **1.10 From AIMP1 to EMAP II**

AIMP1 is proteolytically cleaved to produce EMAP II under conditions of cellular stress like apoptosis, hypoxia and treatment with chemotherapeutic agents (Knies *et al.*, 1998; Barnett *et al.*, 2000 ;Matschurat *et al.*, 2003). The mechanism(s) of AIMP1 cleavage and especially which proteases are involved turned out to be very complex and are still under debate.

*In vitro* cleavage experiments performed using mouse recombinant AIMP1 identified caspase-7, and to a lesser extent caspase-3, as proteases capable of AIMP1 cleavage (Behrendorf *et al.*, 2000). In line with these findings is the fact that caspase-7 is capable of cleaving EMAP II out of the whole murine multi tRNA synthetase complex (Shalak *et al.*, 2001). The cleavage site within mouse recombinant AIMP1 sequence was mapped at the critical aspartate residue (Asp-144) in the ASTD-motif. Although this motif is absent in humans, Asp-146 had been suggested to be critical in cleavage of human AIMP1 (Berger *et al.*, 2000). Experiments with human proteins showed very different results and questioned the suggested similarity on cleavage mechanisms. Data on recombinant human AIMP1 showed that human caspase-3 and -7 are not capable of AIMP1 cleavage *in vitro*, and in lysates of human tumour cell lines triggered with apoptosis-inducers no EMAP II was found (Zhang & Schwarz, 2002). In another study in which mouse

melanoma tumour cells were used, EMAP II release was induced by hypoxia; this induction was also shown to be independent of caspase-3 and -7 activation (Matschurat *et al.*, 2003). The involvement of caspases in AIMP1 cleavage is very contradictory and at least dependent on experimental setting.

Shalak *et al.* (Shalak *et al.*, 2007) identified a new intermediate in the pathway that, starting from the AIMP1 subunit of the complex, leads to the extracellular cytokine. This new intermediate was named AIMP1(ARF) for Apoptosis-released Factor and is produced *in cellulo* by proteolytic cleavage of endogenous AIMP1 and is rapidly recovered in the culture medium. This AIMP1 derivative was purified from the medium of human U937 cells subjected to serum starvation. It contains 40 additional N-terminal amino acid residues as compared with EMAP II and may be generated by a member of the matrix metalloproteinase family.

In conclusion, the cleavage of AIMP1 varies strongly between different settings, species and likely even between tumour types. The exact mechanisms, cleavage sites and whether this affects the cytokine properties and activity of EMAP II are still unknown.

### **1.11 Receptors mediating AIMP1/EMAP II cytokine activities on endothelial cells**

It does not seem plausible that soluble AIMP1 and EMAP II use a unique receptor on target cells to carry out the many functions described. It is more likely that different receptors are involved for different activities on diverse target cells.

Different receptors have been proposed as mediators of the cytokine activities of AIMP1 and EMAP II on endothelial cells. An interaction between the C-terminal portion of AIMP1 (EMAP II) and the  $\alpha$ -subunit of ATP synthase has been demonstrated and, furthermore, this interaction may function as a mechanism for the inhibition of BAEC (Bovine Aortic Endothelial Cells) growth (Chang *et al.*, 2002). Schwarz *et al.* (Schwarz *et al.*, 2005) demonstrated that EMAP II inhibits MEC (Microvascular Endothelial Cells) adhesion to fibronectin through direct interaction with  $\alpha 5\beta 1$  integrin. Moreover, it was reported that AIMP1 employs the chemokine receptor CXCR3 to stimulate endothelial

progenitor cell (EPCs) migration (Hou *et al.*, 2006). Yi *et al.* (Yi *et al.*, 2005) monitored the binding patterns to the cell surface and the internalization of AIMP1 in endothelial cells (BAEC) and determined that the protein may be internalized via lipid rafts, which are plasma membrane platforms that organize various receptors and their downstream molecules. Finally, EMAP II was demonstrated to bind to VEGFR1 and VEGFR2 in HUVEC (Human Umbilical Vein Endothelial Cells), thus interfering with VEGF-induced pro-angiogenic signalling and inhibiting endothelial cell proliferation and migration (Awasthi *et al.*, 2008).

Figure 1.10 reports a schematization of some of the activities exerted by AIMP1 on endothelial cells and the receptors responsible for such activities.

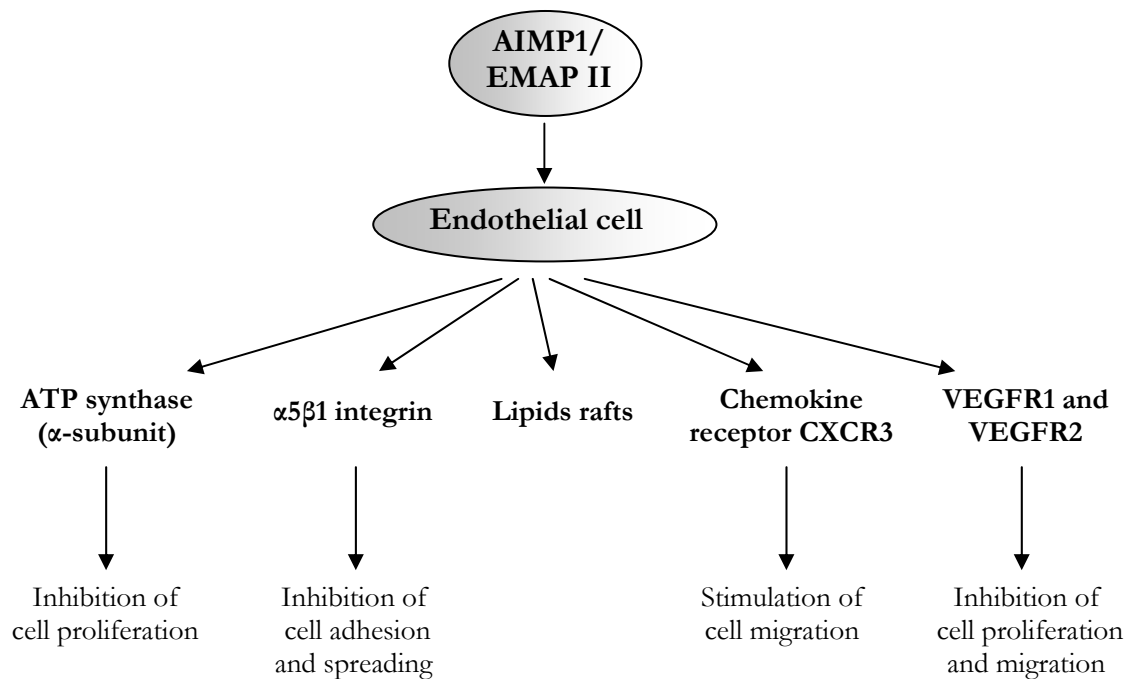


**Fig. 1.10 AIMP1 acts on endothelial cells by interacting with different receptors.** Schematization of some of the receptors identified for AIMP1 in endothelial cells and correspondent cellular effects.

## 2. Materials and methods

### 2.1 Materials

Unless otherwise indicated, all chemicals, solvents and reagents were purchased from Sigma Aldrich Co. (St. Louis, MO, USA).

Primary antibodies used were provided by Santa Cruz Biotechnology (Santa Cruz, CA), except for rabbit anti-pERK/ERK, anti-pJNK/JNK, anti-pAKT/AKT antibodies, which were from Cell Signalling Technology (Beverly, MA), mouse anti- $\alpha$ 5 $\beta$ 1 integrin antibody from Millipore (Billerica, MA), mouse anti-vinculin antibody from Sigma and anti-ARHGAP29 antibody from Abnova.

### 2.2 Cell cultures

Immortalized porcine aortic endothelial cells (PAEC) were a kind gift of Prof. Bussolino (IRCC – Candiolo - TO). Cells were cultured in Ham's F-12 medium, supplied with 10% Fetal Bovine Serum (FBS) (Gibco Life Technologies), 100  $\mu$ g/ml penicillin-streptomycin 10U/ $\mu$ l and 2 mM glutamine in a humidified 5% CO<sub>2</sub> incubator at 37°C.

Bovine aortic endothelial cells (BAEC) were isolated from descending thoracic aortas and cultured in DMEM, supplied with 10% FBS, 100  $\mu$ g/ml penicillin-streptomycin 10U/ $\mu$ l

and 2 mM glutamine in a humidified 5% CO<sub>2</sub> incubator at 37°C and used at early passages (I-VI).

Porcine aortic endothelial cells (PAEC) were isolated from descending thoracic aortas and cultured in Ham's F-12 supplied with 10% FBS, 100 µg/ml penicillin-streptomycin 10U/µl and 2 mM glutamine in a humidified 5% CO<sub>2</sub> incubator at 37°C and used at early passages (I-VI).

Human umbilical vein endothelial cells (HUVEC) were isolated from human umbilical cords by collagenase digestion according to the protocol of Jaffe *et al.* (Jaffe *et al.*, 1973) and grown in M199 medium containing 20% FBS supplemented with 100 µg/ml penicillin-streptomycin 10U/µl and 2 mM glutamine, porcine heparin and 0,2% bovine brain extract (BBE) in a humidified 5% CO<sub>2</sub> incubator at 37°C. Cells were grown on plates coated with 1% porcine gelatin and used at early passages (I-V).

Human urinary bladder carcinoma ECV-304 cells and mouse macrophages RAW 264.7 were purchased from the American Type Culture Collection (Manassas, VA) and cultured in DMEM supplied with 10% Fetal Bovine Serum, 100 µg/ml penicillin-streptomycin 10U/µl and 2 mM glutamine, in a humidified 5% CO<sub>2</sub> incubator at 37°C.

Serum starved cells were cultured for 16 hours in serum free cell culture medium.

Since it was shown that starvation increases the binding of EMAP II to the cell surface (Chang *et al.*, 2002), serum starvation was used as an experimental condition for every biological assay before treatment with AIMP1.

### **2.3 Production and purification of human recombinant AIMP1**

Human AIMP1 cDNA was obtained by retrotranscription of U937 cells RNA, cloned in pBAD/Myc/HisA vector using Hind III and Nco I restriction enzymes using the following primers: 5'-CACGCCATGGCAAATAATGAT-3' (forward primer) and 5'-CCCAAGCTTTTGGATTCCACT-3' (reverse primer). *Escherichia coli* TOP F10 cells were transformed with this plasmid and let to grow in Luria Broth at 37°C until the absorbance at 600 nm reached 0.6 units. L-Arabinose (0.002%) was added to the culture to induce

AIMP1 expression. After 16 hours at 20°C cells were harvested by centrifugation (6,000 rpm, 30 min, 4°C) and resuspended in phosphate buffer (50 mM NaH<sub>2</sub>PO<sub>4</sub>, 300 mM NaCl, 50 µg/ml RNase, 4U/ml benzonase nuclease, 2 mM DTT, 0.5 mM PMSF, 1x Protease Inhibitor Cocktail, pH 8.0), sonicated, centrifuged, filtered and loaded on a Ni-Sepharose column (Ni-Sepharose high performance, GE Healthcare, Uppsala, Sweden). After having washed the unbound proteins, recombinant AIMP1 (rAIMP1) was eluted through a step gradient of 500 mM imidazole elution buffer. The fractions containing rAIMP1 were identified through SDS-PAGE analysis followed by MS/MS spectrometry analysis. Then, the fractions containing rAIMP1 were loaded on a Hi-Trap cationic-exchange column (Hi-Trap SP HP, GE Healthcare) and eluted through a linear gradient of 1 M NaCl phosphate buffer (30 mM NaH<sub>2</sub>PO<sub>4</sub>, 1M NaCl, pH 7.2).

In order to remove lipopolysaccharides (LPS), the protein underwent 5 cycles of Triton X-114 extraction (Liu *et al.*, 1997) after which the buffer was exchanged, through dialysis with a 10 kDa cut-off, against pyrogen-free PBS containing 20% of cell culture tested glycerol. The protein was then filtered through a Posidyne membrane (0.2 µm) (Pall Gelman Laboratory, Ann Arbor, USA). The concentration of LPS in the final rAIMP1 preparation was below 20 pg/mg, as determined with a Limulus Amebocyte Lysate QCL-1000 kit (BioWhittaker). In parallel, 10 ml of PBS-20% glycerol underwent the same protocol used for LPS extraction from rAIMP1 to be used as the vehicle for control samples in all experiments.

## **2.4 Circular Dichroism spectrometry**

For circular dichroism analysis recombinant AIMP1 and vehicle (used as a control) were diluted in deionised water to a concentration of 0.1 mg/ml. Circular dichroism spectra were recorded for rAIMP1 protein at temperatures between 20 and 90°C, on a JASCO J-815 spectrometer equipped with a Peltier temperature controller, using a 1 cm path length quartz cuvette. Spectra were recorded between the wavelengths of 195 nm and 250 nm with a 1.0 nm step size and slit bandwidth of 1.0 nm. Signal averaging time was 8 s and

ellipticities reported as mean residue ellipticity in deg.cm<sup>2</sup>/dmol. Spectra recorded for vehicle were subtracted from rAIMP1 spectra.

## **2.5 AIMP1 stability in conditioned cell culture medium**

Recombinant AIMP1, at a concentration of 250 nM, was incubated at 37°C in conditioned Ham's F-12 medium supplied with 10% FBS. The cultured medium used was taken from a PAEC plate that had been kept in culture for 48 hours. At defined time points 30 µl of sample were collected and loaded on SDS-PAGE for Western blot analysis.

## **2.6 Western blotting analysis**

Protein samples were loaded on SDS-PAGE, transferred to nitrocellulose membrane and blocked in 5% non-fat milk in TBS containing 0.1% Tween 20 (TBST). The membrane was incubated with specific primary antibody diluted in TBST 1% milk O.N. at 4°C; the appropriate HRP-conjugated secondary antibody was diluted 1:10,000 in TBST 1% milk and incubated for 1 hour at room temperature and developed using ECL Western Blotting substrate kit (Thermo Fisher Scientific, Rockford, IL, USA). For normalization, membranes were stripped with a stripping buffer (62.5 mM Tris HCl pH 6.8, 2% SDS, 0.7% β-mercaptoethanol) for 30 minutes at 50°C, and blotted against the normaliser. Quantification of the bands was carried out using ImageJ software.

## **2.7 Biological assays**

### ***2.7.1 Cell viability assay***

AIMP1 role in inhibiting cell survival was monitored by measuring the cellular conversion of a tetrazolium salt into a formazan product that is detected using a 96-well plate reader (CellTiter 96 Non-Radioactive MTT Assay, Promega, Madison, Wisconsin, USA). Cells

were serum-starved for 16 hours and plated at a density of  $5 \times 10^3$  /well or  $1 \times 10^4$  /well on 96-well microtitre plates supplemented with 0%, 4% or 10% FBS. Recombinant AIMP1 was added to the medium at the concentrations indicated in the specific experiment. After 24 hours, 15  $\mu$ l of Dye Solution (containing the tetrazolium component) were added to each well, and 4 hours later, the reaction was terminated by addition of 100  $\mu$ l of stop solution to each well. The plates were incubated for 1 hour to solubilise the formazan dye, and the optical density of each well was measured with a multimode microplate reader (Infinite 200, Tecan) at 570 nm. Triplicate wells and blank well without cells were run for each treatment.

For the anti- $\alpha 5\beta 1$  integrin antibody assay, cells were starved for 16 hours in serum-free medium, detached with 5 mM EDTA and  $7 \times 10^4$  cells were incubated with 800 nM anti- $\alpha 5\beta 1$  integrin antibody or control for 15 min at 4°C before plating. 100 nM rAIMP1 was added in presence of 10% FBS and cells were plated in triplicate at a density of 20,000 cells/well. MTT assay was performed after 24 hours as described above.

Absorbances were normalized to vehicle and expressed as values relative to positive control.

### ***2.7.2 Cell Proliferation Assay***

To determine AIMP1 effect on cell proliferation, a proliferation assay based on the measurement of 5-bromo-2'-deoxyuridine (BrdU) incorporation during DNA synthesis in proliferating cells was performed (Cell Proliferation Biotrak Elisa System Version 2 kit, GE Healthcare). Cells were serum-starved for 16 hours and plated at a density of  $5 \times 10^3$  /well on 96-well microtitre plates supplemented with 10% FBS. Recombinant AIMP1 or vehicle were added to the medium at 200 nM. After 24 hours BrdU was added and incubated for 2 hours. During this labelling period, the pyrimidine analogue BrdU is incorporated in place of thymidine into the DNA of proliferating cells. The peroxidase-labelled anti-BrdU binds to the BrdU incorporated in newly synthesized, cellular DNA. The immune complexes are detected by the subsequent substrate reaction and the resultant colour read at 450 nm in a microtitre plate spectrophotometer. The absorbance

values correlate directly to the amount of DNA synthesis and thereby to the number of proliferating cells in culture.

### ***2.7.3 Tubulogenesis assay***

Tubulogenesis assay was performed essentially as described previously by Baatout (Baatout, 1997), using 150  $\mu$ l/well of Matrigel (8 mg/ml) (Becton Dickinson, Franklin Lakes, New Jersey, USA) that allows ECV tubule formation and permits vascular network visualization and quantification by image analysis. Briefly, ECV cells were serum-starved for 16 hours and plated in 48-well plates ( $4 \times 10^4$  cells/well) on Matrigel in culture medium without FBS, supplied with 10 ng/ml EFG; rAIMP1 was added at the indicated concentrations. Triplicate wells were photographed at 4x magnification with a Leica DFC420C camera and analyzed with Leica Application Suite software (Leica Microsystems, Switzerland). The number of closed areas after 6 hours of culturing were counted in triplicate wells.

### ***2.7.4 Migration assay***

Cell migration assay was performed using a 48-well modified Boyden chamber (Neuroprobe, Gaithersburg, MD). A polycarbonate membrane with 8  $\mu$ m pores (Neuroprobe) was coated with 1% gelatin. RAW 264.7 cells were serum-starved for 16 hours and plated in serum-free medium in the upper compartment of the chamber ( $5 \times 10^4$  cells/well). Test substances were added at indicated concentrations to serum-free medium in the lower compartment. After 5 hours, cells migrated to the lower side of the membrane were fixed, coloured with Giemsa stain and counted at 20x magnification using a Leica DFC420C camera and analyzed with Leica Application Suite software (Leica Microsystems, Switzerland). Samples were performed in duplicate, and 20 optical fields were counted per sample.

### ***2.7.5 Adhesion assay***

Cell adhesion assay was performed using fibronectin (FN) pre-coated 96-well plates (Becton Dickinson, Franklin Lakes, New Jersey, USA). Cells were serum-starved for 16 hours, detached with 5 mM EDTA and plated ( $5 \times 10^4$  cells/well) in Ham's F-12 medium supplied with 1% FBS in presence of 100 nM rAIMP1 or vehicle. After 20 minutes cells were fixed with paraformaldehyde (PFA) 4% in PBS, stained with 50  $\mu$ l crystal violet solution (0.5% crystal violet, 20% methanol) for 10 minutes at room temperature and stain was solubilised with 100  $\mu$ l Sorenson's buffer (0.1 M sodium citrate, 50% ethanol, pH 4.2). After solubilisation the optical density of each well was measured with a multimode microplate reader (Infinite 200, Tecan) at 595 nm. Triplicate wells and blank well without cells were run for each treatment.

## **2.8 Immunofluorescence**

Indirect immunofluorescence analysis was performed on time course experiments of PAEC stimulated with rAIMP1 to study the subcellular localization of the exogenous protein after treatment. PAEC, maintained in their growth medium, were plated at a density of  $2 \times 10^4$  cells/well in 24-well plates onto glass coverslips covered with 1% porcine gelatine (coating layered over-night at 4°C). Cells were cultured for 30 hours and then serum-starved for 16 hours; they were then washed and 50 nM of AIMP1 in 500  $\mu$ l of 10% FBS containing culture medium was added. After stimulation, cells were washed twice with PBS and fixed in 4% PFA, permeabilized in PBS-0.1% Triton X-100 and blocked in PBS, 1% BSA, 5% goat serum for 1 hour. Cells were then incubated with primary antibodies for 1 hour. After two 5 minute washes with PBS and one 5 minute wash with PBS, 1% goat serum, cells were incubated with Alexa Fluor 488- or Alexa Fluor 568- (Invitrogen, Carlsbad, CA) conjugated secondary antibodies for 1 hour. Moreover, cells were stained for 30 minutes with propidium iodide to decorate nuclei or for 20 minutes with phalloidin to stain the cytoskeleton. Fluorescence was examined with

a Leica confocal microscope (Leica TCS SPE). Pictures were handled with Leica Application Suite (Leica Microsystems, Switzerland) and Adobe Photoshop software.

## **2.9 Analysis of AKT, ERK and JNK activation through phosphorylation**

In order to analyse activation through phosphorylation of AKT, ERK and JNK, cells were serum starved for 16 hours and treated with 200 nM AIMP1 or vehicle (as a control) for 10 to 180 minutes in Ham's F-12 without FBS. Four biological replicates were performed for each treatment. After treatment, cells were washed twice with PBS and lysed in lysis buffer (50 mM Tris-HCl pH 6.8, 120 mM NaCl, 1% SDS, 1x PhosStop Cocktail (Roche), 0.5 mM PMSF, 1x Protease inhibitor cocktail). Samples were kept in ice for 15 minutes, vortexed, passed 15 times through a 1 ml syringe needle and centrifuged for 10 minutes at 14,000 rpm at 4°C. The supernatants were collected, quantified using the BCA method and 50 µg of proteins were loaded on SDS-PAGE.

## **2.10 Subcellular fractionation**

PAEC were serum-starved for 16 hours and subcellular fractionation was performed according to Kim *et al.* (Kim *et al.*, 1999) with some modifications. All procedures were done at 4°C. PAEC from one 150-mm culture dish (8 x 10<sup>6</sup> cells) were resuspended in 1 ml of buffer A (25 mM Tris pH 7.4, 1 mM EDTA, 0.5 mM EGTA, 10 mM NaCl, 0.5 mM PMSF, 1x Protease inhibitor cocktail), put through 3 freezing and thawing cycles in liquid nitrogen and homogenized 40 times with a tight Dounce homogenizer (Kontes Glass, Vineland, NJ). A one-tenth volume buffer A containing 2.5 M sucrose was added to the homogenate. The homogenate was centrifuged at 1,000 x g for 10 min (step A). The supernatant of step A was centrifuged at 100,000 x g for 1 h (step B). The pellet of step B was resuspended in PBS, 1% NP40 (containing 1x Protease inhibitor cocktail and 0.5 mM PMSF) and stored as the membrane fraction; the supernatant of step B was stored as the cytosolic fraction.

## **2.11 Affinity purification of AIMP1-binding proteins**

The subcellular fractions were dialyzed for 16 hours at 4°C against PBS containing 1x Protease inhibitor cocktail, then incubated with rAIMP1 or vehicle for 2 hours at 4°C; rAIMP1 was then precipitated using nickel affinity interaction (Ni-Sepharose high performance, GE Healthcare) for 1 hour at 4°C.

After incubation, the resin was spun down, washed with washing buffer (50 mM Na<sub>2</sub>HPO<sub>4</sub>, 200 mM NaCl, 0.1% NP40, 2 mM EDTA, 2 mM Na<sub>3</sub>VO<sub>4</sub>, 1 mM PMSF, 1x Protease inhibitor cocktail) and resuspended in 30 µl loading buffer (62.5 mM Tris-HCl pH 6.8, 20% glycerol, 2% SDS, 5% β-mercaptoethanol, 0.025% bromophenol blue). Samples were resolved on SDS-PAGE and stained with Coomassie Brilliant Blue; the differential bands were excised and identified by mass spectrometry analysis.

## **2.12 Protein identification by mass spectrometry (MS)**

The selected protein spots or bands were excised from the gel and destained over night with 40% ethanol in 25 mM ammonium bicarbonate, washed twice with 25 mM ammonium bicarbonate, three times with acetonitrile, and dried. Each gel fragment was reswollen in 25 mM ammonium bicarbonate containing 0.6 µg of modified porcine trypsin and digested overnight at 37°C. Peptides were extracted by sonication in 25 mM ammonium bicarbonate, loaded onto a ZORBAX 300 SB C18 RP column (75 µm x 150 mm, 3.5 µm particles, Agilent, Santa Clara, CA, USA) and eluted with a gradient of acetonitrile from 5% to 80% (containing 0.1% formic acid) at a flow rate of 0.3 µl/min by a HP 1100 nanoLC system coupled to a XCT-Plus nanospray-ion trap mass spectrometer (Agilent, Santa Clara, CA, USA). MS parameters were the following: scan range  $m/z = 100-2,200$ , scan speed 8,100  $m/z$  s<sup>-1</sup>, dry gas flow 5 l/min, dry temperature 300°C, capillary 1.8 kV, skimmer 40 V, ion charge control (ICC) target 125,000, maximum accumulation time 300 ms. Positively charged peptides ions were automatically isolated and fragmented, and spectra were deconvoluted by the DataAnalysis software version 3.4 (Bruker Daltonics, Bremen, Germany). Mass spectrometry data were fed to the Mascot

search algorithm for searching against the NCBI non-redundant database number 20100402 (<http://www.Matrixscience.com>). Mass tolerance for the monoisotopic peak masses was set to 1.2 Da (parent ion) or 0.6 Da (fragments), while the maximum number of missed cleavages was set to 3. Allowed modifications were cysteine carbamidomethylation and methionine oxidation for spots deriving from 2-DE gels. Hits with a probability-based Mowse score higher than 47 were considered significant ( $p < 0.05$ ). Since the protein database for *Sus scrofa* is not complete, when a protein was not present as porcine in the database, we accepted its identification from *Bos taurus* or *Homo sapiens*.

### **2.13 Pull-down assay**

Subcellular fractions were dialyzed for 8 hours against PBS containing 1x Protease inhibitor cocktail at 4°C and were then incubated with rAIMP1 or vehicle for 16 hours at 4°C. Ni-Sepharose high performance beads were added to the cellular fractions and incubated for 1h at 4°C. The samples were then centrifuged and the supernatant was removed. The beads were washed with washing buffer (50 mM Na<sub>2</sub>HPO<sub>4</sub>, 200 mM NaCl, 0.1% NP40, 2 mM EDTA, 2 mM Na<sub>3</sub>VO<sub>4</sub>, 1 mM PMSF, 1x Protease inhibitor cocktail) and resuspended in 200 µl loading buffer. 20 µl of sample were loaded on an SDS-PAGE and the putative rAIMP1-binding proteins were identified through Western blot analysis.

### **2.14 Co-immunoprecipitation**

Subcellular fractions were dialyzed for 8 hours against PBS containing 1x Protease inhibitor cocktail at 4°C, incubated with rAIMP1 for 16 hours at 4°C and mixed, for 1h at 4°C, with anti-filamin-A, anti- $\alpha$ -tubulin, anti-vinculin, anti-cingulin or control antibodies, pre-coupled with protein A or G Sepharose beads. The samples were then centrifuged and the supernatants removed. Beads were washed with PBS 0.1% NP40 and resuspended in 20 µl loading buffer. Samples were then loaded on an SDS-PAGE and immunoblotted with anti-His-probe antibody to recognize rAIMP1.

## **2.15 Cell treatment, protein extraction and sample preparation for 2-D electrophoresis**

For phosphoproteomic analysis, cells were serum starved for 16 hours and treated with 200 nM AIMP1 or vehicle (as a control) in Ham's F-12 without FBS for 10 or 30 minutes. Four biological replicates were performed for each treatment. After treatment, cells were washed twice with PBS and twice in sucrose buffer (250 mM sucrose, 10 mM Tris-HCl, pH 7). Protein extraction was performed following the protocol from Yan *et al.* (Yan *et al.*, 2007). Cell samples were lysed in solubilisation buffer (40 mM Tris, 7 M urea, 2 M thiourea, 4% 3-[(3-cholamidopropyl)dimethylammonio]-1-propanesulfonate (CHAPS), 65 mM dithiothreitol (DTT), 1 mM ethylenediamine-tetra-acetic acid, 1x Protease inhibitor cocktail, 0.1 g/l RNase A, and 0.1 g/l DNase) and sonicated (5 s/cycle, 3 cycle; 0 °C). After centrifugation at 13,000 x g for 30 min at 4°C, the supernatant was collected as the protein sample. Before subsequent analysis the sample was concentrated and desalted using the Ultrafree-0.5 Centrifugal Filter Device (Millipore) according to manufacturer's protocol. Protein concentration was determined using Bradford protein assay kit (BioRad, Marnes-la-Coquette, France).

## **2.16 2-D electrophoresis**

2-D electrophoresis (2-DE) was performed according to Jacobs *et al.* (Jacobs *et al.*, 2001), with some modifications. Isoelectrofocusing of proteins was performed at 20°C in 18 cm IPG 4-7 strips (GE Healthcare), using the Ettan IPGphor system (GE Healthcare). Prior to SDS-PAGE, the IPG strips were equilibrated twice for 15 minutes in a buffer containing 50 mM Tris-HCl pH 8.8, 6 M urea, 30% glycerol, 2% SDS, plus 1% DTT for the first equilibration step, 2.5% iodoacetamide and traces of bromophenol blue for the second one. SDS-PAGE was performed on 12.5% polyacrylamide gels according to Laemmli (Laemmli, 1970) but without stacking gel, in a PerfectBlue Dual gel System, 20x20 cm (PeQLab, Erlangen, Germany). The run was carried out at 60 mA/gel at 16°C until the tracking dye front reached the bottom of the gel. Each treated sample was run

simultaneously to its control. In order to visualize phosphorylated proteins, gels were stained with Pro-Q Diamond (Molecular Probes Inc, Eugene, OR) following the protocol of Agrawal and Thelen (Agrawal & Thelen, 2005). After image acquisition, gels were stained for total protein with SYPRO Ruby protein gel stain (Molecular Probes) according to the manufacturer's protocol.

Images were acquired by CCD camera (ProXPRESS 2-D Perkin Elmer) with the following parameters: excitation 540/25 and emission 590/35 nm for phosphoprotein staining, and excitation 460/80, emission 650/150 for Sypro staining respectively. Before MS/ spectrometry analysis the gels were stained in Coomassie Blue R350 (Marchetti-Deschmann *et al.*, 2009).

## **2.17 Image analysis**

Image analysis was performed by the ImageMaster 2D Platinum 5.0 software package (GE Healthcare). Spot detection and gel matching were carried out automatically and checked manually. The volume of each spot was normalized to the total volume of spots in the gel (%Vol). Analysis was performed in order to identify spots with qualitative (presence/absence) and quantitative ( $\geq 1.5$ -fold) spot volume increase/decrease between treatment and control. Spots that fulfilled these criteria in at least three experiments were considered significant and underwent mass spectrometry analysis. For ProQ Diamond stained gels all spots were also required to be detected and matched in SYPRO Ruby image counterpart. Quantitative differences were calculated for both SYPRO Ruby and ProQ Diamond images. Proteins found as having differential spot volumes by ProQ Diamond staining were considered as differentially phosphorylated only if they did not also show a significant variation by SYPRO Ruby staining.

## **2.18 Cell treatment, RNA extraction and retrotranscription for Real Time PCR analysis**

In order to investigate transcriptional gene regulation, Real Time PCR experiments were performed. Cells were serum starved for 16 hours and treated with the indicated concentrations of AIMP1 or vehicle (as a control) in Ham's F-12 medium supplied with 10% FBS in time course experiments (from 1 hour to 24 hours). After treatment, total RNA was extracted from cell cultures which were about 80% confluent using the Trizol Reagent (Invitrogen). RNA was extracted according to the "acid phenol" method of Chomczynski and Sacchi (Chomczynski & Sacchi, 1987), where, by using acid phenol, a selective separation of RNA from DNA and the other lipidic and proteic components was obtained. Purification was carried out according to manufacturer's instructions. Extracted RNA was treated with DNase to eliminate residual genomic DNA, using the DNA free kit (Ambion, Austin, Texas). Quantification of RNA was performed by NanoDrop spectrophotometer ND-1000 (Celbio) at 260 nm. 0.5 µg of RNA from each sample were retrotranscribed into cDNA using the reverse transcriptase enzyme (M-MLV) (Ambion, Austin, TX). The obtained cDNA was diluted 1:4 with sterile water and stored at -20°C.

Real Time-PCR assays were designed using the Probe Finder Software, and reactions were carried out in 96-well plates, using Probe Master Mix (Roche) on the LC 480 instrument (Roche).

The set of genes analysed was chosen either on the basis of literature data reporting a correlation between gene transcriptional regulation and AIMP1 treatment or on the basis of the role of a specific protein in a process important in the frame of our study (that is the example of VEGFA, VEGFR1 and VEGFR2 that were chosen for their roles in angiogenesis). The list of analysed genes is reported in table 2.1, together with the primers sequences and the UPL probe number.

The primers were purchased from Sigma, while probes were from the UPL probe library (Roche). Fold induction was calculated by the  $\Delta\Delta Ct$  method. Data were normalized to 18S ribosomal RNA levels.

Primers	Sequences	Probe number
18S_fw	GGGACTTAATCAACGCAAGC	48
18S_rev	GCAATTATTCCCCATGAACG	48
VEGFA_fw	CTACCTCCACCATGCCAAGT	64
VEGFA_rev	GTGGGGTTTCTGGTCTCCTT	64
VEGFR1_fw	TGTCACGCTAACGGTGTCC	45
VEGFR1_rev	GGCTCCTGTTGTATTTTGTGG	45
VEGFR2_fw	ACTGCAGTGATTGCCATGTT	71
VEGFR2_rev	CTTAACGGTCCGGAGAACG	71
MMP2_fw	CTGGTGCTGCCACACTTAG	12
MMP2_rev	GGGTGCTGTAAGCCACAGA	12
MMP9_fw	CGGGAGACCTACGAACCA	27
MMP9_rev	AGCGGTACAGATATTCCTCTGC	27
ICAM1_fw	TCATGTCTGCCTCTATTGCTG	79
ICAM1_rev	GCAGGACGAGGCACTAAGAC	79
COL1a2_fw	CTGGCCCTCAAGGTTTCC	62
COL1a2_rev	GACCAGTCTGACCAGGTTTCG	62
CCNG2_fw	GCAATAAATGGGGGAGTAGGT	72
CCNG2_rev	GGCTATGCAATTCCTGCCTA	72
TNFAIP3_fw	CAGTCCCCAAACCTCCATC	82
TNFAIP3_rev	CCTCAGTGGGGACCACTTC	82
KLF4_fw	GAGGAGCCAAAGCCAAAGA	7
KLF4_rev	GTGAGTGGCCGTCTTTTC	7
BIRC3_fw	CTTCAGACAATCCAGAAGATGAAA	21
BIRC3_rev	TTCCGGATCAATGATAGGTCA	21

**Table 2.1.** List of the genes analysed following AIMP1 treatment of PAEC. The table lists the names of the genes, the sequences of the primers used for the amplification reaction and the number of the UPL probe used for each gene.

## 3. Results

### 3.1 Production and purification of recombinant AIMP1

Human recombinant AIMP1 was cloned in a pBAD/Myc/HisA vector, which produces a protein with a C-terminal 6-histidine tag and a myc tag.

The recombinant protein was expressed in *Escherichia coli* TOP F10 and purified using an FPLC Akta Purifier (Amersham Biosciences) in a two-step chromatography process. The software used to control the chromatography process was Unicorn 5.01, which provides a chromatogram that shows the data relative to the ongoing purification, such as absorbance at 280 nm, conductivity, concentration of elution buffer, etc. (Fig. 3.1).

The elution flux was collected in different fractions and, on the basis of the information given by the absorbance at 280 nm, selected fractions were loaded on SDS-PAGE (Fig. 3.2), in order to identify the samples containing the recombinant protein. To confirm the presence of recombinant AIMP1, mass spectrometry analysis was performed on the putative protein containing bands (Fig. 3.2, red panel). Fractions C1 to C6 from the nickel affinity purification step were pooled and loaded on the cationic exchange column.

The recombinant protein eluted from the second purification step was highly pure (>98%). Recombinant AIMP1 purity was analyzed through SDS-PAGE analysis, comparing it with commercial BSA (Fig. 3.3).

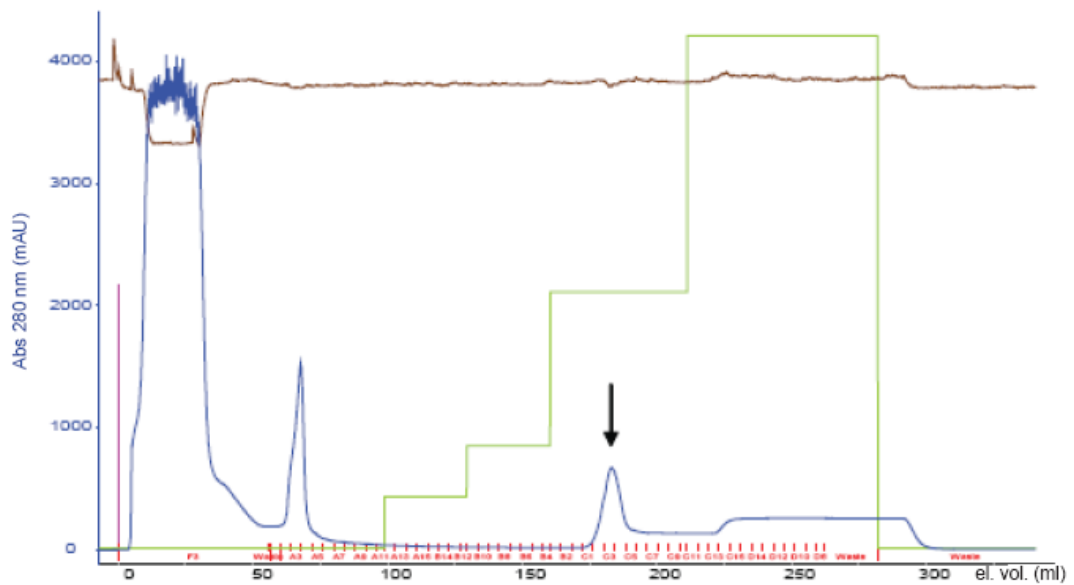


**Fig. 3.1. Chromatogram of the nickel affinity purification step.** The x-axis shows the elution volume expressed in ml, the y-axis shows the absorbance at 280 nm expressed in mAU (milli Absorbance Units). Brown line: conductivity, green line: concentration of elution buffer, blue line: absorbance at 280 nm; the red dashes on the x-axis represent the different fractions in which the elution was divided. The blue peak indicated with the black arrow represents recombinant AIMP1 elution peak.

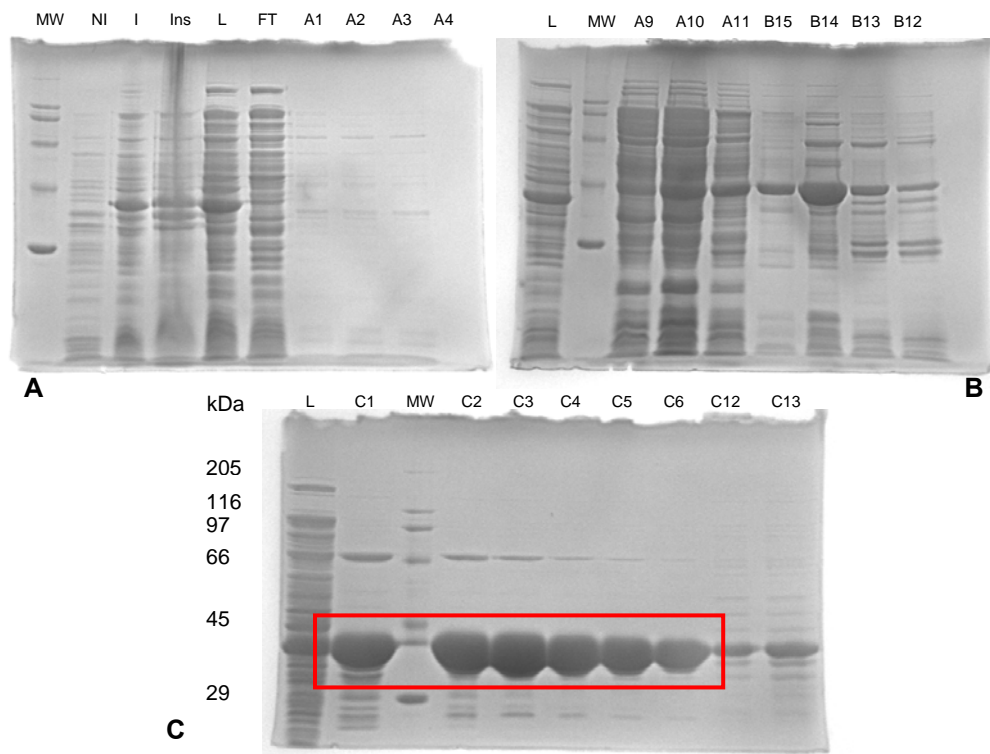


**Fig. 3.2. Elution fractions from the nickel affinity chromatography.** Reducing SDS-PAGEs (12% acrylamide/bisacrylamide) of the elution fractions deriving from the nickel affinity purification step. MW: molecular weight, NI: not induced, I: induced, Ins: insoluble, L: load, FT: flow through, A1 to C13: different elution fractions. Red panel: fractions C1 to C6 contained recombinant AIMP1 and were pooled to be loaded on the cationic exchange column.

The recombinant protein concentration was calculated with the BCA method (according to Manufacturer's instructions) using as reference a curve of known concentrations of commercial BSA and resulted equivalent to 1  $\mu\text{g}/\mu\text{l}$ .

Finally, LPS were removed through a 5-cycle extraction with Triton X-114 and protein buffer was substituted with pyrogen-free PBS, 20% glycerol through dialysis with a 10 kDa cut-off, to remove any trace of the detergent and to have the protein in an optimal buffer for conservation and for use in *in vitro* assays.

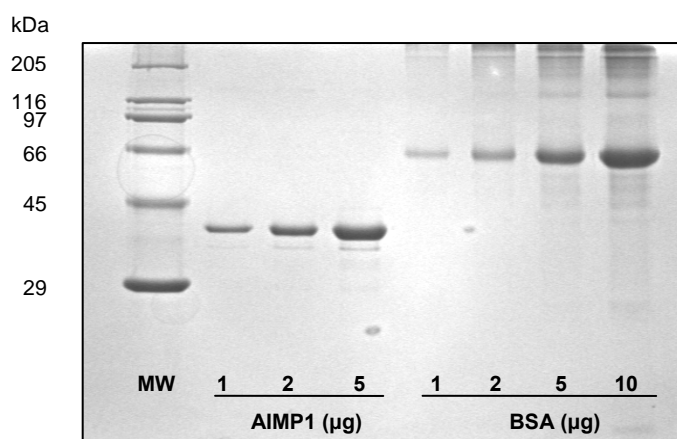


**Fig. 3.3. Recombinant AIMP1 purity is over 98%.** Reducing SDS-PAGE (10% acrylamide/bisacrylamide) to verify the purity of human recombinant AIMP1 in comparison to commercial BSA.

In order to obtain information about the secondary and tertiary structure of rAIMP1, circular dichroism (CD) experiments were performed using a JASCO spectrometer.

CD can be used to study how the secondary and tertiary structure of a molecule changes as a function of temperature. Recombinant AIMP1 circular dichroism spectrum was recorded between 195-250 nm, at temperatures ranging from 20°C to 99°C. A decrease in signal was seen when temperature increased, suggesting a progressive loss of the molecule three-dimensional organization. Notably, a steep decrease in CD signal was observed around 50-70°C, suggesting that denaturation of the protein occurs at temperatures above 50°C (Fig. 3.4).

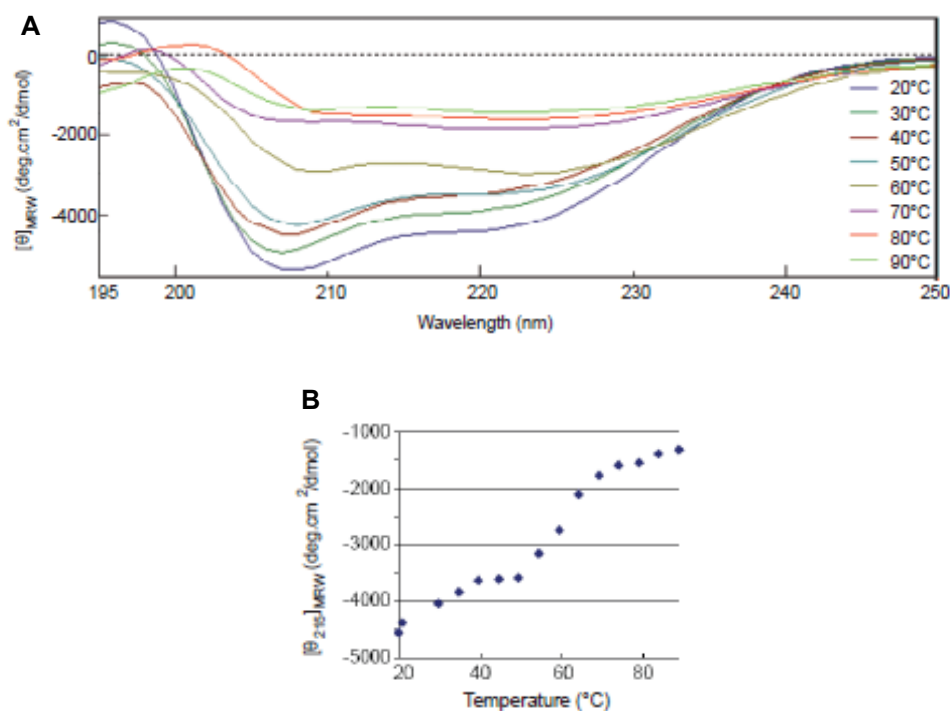


**Fig. 3.4. CD analysis of AIMP1.** **A:** Thermal denaturation of AIMP1. Circular dichroism spectra were recorded for AIMP1 (0.1 mg/ml) between 195 and 250 nm during heating from 20 to 90°C and reported as mean residue ellipticity ( $\theta_{MRW}$ ). Data were plotted for each 10°C interval as indicated in the figure. **B:** Quantification of thermal denaturation of AIMP1. Mean residue ellipticity (deg.cm<sup>2</sup>/dmol) at 215 nm was plotted against temperature.

### 3.2 AIMP1 stability in conditioned cell culture medium

The stability of AIMP1 in conditioned medium was verified. This experiment was performed in order to obtain information about AIMP1 resistance to secreted proteases. 250 nM AIMP1 was incubated at 37°C in conditioned Ham's F-12 medium supplied with 10% FBS. The cultured medium used was taken from a PAEC plate that had been kept in culture for 48 hours. At defined time points 30  $\mu$ l of sample were collected for SDS-PAGE and Western blot analysis. The results showed that a high amount of undegraded AIMP1 is still present after 54 hours of incubation (Fig. 3.5). These data show that, when administered to cells AIMP1 remains in the medium even after 48 hours.

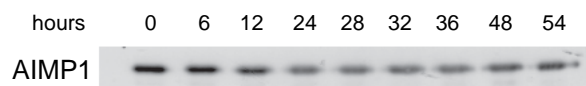


**Fig. 3.5. AIMP1 stability in conditioned medium.** Recombinant AIMP1 was incubated with conditioned Ham's F-12 supplied with 10% FBS at 37°C for the times indicated. The protein was immunoblotted using anti-EMAP II antibody recognizing AIMP1.

### 3.3 Biological assays

In order to understand if the recombinant AIMP1 produced in our laboratory was biologically active, a series of *in vitro* assays were performed on different cell cultures. Among these biological assays, some were carried out in accordance with literature data to confirm the biological activity of the protein, while others provided new information about exogenous AIMP1 biological activity.

#### 3.3.1 AIMP1 has a dose-dependent role on ECs proliferation

AIMP1 is reported to have a dose-dependent role in angiogenesis, inducing endothelial cell migration at low doses and inhibiting endothelial cell survival at high doses (Park *et al.*, 2002c).

To confirm the anti-angiogenic activity of AIMP1 on endothelial cells, the protein was tested at concentrations up to 200 nM on primary BAEC, primary PAEC and on immortalized PAEC in presence of medium containing 10% FBS in viability assays. At 200 nM, the survival inhibition percentage is, respectively, 30%, 28,1% and 41% on primary BAEC, primary PAEC and immortalized PAEC, in comparison to the positive control (Fig. 3.6).

To test whether this activity was dependent on AIMP1 folding state, the recombinant protein was heated for 30 minutes at 99°C before stimulation. The inhibitory effect of AIMP1 was completely reverted when the protein was heat-inactivated, confirming the specificity of the effect (Fig. 3.6) and excluding that the inhibitory effect could be elicited by a contaminant present in the protein solution.

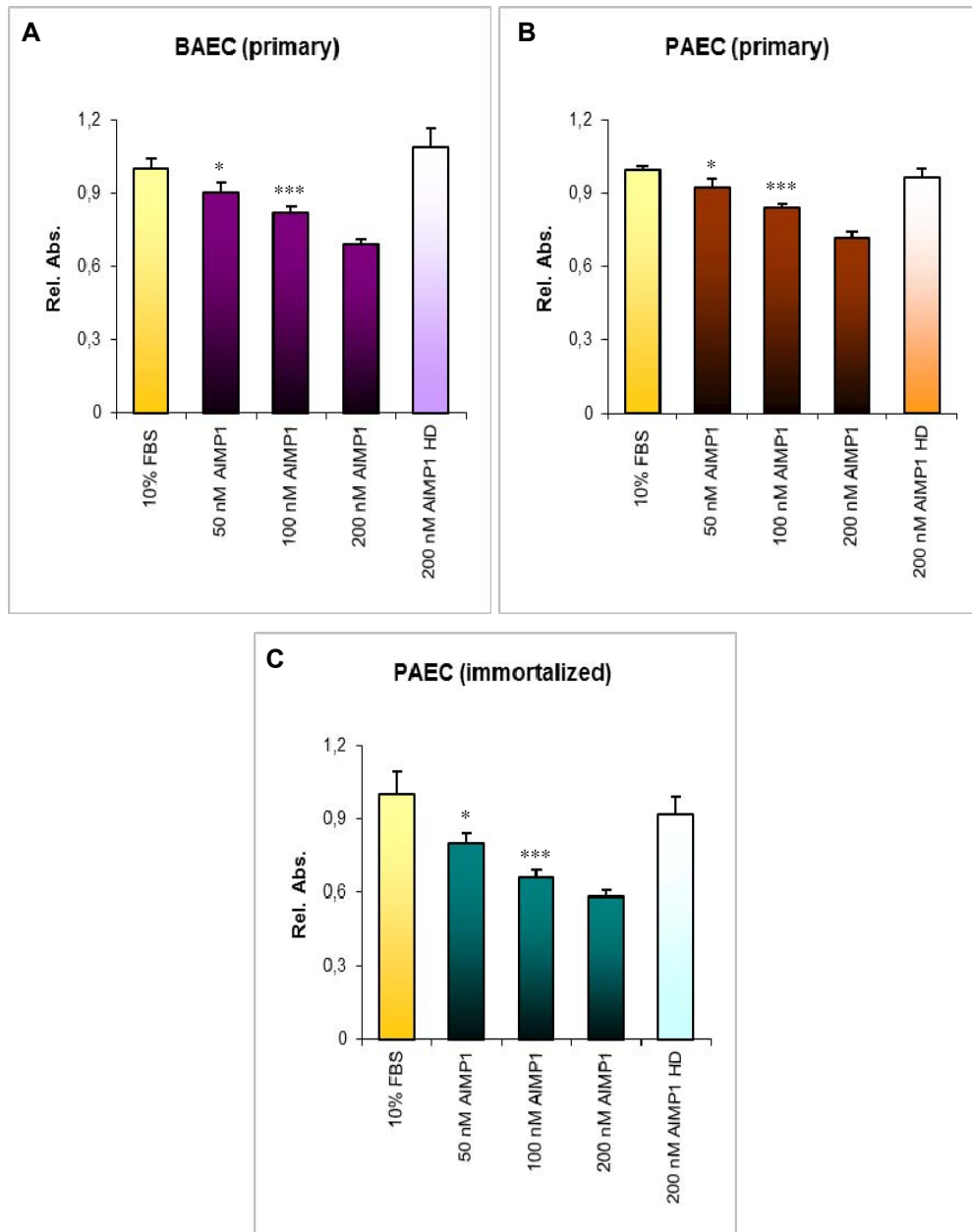


**Fig. 3.6. Viability of BAEC (A), PAEC (B) and immortalized PAEC (C) is inhibited by high concentrations of AIMP1.** Cells were cultured in medium containing 10% FBS in presence of indicated stimuli. After 24 hours, MTT viability assay was performed; AIMP1 HD indicates the heat denaturated protein. \*Statistically significant difference compared with control (\* =  $p < 0.05$ ; \*\*\* =  $p < 0.005$ ).

To assess whether AIMP1 interfered with the proliferative process or the survival, two biological assays were performed in parallel on immortalized PAEC: a proliferation assay based on the measurement on 5-bromo-2'-deoxyuridine (BrDU) incorporation during DNA synthesis in proliferating cells and a viability assay that is based on cellular

conversion of a tetrazolium salt (MTT) into a formazan product by living cells. The results show that AIMP1 does not interfere with the proliferative process (no inhibition in the BrDU assay), but it impairs cell viability (inhibitory effect in the MTT assay) (Fig. 3.7).

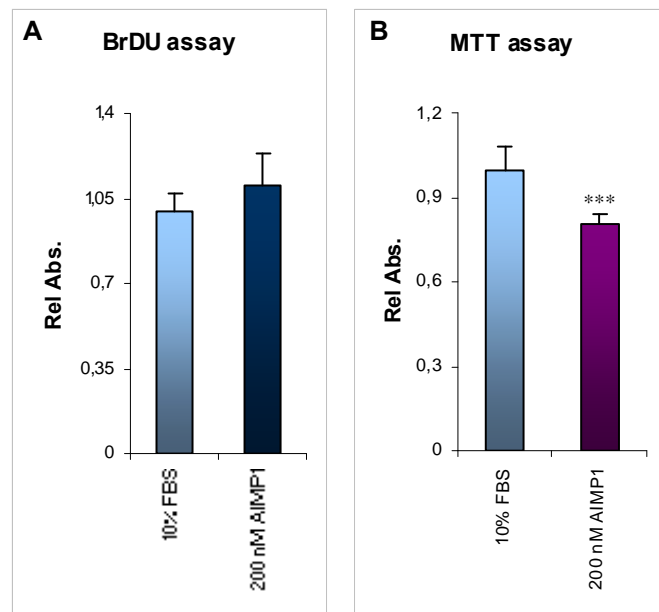


**Fig. 3.7. AIMP1 impairs cell viability but not cell proliferation of PAEC.** Cells were cultured in medium containing 10% FBS and stimulated with 200 nM AIMP1. After 24 hours, BrDU proliferation assay (A) and MTT viability assay (B) were performed. \*Statistically significant difference compared with control (\*\*\*) =  $p < 0.005$ ).

On the other hand, it is known that low concentrations of AIMP1 induce endothelial cell migration (Park *et al.*, 2002c). In this study we tested other possible effects of low doses of AIMP1 on endothelial cells and, in particular, the effects of low concentrations of AIMP1 on endothelial cells survival.

On the basis of the experiments performed, it was observed that low doses of AIMP1 increases endothelial cell viability. AIMP1 was tested on primary BAEC and HUVEC with, respectively, no FBS and 4% FBS containing medium for 24 hours. At a concentration of 1 nM, AIMP1 increases cell viability of about 70% in BAEC and 11% in HUVEC (Fig. 3.8).

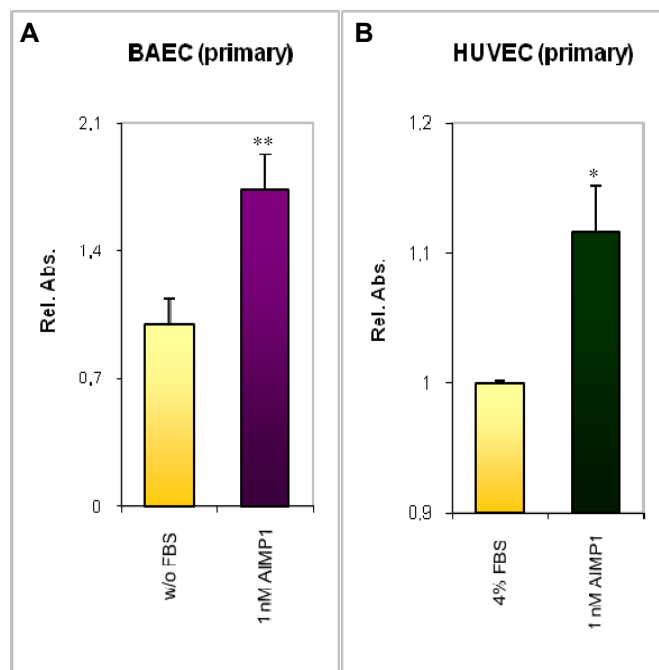


**Fig. 3.8. Viability of BAEC (A) and HUVEC (B) is increased by low concentrations of AIMP1.** Cells were cultured respectively in 0% and 4% FBS containing medium and stimulated with 1nM AIMP1. 24 hours after stimulation MTT viability assay was performed. \*Statistically significant difference compared with control (\* =  $p < 0.05$ ; \*\* =  $p < 0.01$ ).

### ***3.3.2 AIMP1 inhibits ECV tubulogenesis in matrigel***

On the basis of AIMP1 known anti-angiogenic properties (Lee *et al.*, 2006), a tubulogenesis assay was performed to test AIMP1 activity on ECV tubule formation. Cells were seeded in a matrigel three-dimensional matrix in presence of 10 ng/ml of EGF. AIMP1 was added at concentrations of 50, 100 and 200 nM. The quantification of the number of closed areas after 6 hours of culturing showed that at the concentration of 200 nM AIMP1 produces a 22% inhibitory effect on ECV tubulogenesis in matrigel, when induced by EGF (Fig. 3.9).

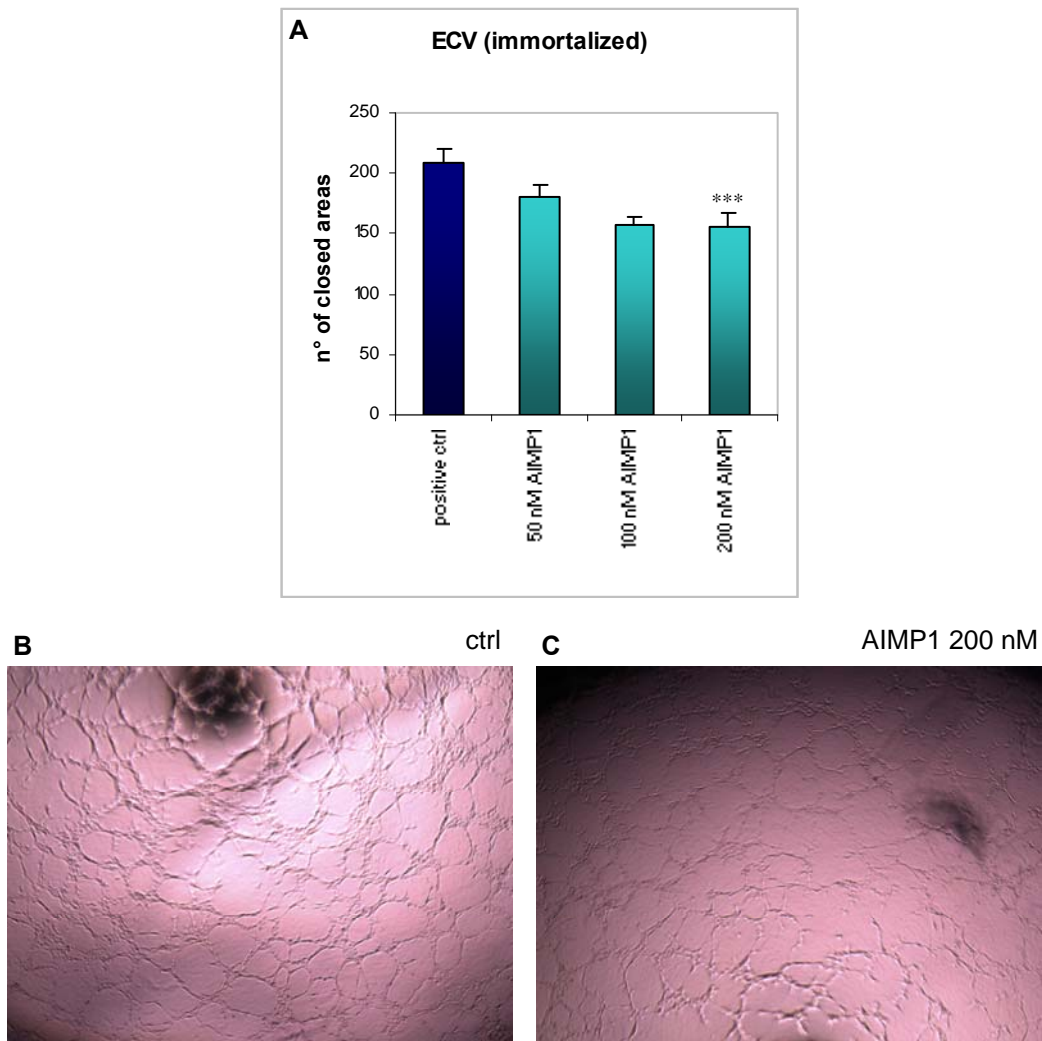


**Fig. 3.9. Tubulogenesis of ECV is inhibited by AIMP1.** **A:** Cells were plated in 0% FBS medium with 10 ng/ml EFG for 6 h in presence of the indicated stimuli. The number of closed areas were counted in triplicate wells. **B** and **C:** magnified pictures (4x magnification) of untreated (ctrl) and AIMP1 treated cells. \*Statistically significant difference compared with control (\*\*\*) =  $p < 0.005$ ).

### 3.3.3 AIMP1 stimulates macrophages migration

EMAP II has been reported to have a chemoattractant role for monocytes/macrophages and granulocytes (Kao *et al.*, 1992). In order to investigate whether also AIMP1 exerted a chemoattractant role towards immune system cells, a range of different concentrations of AIMP1 (from 1nM to 500 nM) was tested on RAW 264.7 mouse macrophages to verify its ability to stimulate their migration. Upon a 4 hour treatment, AIMP1 stimulated macrophages migration with a dose-dependent response. At the concentration of 500 nM,

AIMP1 more than triplicates macrophage migration rate in comparison to the negative control (Fig. 3.10).

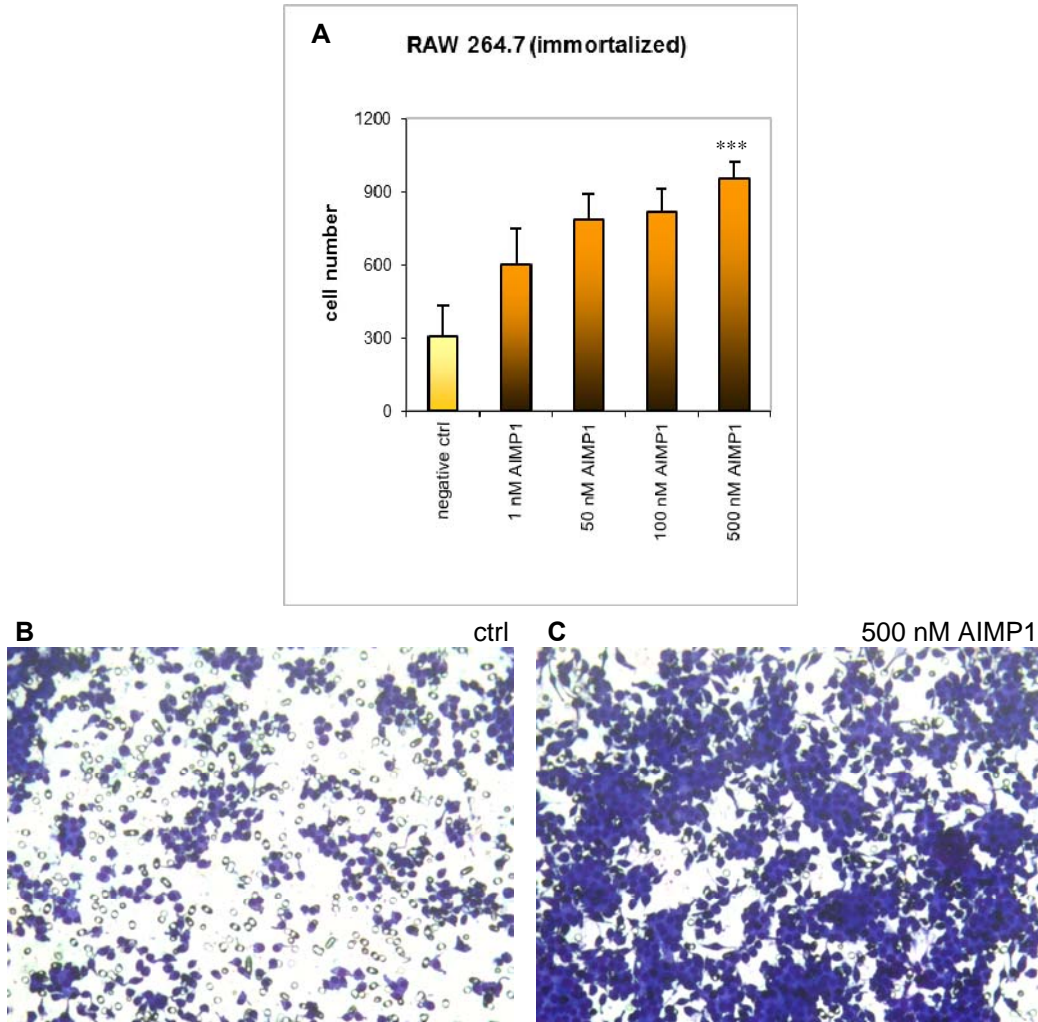


**Fig. 3.10. Migration of RAW 264.7 is increased upon AIMP1 treatment.** **A:** Cells were plated in 0% FBS medium for 4 h in presence of the indicated stimuli. The migrated cells from three experiments were counted. **B** and **C** are magnified pictures (4x magnification) of untreated (ctrl) and AIMP1 treated migrated cells. \*Statistically significant difference compared with control (\*\*\*) =  $p < 0.005$ ).

At this point the immortalized PAE cell line was selected as a model to investigate the cellular mechanisms and the signalling pathways activated by exogenous AIMP1 and to identify new cellular interactors of AIMP1 in endothelial cells.

This model was selected because treatment of immortalized PAEC with exogenous AIMP1 leads to strong and reproducible cellular effects and because these cells are easier to manage than primary cell lines.

### 3.4 AIMP1 inhibitory effect on PAEC viability is reverted by pre-treatment with anti- $\alpha 5\beta 1$ integrin antibody

In order to try to identify the receptor responsible for the transduction of exogenous AIMP1 signal inside the cell, we focused our attention on  $\alpha 5\beta 1$  integrin. This because  $\alpha 5\beta 1$  integrin has been shown to bind EMAP II on MEC (microvascular endothelial cells) (Schwarz *et al.*, 2005). We hypothesized that this receptor could also have a role in the anti-angiogenic effect exerted by AIMP1 on PAEC. To verify this hypothesis an MTT viability assay was performed incubating the cells with anti- $\alpha 5\beta 1$  integrin antibody before incubation with AIMP1, in order to block the receptor activity before stimulating the cells. Indeed, pre-treatment of PAEC with the anti- $\alpha 5\beta 1$  integrin antibody is able to revert AIMP1 inhibitory effect on PAEC survival (Fig. 3.11).

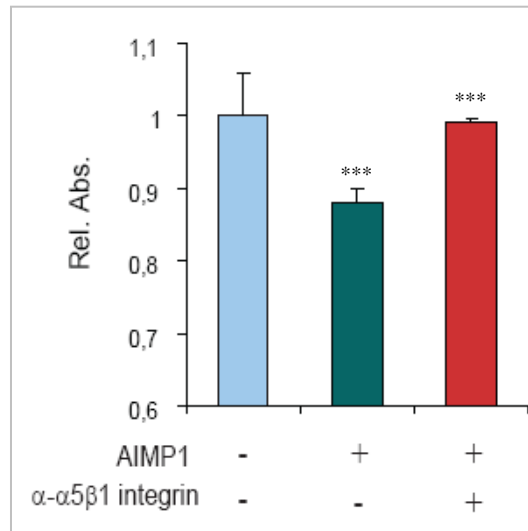


**Fig. 3.11. Pre-treatment of cells with anti- $\alpha 5\beta 1$  integrin antibody reverts AIMP1 inhibitory effect on survival.** Cells were incubated with anti- $\alpha 5\beta 1$  integrin antibody (0.8  $\mu$ M) before treatment with AIMP1 (100 nM). MTT assay was performed after 24 hours. Data represent mean  $\pm$  SD. Graphics report relative absorbance values normalized to vehicle (ctrl). \*Statistically significant difference compared with control (\*\*\*) =  $p < 0.005$ ).

### 3.5 AIMP1 inhibits cell adhesion on fibronectin

On the basis of the experimental results obtained through the viability assays, in addition to literature describing EMAP II inhibitory effect on MEC adhesion through a direct interaction between EMAP II and  $\alpha 5\beta 1$  integrin (Schwarz *et al.*, 2005), the hypothesis of an inhibitory effect elicited by AIMP1 on PAEC adhesion was investigated. To do this, a cell adhesion assay was performed: cells were treated with 100 nM AIMP1 or vehicle, plated on fibronectin pre-coated plates and let to adhere for 20 minutes. The fibronectin coating was chosen on the basis of data demonstrating that integrin is the receptor for fibronectin during angiogenesis (Kim *et al.*, 2000a).

Measurement of absorbance values after crystal violet staining showed that AIMP1 inhibits cell adhesion on fibronectin (Fig. 3.12). These results show that, as was previously demonstrated for EMAP II (Schwarz *et al.*, 2005), also AIMP1 is able to interfere with the process involved in endothelial cell adhesion on fibronectin.

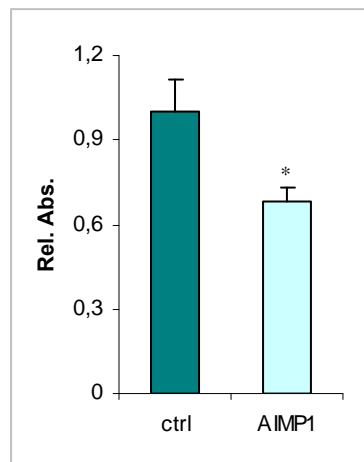


**Fig. 3.12. AIMP1 inhibits PAEC adhesion on fibronectin.** Cells were treated with 100 nM AIMP1 and plated on fibronectin pre-coated plates. After 20 minutes, cells were fixed and stained with crystal violet. Absorbance values (595 nm) represent mean  $\pm$  SD. Graphics report relative absorbance values normalized to vehicle (ctrl). \*Statistically significant difference compared with control (\* =  $p < 0.05$ ).

### 3.6 Subcellular localization of exogenous AIMP1 in PAEC

Since one of the objectives of this study was to identify new AIMP1 interactors, it was important to obtain information about exogenous AIMP1 subcellular localization in PAEC. These data were fundamental in order to understand which were the subcellular fractions to be analysed for the “fishing” of AIMP1-interacting molecules.

For this purpose, immunofluorescence experiments were performed on PAEC to analyse exogenous AIMP1 subcellular localization.

PAEC were treated with 50 nM AIMP1 in time course experiments from 15 minutes to 24 hours. The stainings performed in this phase were the following: exogenous AIMP1 was stained, using the anti-myc antibody, to analyse its subcellular localization; actin and the nucleus were stained using, respectively, phalloidin and propidium iodide to have precise cell structure references of the cytoplasm and the nucleus.

Exogenous AIMP1 was previously demonstrated to be internalized almost immediately after cellular incubation (Yi *et al.*, 2005) and this *datum* was confirmed in this work using immunofluorescence technique. As soon as 30 minutes after AIMP1 treatment, the exogenous protein enters the cell, but does not enter the nucleus: this was indicated by collection of confocal optical sections at 0.5  $\mu\text{m}$  intervals throughout the cells. AIMP1 localization inside the cell or on the cell membrane does not occur when the protein is heat inactivated for 30 minutes at 99°C before stimulation (Fig. 3.13).

Interestingly, AIMP1 distribution appears to be asymmetrical and, furthermore, it seems to be localized at the level of the cell protrusions (Fig. 3.14). The observation that exogenous AIMP1 does not distribute in an homogeneous way throughout the cell and the cell membrane, together with the experimental results on AIMP1 effect on endothelial cell adhesion, lead us to hypothesize that AIMP1 may interact with or activate cytoskeletal or cytoskeleton-associated proteins, thus affecting cellular architecture remodelling and the adhesion process.

In long term stimulations, after 6 and 24 hours, AIMP1 accumulates in clots under the cell membrane (Fig. 3.15). This particular distribution pattern could represent an expulsion mechanism carried out by phagosomes or liposomes, but would need a deeper

investigation to be understood.

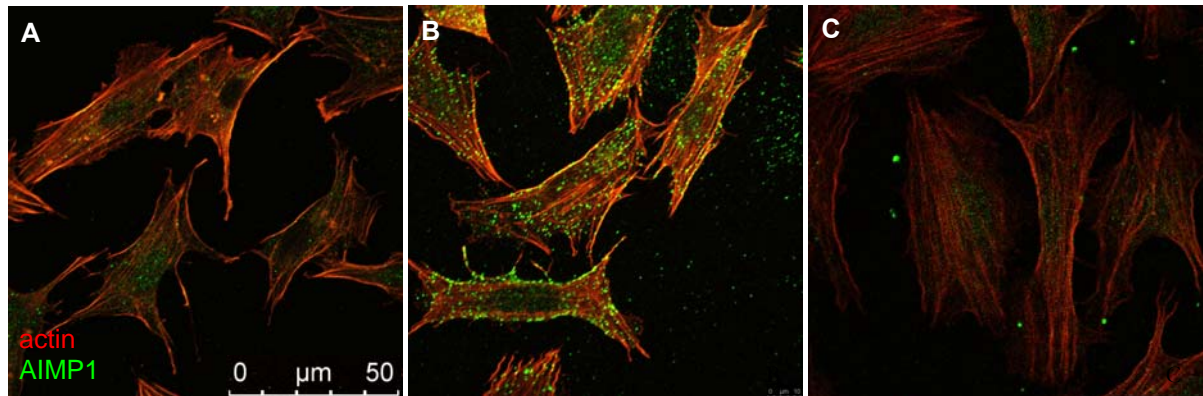


**Fig. 3.13. Exogenous AIMP1 subcellular localization.** PAEC were treated with 100 nM AIMP1 for 1 hour. After treatment cells were fixed and stained. Actin was stained in red (phalloidin) and AIMP1 in green (anti-myc antibody). **A:** untreated cells, **B:** 1h AIMP1 treated cells and **C:** 1h heat denaturated AIMP1 treated cells. AIMP1 does not bind the cells when heat inactivated before treatment.

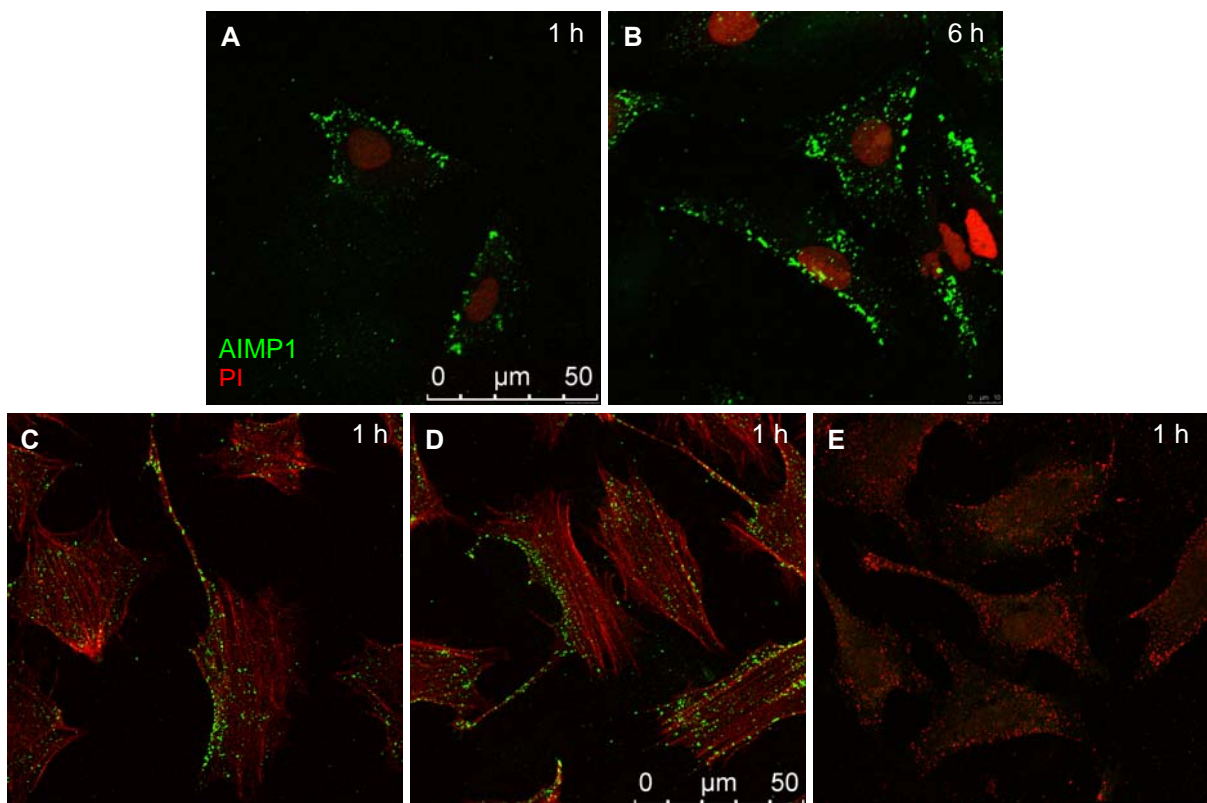


**Fig. 3.14. Exogenous AIMP1 subcellular localization is asymmetrical and it concentrates at the cell protrusions.** After treatment cells were fixed and stained. AIMP1 subcellular localization is asymmetrical (**A** and **B**) and it accumulates at the level of cell protrusions (**C-E**). In **A** and **B** the nucleus was stained in red (PI) and AIMP1 in green (anti-myc antibody). In **C** and **D** actin was stained in red (phalloidin) and AIMP1 in green (anti-myc antibody). In **E** AIMP1 was stained in red (anti-myc antibody).

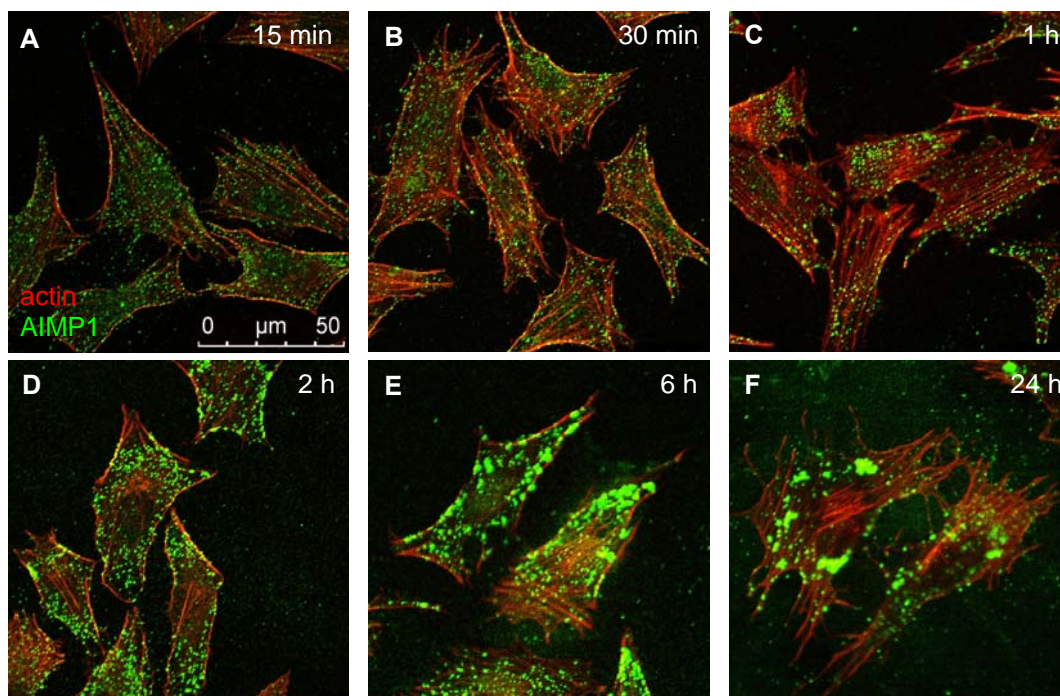


**Fig. 3.15. Exogenous AIMP1 subcellular localization in a time course experiment.** Time course treatment of PAEC with 100 nM AIMP1 from 15 minutes (A) to 24 hours (F). After treatment cells were fixed and stained. Actin was stained in red (phalloidin) and AIMP1 in green (anti-myc antibody).

### **3.7 AIMP1 treatment of PAEC activates ERK and JNK, but not AKT**

In the biological assays, AIMP1 showed an inhibitory activity on endothelial cell viability and adhesion at high concentrations. On the basis of these data, in order to investigate the signalling pathways activated in PAEC, Western blot analysis was performed to identify some of the molecules activated upon high concentrations of AIMP1 treatment. On the basis of the experimental results which show that AIMP1 activity on PAEC could be mediated by a membrane receptor ( $\alpha 5\beta 1$  integrin), we decided to investigate the possible activation of phosphorylated proteins.

As a first step the activation of a small group of kinases was analysed during a time course experiment of PAEC stimulation with AIMP1.

This group included AKT, a protein involved in cellular survival pathways by inhibiting apoptotic processes; JNK, which is involved in apoptosis, cell differentiation and

proliferation and ERK, involved in functions including the regulation of meiosis, mitosis, post-mitotic functions in differentiated cells and in a great variety of signalling transduction pathways activated by extracellular molecules.

Cells were treated with AIMP1 at a concentration of 200 nM in time course experiments, with 6 time points from 0 to 180 minutes (Fig. 3.16). AIMP1 induces activation of ERK and JNK through phosphorylation after a 10 minute treatment of PAEC, but it does not regulate AKT expression.

In order to confirm that the effect observed was due to AIMP1 activity and not to the cells manipulation, an experiment was performed treating PAEC for 10 minutes with AIMP1 or with vehicle. This last experiment confirmed a very rapid activation of ERK and JNK, and no regulation of AKT, after stimulation of PAEC with AIMP1 (Fig. 3.17).

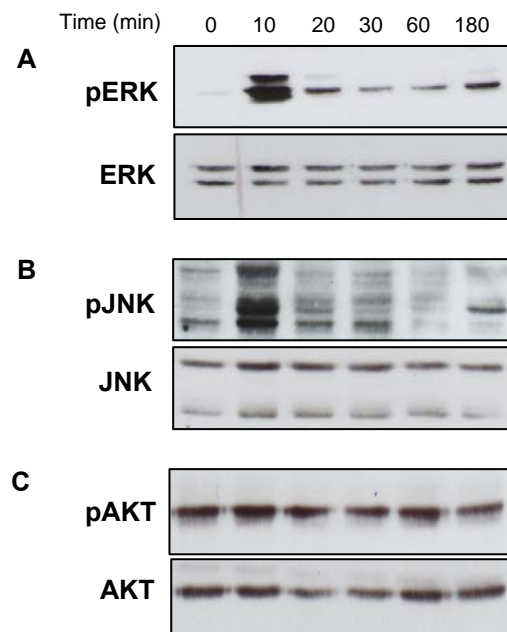


**Fig. 3.16. AIMP1 activates ERK and JNK but not AKT in PAEC.** Western blot analysis of a time course treatment of PAEC with AIMP1. Cells were treated with 200 nM AIMP1 for 0 to 180 minutes. Membranes were blotted with anti-pERK (**A**), anti-pJNK (**B**) and anti-pAKT (**C**) antibodies and normalized to total ERK, JNK and AKT proteins respectively.

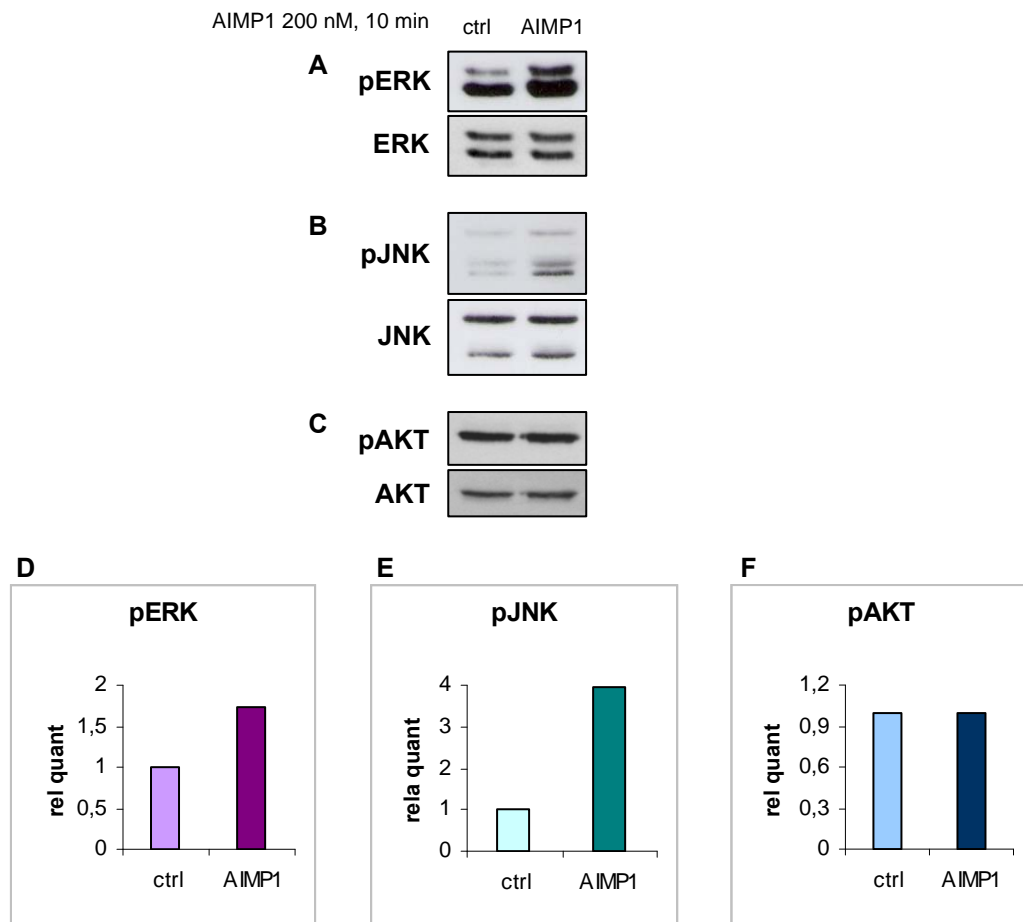


**Fig. 3.17. AIMP1 activates ERK and JNK but not AKT in PAEC.** Western blot analysis of PAEC treated with 200 nM AIMP1 for 10 minutes. Control samples were treated with vehicle (PBS 20% glycerol). Membranes were blotted with anti-pERK (A), anti-pJNK (B) or anti-pAKT (C) antibodies and normalized to total ERK, JNK and AKT proteins, respectively. The relative quantification is shown in the histograms below (D, E and F).

The activation of ERK through phosphorylation after a 10 minute treatment of PAEC with 200 nM AIMP1 was confirmed performing a Western blot analysis on a two-dimensional gel (Fig. 3.18). Indeed spot intensity of pERK in treated cells is 1.4 times higher respect to the control (total ERK was used for normalization).

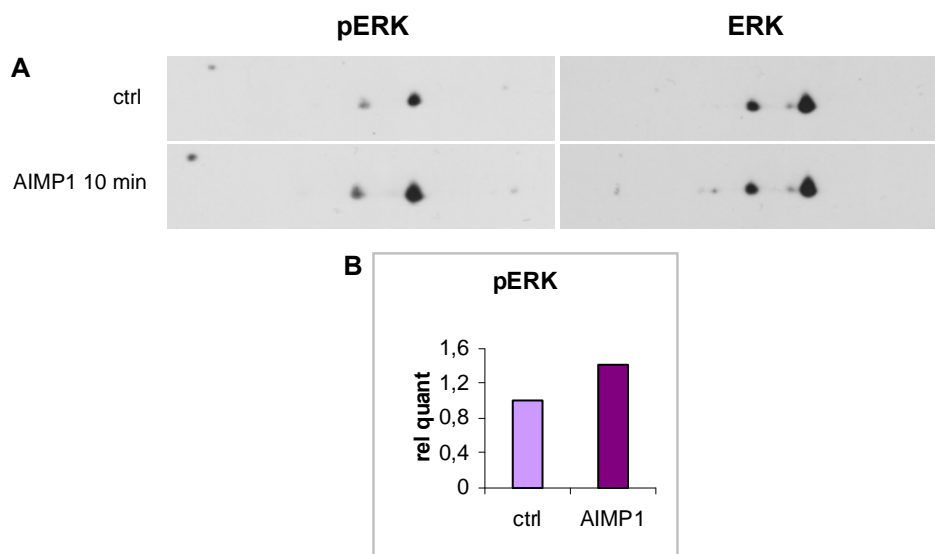


**Fig. 3.18. AIMP1 activates ERK in PAEC.** 2DE-Western blot analysis on PAEC treated with 200 nM AIMP1 for 10 minutes. Control samples were treated with the vehicle (PBS, 20% glycerol). **A:** Membranes were blotted with anti-pERK and normalized to total ERK. The different spots indicate different phosphorylation degrees of ERK. The relative quantification is shown in the histogram **(B)**.

### 3.8 Affinity purification of AIMP1-binding molecules

On the basis of the information obtained by the immunofluorescence experiments about exogenous AIMP1 subcellular localization, two PAEC subcellular fractions were analysed to search for AIMP1-interacting molecules: the cytosolic and the membrane fraction. Figure 3.19 shows an SDS-PAGE on which the two subcellular fractions were loaded, showing distinct protein patterns.

The subcellular fractions were incubated with AIMP1 and affinity purification of AIMP1-binding molecules was performed using a Ni-Sepharose resin in order to precipitate the recombinant protein together with its interactors. In the control sample the vehicle (PBS, 20% glycerol) was used instead of AIMP1, in order to discard the proteins aspecifically interacting with the resin. Samples obtained by affinity purification were loaded on SDS-PAGE and differential bands between control samples and AIMP1 samples were identified and excised (Fig. 3.20). Identification of the bands was performed through MS/MS spectrometry analysis.

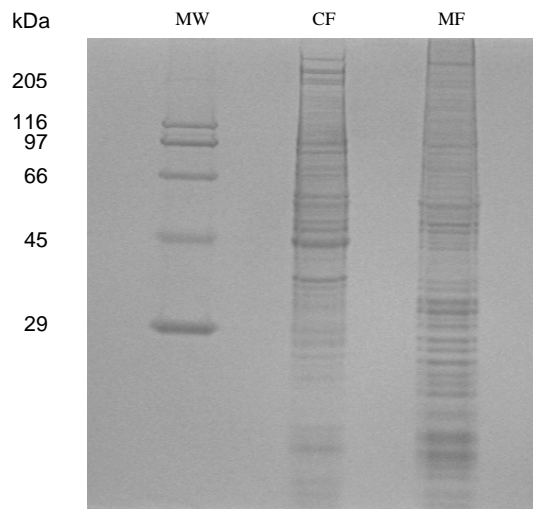


**Fig. 3.19. SDS-PAGE of the two protein fractions obtained by the subcellular fractionation of PAEC.** Reducing SDS-PAGE (10% acrylamide/bisacrylamide). MW: molecular weight, CF: cytosolic fraction, MF: membrane fractions.

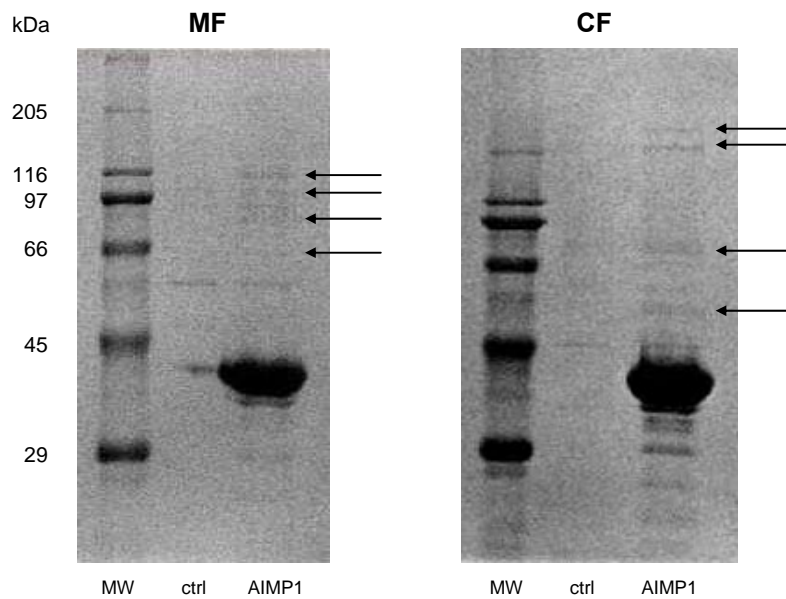


**Fig. 3.20. Affinity purification of AIMP1-interacting molecules.** Reducing SDS-PAGE (10% acrylamide/bisacrylamide) stained in Coomassie Brilliant Blue of two representative experiments performed with the membrane fraction (MF, on the left) or the cytosolic fraction (CF, on the right). MW: molecular weight. The black arrows indicate the differential bands between AIMP1 functionalized resin and control. In both images, the huge band at 34 kDa is the recombinant AIMP1 incubated with the subcellular fractions.

Table 3.1 reports the putative AIMP1-interacting proteins identified in membrane and cytosolic fractions. Other proteins were found, including glycyl-tRNA synthetase and coatomer subunit beta protein ( $\beta$ -cop), the interaction of which with AIMP1 has already been described (Han *et al.*, 2007) (data not shown). Interestingly, 6 of the identified proteins were cytoskeletal or cytoskeleton-associated proteins which are involved in cellular architecture maintenance and remodelling.

Fr	LC-MS/MS identification	Accession number	Peptide number	Seq cov (%)	Score
CF	filamin-A	gi116241365	34	32%	1791
	GRP78	gi14916993	23	28%	1058
	vimentin	gi76097691	13	41%	695
	$\alpha$ -tubulin	gi81174755	4	11%	313
	glycogen phosphorylase	gi106073338	6	7%	213
MF	cingulin	gi194036221	4	3%	67
	vinculin	gi50403675	3	3%	59
	ras GTPase-activating-like protein (IQGAP3)	gi229462887	2	2%	59
	protocadherin-11 X-linked	gi75071591	2	2%	57
	rho GTPase-activating protein 29 (ARHGAP29)	gi194036908	2	2%	52

**Table 3.1. AIMP1-interacting proteins obtained by affinity purification.** First column indicates the subcellular fraction in which the protein was found, second and third column report the name of the identified protein and its gi accession number; the table also shows the number of peptides recognized by Mascot algorithm and the percentage of sequence coverage; hits with a probability-based MOWSE score higher than 47 were considered significant ( $p < 0.05$ ).

### 3.9 Validation of putative AIMP1-interacting proteins through pull-down and co-immunoprecipitation

In order to validate the data obtained by the affinity purification, pull-down and co-immunoprecipitation experiments were performed. The use of these two techniques confirmed AIMP1 interaction with cingulin, filamin-A,  $\alpha$ -tubulin, vinculin, GRP78 and PYG (Fig. 3.21).

However, using these experimental procedures, no information could be obtained about the interaction of AIMP1 with these proteins being direct or indirect. Therefore, it is possible that a complex of more than two proteins is formed.

Among the cytoskeletal and cytoskeleton-associated proteins, the interaction with 4 out of 6 proteins was confirmed. This result strengthens the hypothesis of an involvement of proteins implied in cellular architecture maintenance and remodelling in AIMP1 activity on PAEC.

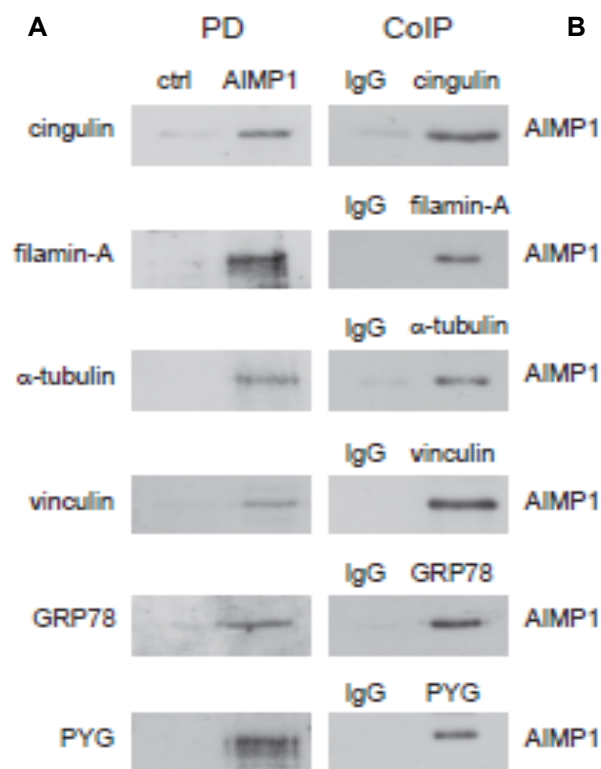


**Fig. 3.21. Validation of AIMP1-putative interactors.** **A: Pull-down assay.** Subcellular fractions (membrane fraction or cytosolic fraction) were incubated with AIMP1 or vehicle and precipitated by nickel affinity. Cingulin, filamin-A,  $\alpha$ -tubulin, vinculin, GRP78 and PYG were immunoblotted with the respective antibodies. **B: Co-immunoprecipitation assay.** Subcellular fractions were incubated with AIMP1 and immunoprecipitated with anti-cingulin, anti-filamin-A, anti- $\alpha$ -tubulin, anti-vinculin, anti-GRP78 and anti-PYG antibodies or control IgG. Precipitated proteins were immunoblotted with anti-his-probe antibody recognizing recombinant AIMP1.

### 3.10 AIMP1 co-localizes with cingulin and filamin-A in endothelial cells

To see whether AIMP1 co-localized in the cell or at the cell membrane with the AIMP1-interacting proteins previously identified or with  $\alpha 5\beta 1$  integrin, immunofluorescence double-staining experiments were performed. This technique allowed us to have an overview of these interactions in physiologic conditions. After a 1 hour treatment of subconfluent PAEC with 50 nM AIMP1, co-localization was observed between AIMP1 and cingulin and between AIMP1 and filamin-A (Fig. 3.22), but no co-localization was observed between AIMP1 and vinculin,  $\alpha$ -tubulin, GRP78, PYG or  $\alpha 5\beta 1$  integrin (data not shown).

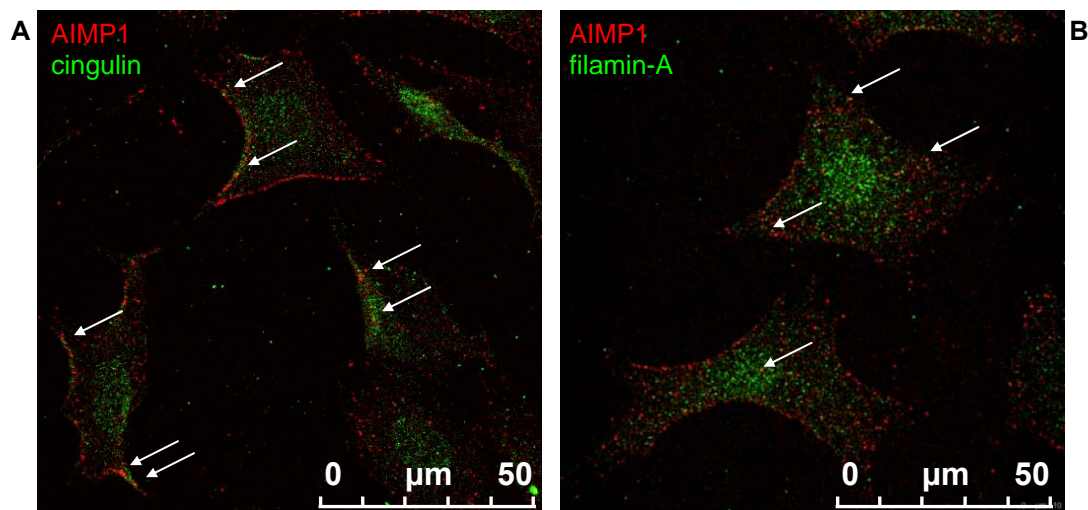


**Fig. 3.22. AIMP1 co-localizes with cingulin and filamin-A in the cells.** Cells were treated with 100 nM AIMP1 for 1 hour. After treatment cells were fixed and immunostained. AIMP1 was stained in red (anti-myc antibody), cingulin and filamin-A were stained in green. **A:** Merge between  $\alpha$ -cingulin (green) and anti-myc (red) staining. **B:** Merge between anti-filamin-A (green) and anti-myc (red) staining. The co-localization positions are indicated by the arrows.

### 3.11 AIMP1 treatment induces phosphorylation of $\alpha$ -tubulin, EF-1 $\delta$ and RPLP2

To get a deeper insight in the signalling pathway activated by exogenous AIMP1 in PAEC, we further investigated the phosphorylation events upon AIMP1 treatment through a 2-DE phosphoproteomic approach. This technique allows to have an overview of the whole phosphoproteome in definite experimental conditions. PAEC were treated with 200 nM of AIMP1 or vehicle for 10 and 30 minutes.

Each 2-DE gel was stained subsequently with 3 different dyes: gels were first stained with ProQ Diamond fluorescent stain for phosphorylated proteins, then with Sypro Ruby fluorescent stain for total proteins and, finally, with Coomassie Brilliant Blue for MS/MS analysis (Fig. 3.23).

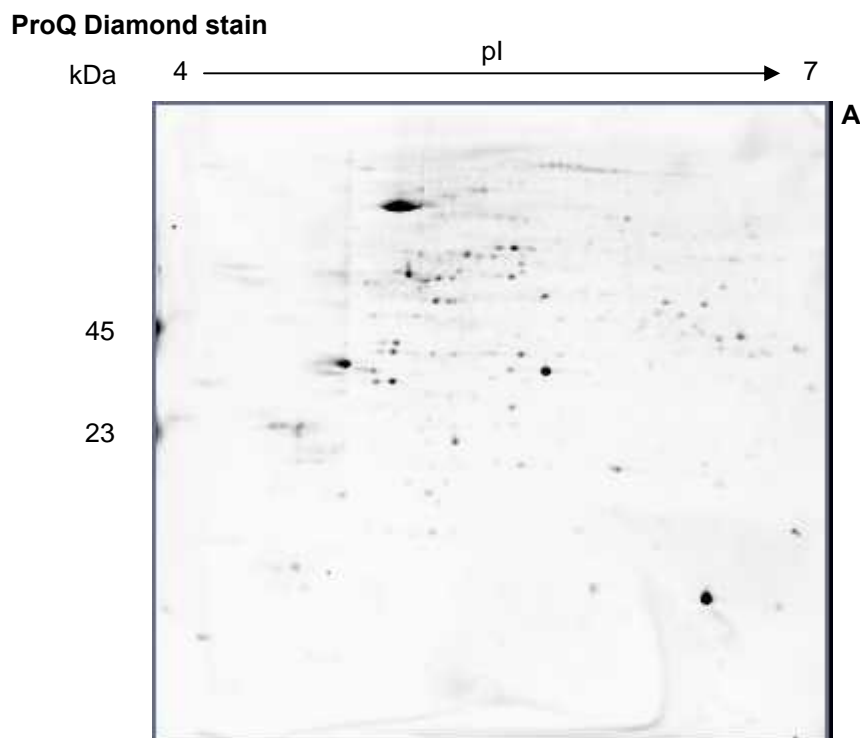
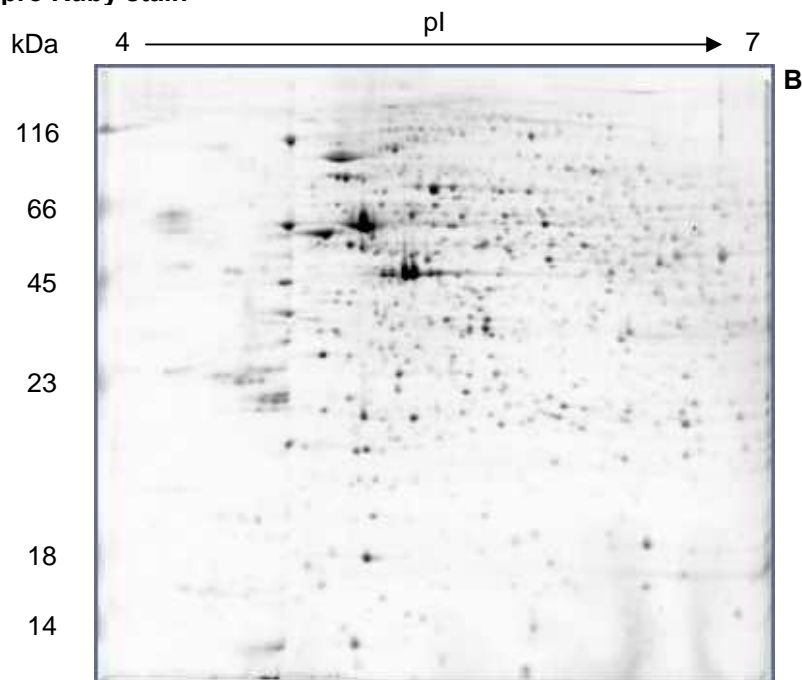
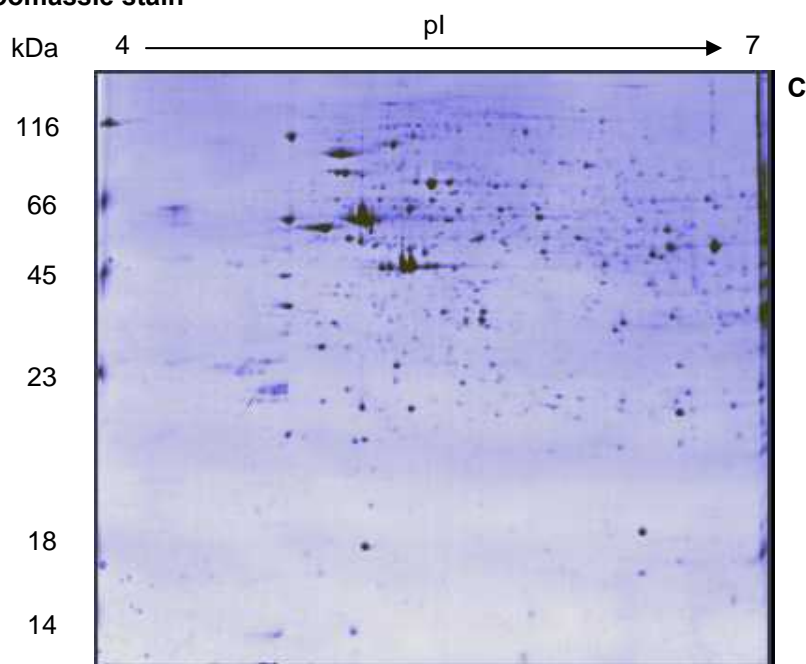


Fig. 3.23. Example of a single 2-DE gel stained with 3 different dyes. Continues.

**Sypro Ruby stain**



**Coomassie stain**



**Fig. 3.23.** Example of a single 2-DE gel stained with 3 different dyes. **A:** ProQ Diamond staining, **B:** Sypro Ruby staining and **C:** Coomassie Brilliant Blue staining. On the x-axis proteins are separate on the basis of their pI (pI gradient from 4 to 7). On the y-axis proteins are separated on the basis of their molecular weight. The numbers on the left side of the gels indicate the weight in kDa of the MW marker (only two proteins of the MW are detectable with the ProQ Diamond staining).

About 1200 protein spots were detected by the SYPRO Ruby stain and about 120 spots were visualized by the phosphoprotein-specific stain. For each treatment (AIMP1 10 min, control 10 min, AIMP1 30 min and control 30 min) a set of 4 gels was stained with ProQ Diamond followed by Sypro Ruby, imaged and analyzed as described in the Methods section. The spots which significantly varied among treated samples and controls were excised and identified by LC-MS/MS. For both time points no qualitative differences were highlighted. As regards the qualitative differences, no significant spots were identified upon 30 minute treatment. The proteins which resulted differentially phosphorylated between treated cells and controls upon 10 minute treatment in all the four experiments were  $\alpha$ -tubulin, elongation factor 1 $\delta$  (EF-1 $\delta$ ) and 60S acidic ribosomal protein P2 (RPLP2) (table 3.2 and figure 3.24).

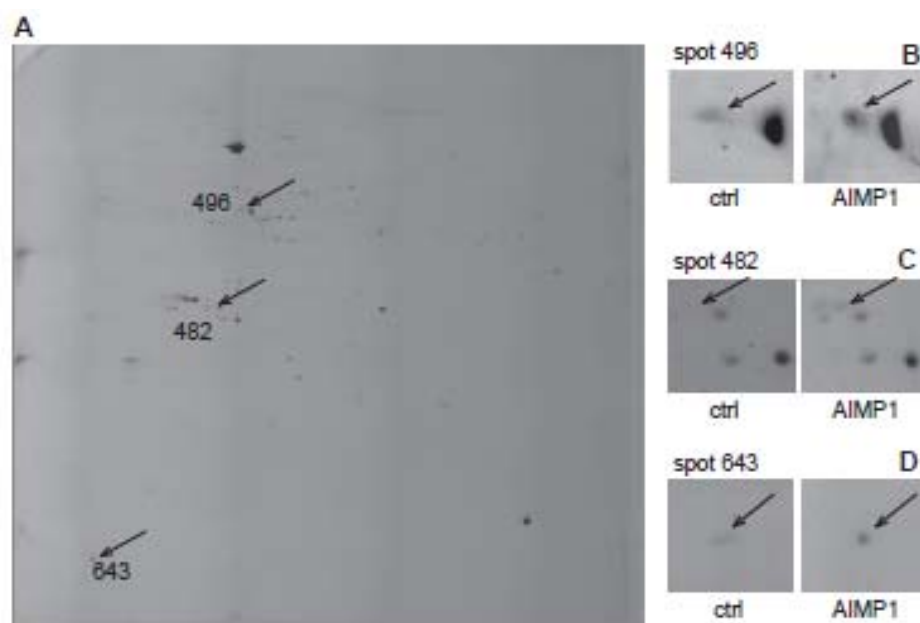


**Fig. 3.24. The phosphorylation of  $\alpha$ -tubulin, elongation factor 1 $\delta$  and 60S acidic ribosomal protein P2 is up-regulated upon 10 minute AIMP1 treatment of PAEC.** Cells were treated with 200 nM AIMP1 for 10 minutes. After treatment cells were lysed, protein were extracted and 2D-gels were run as described in the Methods section. Gels were stained with ProQ Diamond. **A.** ProQ Diamond stained gel of a representative experiment. Spots that showed a significant change in volume percentage are indicated by the arrows and identified by the spot number. **B, C** and **D** are single spot magnifications of ProQ Diamond stained gels from control (vehicle) and treated samples (spots of interest are indicated by the arrows).

Spot num	Change-fold	LC-MS/MS identification	Accession number	Peptide number	Seq cov (%)	Apparent pI/MW	Theoretical pI/MW	Mascot score
496	↑ 1.8	$\alpha$ -tubulin	gi81174755	18	42%	~5/~50 kDa	4.86/50 kDa	589
482	↑ 2.6	elongation factor 1 $\delta$	gi172047287	15	32%	~5/~30 kDa	4.94/30 kDa	564
643	↑ 2.1	60S acidic ribosomal protein P2	gi3914781	4	21%	~4.5/~12 kDa	4.42/11.6 kDa	218

**Table 3.2. Phosphorylated proteins upon 10 minute AIMP1 treatment of PAEC.** Cells were treated with 200 nM AIMP1 for 10 minutes. After treatment cells were lysed, protein were extracted and 2D gels were run as described in the Methods section. Gels were stained, subsequently, with ProQ Diamond, SyproRuby and Coomassie staining. Image analysis and spot quantification was carried out as described in the Methods section. The spot number corresponding to each identified protein is indicated in the first column. Change fold values indicate the mean obtained from at least three experiments (↑: up-regulated in AIMP1 samples). Name of identified protein and gi accession number are shown in the third and fourth columns. The sequence of elongation factor 1 $\delta$  is not present in the *Sus scrofa* database, thus we accepted the identification for *Bos taurus*. The table also shows the number of peptides recognized by Mascot algorithm and the percentage of sequence coverage; hits with a probability-based MOWSE score higher than 47 were considered significant ( $p < 0.05$ ). Apparent pI and MW are obtained from the 2DE gel, theoretical pI and MW are obtained from Mascot database.

### 3.12 AIMP1 treatment regulates gene expression in PAEC

As a last investigative field, the effect of AIMP1 on the transcriptional regulation of some genes was determined. The set of genes to be analysed was chosen either on the basis of literature data reporting a correlation between gene transcriptional regulation and AIMP1 treatment or on the basis of the role of a specific protein in processes important in the frame of our study (adhesion, angiogenesis). The analysed genes were: VEGFA, VEGFR1, VEGFR2, MMP2, MMP9, ICAM1, COL1a2, CCNG2, TNFAIP3, KLF4, BIRC3 (18S was used as normaliser).

Cells were serum starved for 16 hours, then stimulated with different concentrations of AIMP1 in time course experiments. The experimental conditions were identical for all the genes (a time course experiment was carried out from 1 to 24 hours, stimulating the cells with 100 nM AIMP1) apart from MMP2 and MMP9 (in this case the cells were treated with different concentration of AIMP1 -1, 10, 100 nM- for 1 hour and 24 hours). After treatment cells were lysed, RNA was extracted, quantified and retrotranscribed, Real Time PCR was performed

Relative quantification of the expression level of these genes indicated that, in the tested conditions, AIMP1 treatment regulates the expression of VEGFA, VEGFR2, MMP2 and

MMP9. AIMP1 up-regulates VEGFA and VEGFR2 transcripts at a concentration of 100 nM after a two-hour treatment. Instead, transcription of MMP2 is induced after 24-hour treatment with 10 nM AIMP1 and MMP9 expression is up-regulated upon 1 hour treatment with 10 nM AIMP1 and 24 hour treatment with 1nM AIMP1 (Fig. 3.25).

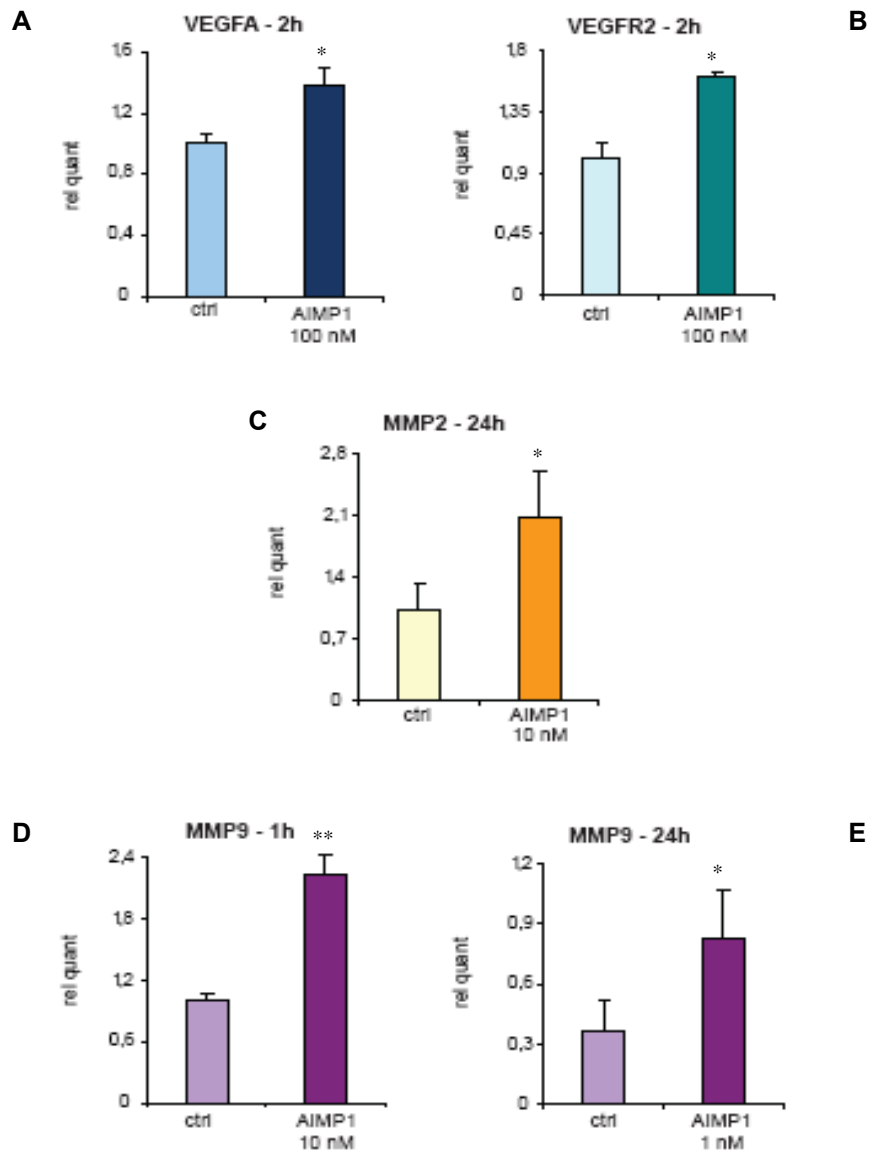


**Fig. 3.25. Real Time analysis of gene transcription regulation upon AIMP1 treatment.** Cells were treated with the indicated concentrations of AIMP1 or vehicle (as a control) for the indicated times. After treatment cells were lysed, RNA was extracted, quantified and retrotranscribed, Real Time PCR was performed. Relative quantification was performed by second derivative analysis and the DDCT calculation method. Control **A** and **B**: VEGF and VEGFR2 transcription is up-regulated after 2 hours of 100 nM AIMP1 treatment. **C**: MMP2 expression is up-regulated after 24 hours of 10 nM AIMP1 treatment. **D**: MMP9 expression is up-regulated after 1hour of 10nM AIMP1 treatment. **E**: MMP9 expression is up-regulated after 24 hours of 1nM AIMP1 treatment. \*Statistically significant difference compared with control (\* =  $p < 0.05$ ; \*\* =  $p < 0.01$ ).

In the described experiments the transcriptional regulation of a set of genes upon AIMP1 treatment of PAEC was investigated through Real Time PCR analysis. Nearly all of the tested genes were reported in previous studies to be regulated in endothelial or immune cells following different conditions of AIMP1 treatment. While VEGFR1, ICAM1, COL1a2, CCNG2, TNFAIP3, KLF4, BIRC3 were not upregulated under our experimental conditions, VEGFA and VEGFR2 were up-regulated at 2 hours, MMP2 was up-regulated at 24 hours and MMP9 was up-regulated at 1 hour and 24 hours.

## 4. Discussion

### 4.1 Production, purification, conformation and stability of recombinant AIMP1

The method used for production and purification of human recombinant AIMP1 lead to a highly pure and biologically active protein. The choice of the pBAD/Myc/HisA vector was taken in order to obtain a tagged protein, so that the recombinant exogenous protein could be distinguished from the endogenous one. The C-terminal position of the His-tag ensured that the protein purified with affinity chromatography was the entire 312 amino acid long protein and not incomplete fragments.

Nevertheless, this production presented different critical points. AIMP1 shows low solubility (Chang *et al.*, 2002) and, for this reason, bacteria tend to confine it in the inclusion bodies. For this reason, induction of protein expression had to be carried out reducing temperature of bacteria culture and increasing time of expression. Furthermore, during the purification process, two precautions had to be taken. First, the two-step purification had to be performed in a short time, keeping the protein at 4°C but without freezing it. Second, glycerol had to be add to the protein buffer before freezing the sample to enhance protein solubility. This because the freezing-thawing process is very delicate and protein can precipitate during this step.

Another critical point was that, given that AIMP1 is positively charged at neutral pH (pI = 8.61), it strongly binds to lipopolysaccharides (LPS), which are produced by Gram-negative bacteria and elicit strong immune responses in mammal cells. For this reason a strong method for LPS removal had to be applied (Triton-X114 extraction).

The circular dichroism analysis showed that recombinant AIMP1 had maintained a three-dimensional structure, which was progressively lost with increase of temperature. These data also showed that AIMP1 three-dimensional structure remains quite stable up to 50°C. Besides showing high temperature stability, AIMP1 showed also a high stability to cell proteases. Indeed, there is still undegraded AIMP1 in conditioned cell culture medium after 54 hours.

## **4.2 AIMP1 biological activities**

Numerous literature references have reported that AIMP1 has cytokine properties and, when secreted, works on different target cells such as monocyte/macrophages (Hou *et al.*, 2006; Ko *et al.*, 2001; Park *et al.*, 2002a; Park *et al.*, 2002b), endothelial cells (Chang *et al.*, 2002; Park *et al.*, 2002c), and fibroblasts (Park *et al.*, 2005b).

In this work we have focused our attention on the activities elicited by AIMP1 on endothelial cells and, in particular, on cell survival and on cell ability to form angiogenic cords in a three-dimensional matrix.

The role of AIMP1 in angiogenesis has turned out to be biphasic and dose-dependent: low concentrations are pro-angiogenic and induce endothelial cell migration (Hou *et al.*, 2006; Park *et al.*, 2002c) while high concentrations are anti-angiogenic and induce endothelial cell death (Park *et al.*, 2002c). Further experiments have demonstrated that different concentrations of AIMP1 activated different intracellular pathways. Low doses of AIMP1 activated ERK kinase that controls expression of matrix metalloproteinase 9. The latter hydrolyses collagen and thus promotes endothelial cell migration. On the other hand, higher doses of AIMP1 stimulated pro-apoptotic kinase JNK and this could be one of the mechanisms for AIMP1-induced apoptosis of endothelial cells (Park *et al.*, 2002c).

The experimental data obtained in this study have confirmed the reduction of endothelial cell survival induced by AIMP1, showing that it has an inhibitory effect on cell viability at relatively high concentrations (above 100 nM). This was observed in two primary endothelial aortic cell line (from a bovine and a porcine source) produced in our laboratory and in an immortalized endothelial cell line (from a porcine source). Comparing the effect of AIMP1 in a proliferation assay (BrDU) and in a cell viability assay (MTT), we could conclude that AIMP1 impairs cell viability and not cell proliferation. This result is in accordance with literature data reporting that AIMP1 induces endothelial cell death at high concentrations (Park *et al.*, 2002c). Moreover, AIMP1 anti-angiogenic activity has been demonstrated by the data obtained in the tubulogenesis assay. At concentrations ranging from 50 to 200 nM, AIMP1 inhibits ECV ability to form angiogenic cords in matrigel. This result is in accordance with the data reported by Tandle *et al.* (Tandle *et al.*, 2009), which show that EMAP II inhibits HUVEC cord formation under hypoxic conditions at a concentration of approximately 110 nM.

On the other hand, viability assays performed with low concentrations of AIMP1 on primary BAEC and HUVEC, showed that 1nM AIMP1 treatment increases endothelial cell viability. These data could find an explanation in the biphasic nature of AIMP1 activity on endothelial cells, which produces different effects on the basis of treatment concentrations. However, an increase in endothelial cell survival upon low concentration treatments with AIMP1 has never been reported before.

The only experiment carried out on a non-endothelial cell line in this work, was a migration assay performed on murine macrophages (RAW 264.7). As soon as it was discovered, EMAP II has been described to activate host-response mechanism, inducing mononuclear phagocyte (mononuclears) and polymorphonuclear leukocyte (PMN) migration (Kao *et al.*, 1992). The authors reported that stimulating these cells with 200 pM EMAP II caused an increase in the migration rate of about five times in PMN and three times in mononuclears. Following works reported that also AIMP1 was able to activate immune system cells such as monocytes and macrophages (Ko *et al.*, 2001; Park *et al.*, 2002a; Park *et al.*, 2002b). Our experiments on RAW 264.7 showed that stimulating cells with 1 nM AIMP1 for four hours duplicates the number of migrating cells respect to a

negative control (carried out with vehicle), while a 500 nM treatment more than triplicates macrophage migration rate.

### **4.3 AIMP1 has an $\alpha 5\beta 1$ integrin-dependent inhibitory effect on PAEC viability and inhibits PAEC adhesion**

EMAP II has been shown to inhibit microvascular endothelial cells (MEC) adhesion to fibronectin and to delay cell spreading through a direct interaction to  $\alpha 5\beta 1$  integrin (Schwarz *et al.*, 2005) Furthermore, EMAP II was shown to disassemble the cytoskeletal architecture of actin fiber networks and fibronectin matrix assembly (Schwarz *et al.*, 2005). Evidence has been provided that  $\alpha 5\beta 1$  integrin and its ligand fibronectin are coordinately up-regulated in blood vessels in human tumour biopsies and play critical roles in angiogenesis, resulting in tumour growth *in vivo*. Three classes of  $\alpha 5\beta 1$  integrin antagonists (antibody, peptide, and a novel non-peptide antagonist) have been shown to block growth factor-stimulated angiogenesis (Kim *et al.*, 2000a). These results implicate that integrin is the receptor for fibronectin during angiogenesis (Kim *et al.*, 2000a) and may be an important target for EMAP II anti-angiogenic function (Schwarz *et al.*, 2005).

In this study we demonstrated that  $\alpha 5\beta 1$  integrin is also involved in the inhibitory effect on cell viability elicited by AIMP1 on PAEC: this was supported by the observation that, when blocking the  $\alpha 5\beta 1$  integrin receptor with the specific antibody, AIMP1 inhibitory effect on PAEC survival was reverted. This result suggests that AIMP1 could affect viability by inhibiting endothelial cell adhesion. This hypothesis was confirmed by the observation that AIMP1 inhibits PAEC adhesion on fibronectin coating. Thus, in this work we demonstrated that also AIMP1, like EMAP II (Schwarz *et al.*, 2005), has an inhibitory effect on endothelial cell adhesion. Furthermore, it can be supposed that the impairment of cell adhesion could be one of the mechanism through which AIMP1 elicits its pro-apoptotic effect on endothelial cells.

Further experiments will have to be performed in order to deeply confirm and investigate these new results, to understand the molecules and signalling pathways involved in this process and to place these findings in the frame of AIMP1 anti-angiogenic role.

#### 4.4 Subcellular localization of exogenous AIMP1 in PAEC

In order to investigate the subcellular localization of exogenous AIMP1 in PAEC, immunofluorescence experiments were performed. Cells were treated with the recombinant protein in time-course experiments and the subcellular localization of the exogenous protein was determined using a confocal microscopy performing z-scans throughout the cells. These data were fundamental in order to understand which were the subcellular fractions to be analysed for the “fishing” of AIMP1-interacting molecules.

Yi *et al.* (Yi *et al.*, 2005) have demonstrated, using electron microscopy, that AIMP1 is internalized by endothelial cells as soon as 30 minutes after treatment. Through uptake experiments, followed by subcellular fractionation and western blot analysis, Tandle *et al.* (Tandle *et al.*, 2009) observed that EMAP II started accumulating in the cytoplasmic compartment as early as 15 minutes with a maximum at 1 hour, and subsequent decrease at 2 hours, following incubation of cells with exogenous EMAP II. The authors also report that a small fraction of EMAP II was detected in the nuclear fraction.

In this work we confirmed exogenous AIMP1 entrance in endothelial cells, but did not observe a localization of the recombinant protein inside the nucleus.

As soon as 30 minutes after AIMP1 treatment of PAEC, the distribution of the exogenous protein shows a very particular pattern. In fact, exogenous AIMP1 subcellular localization shows a strongly asymmetric pattern and, furthermore, AIMP1 accumulates in cell protrusions and prolongations.

Our time course experiments did not point out a decrease of AIMP1 in the cells after long time treatments. What arises is a different distribution pattern, since, after 6 and 24 hours, AIMP1 accumulates in clots under the cell membrane. This particular distribution pattern could represent an expulsion mechanism or, on the other hand, could indicate a functional accumulation of AIMP1 in specific points of the cell. Further investigation should be carried out to shed light on this process.

In immunofluorescence double-staining experiments, exogenous AIMP1 was found to co-localize with filamin-A and cingulin, which represent two of the novel interactors proposed in this work. Cingulin is a protein that has an important role in cell-cell and cell-

substrate junctions; it localizes to tight junctions in confluent cells, while diffusely distributes within the cytoplasm in subconfluent cells (Stevenson *et al.*, 1989). Since colocalization of AIMP1 and cingulin has been evidenced at the level of the cytoplasm in subconfluent cells, it would be interesting to examine whether AIMP1 and cingulin colocalize at the tight junctions in confluent cells. Filamins, on the other hand, are actin-binding proteins that stabilize the three-dimensional actin filament networks and link them to cellular membranes (Zhou *et al.*, 2010). The observation of the peculiar distribution pattern that AIMP1 assumes when administered to cells and the colocalization with two important cytoskeleton-related proteins, made us hypothesize that AIMP1 may act on cellular architecture maintenance and remodelling.

Schwarz *et al.* (Schwarz *et al.*, 2005) have demonstrated that microvascular endothelial cells exposed to EMAP II for 1 hour underwent a rapid disassembly of actin stress fiber network. On the other hand, Keezer *et al.* (Keezer *et al.*, 2003) demonstrated that, in adherent endothelial cells, stimulation with EMAP II caused an increase of intracellular actin fibers and focal adhesions. This result points out a context in which also EMAP II interferes with the cell cytoskeleton organization. In regard to this aspect, it would be interesting to analyse if PAEC treated with AIMP1 show a staining of the actin network different for intensity or pattern.

#### **4.5 Proteins activated upon AIMP1 treatment of PAEC**

In this work we have decided to investigate the signalling pathway activated by stimulation of PAEC with relatively high concentrations of AIMP1. This because high concentrations of AIMP1 have shown to inhibit cell viability (which seems to be  $\alpha 5\beta 1$  integrin-dependent) and cell adhesion.

In order to explore the signalling pathway activated in the described conditions, we decided to analyse protein activation through phosphorylation. This because signalling pathways activated by exogenous stimuli often require phosphorylation, and thus activation, of the proteins involved in the signalling cascade.

The study of the proteins which get phosphorylated in response to AIMP1 stimulation of PAEC was performed using two different techniques. On the one hand a Western blot analysis was carried out to analyse the activation of a small group of kinases known to get phosphorylated in cells activated by exogenous stimuli. This group included AKT, a protein involved in cellular survival pathways by inhibiting apoptotic processes; JNK, which is involved in apoptosis, cell differentiation and proliferation and ERK, involved in functions including the regulation of meiosis, mitosis, post-mitotic functions in differentiated cells and in a great variety of signalling transduction pathways activated by extracellular molecules. Our experiments confirmed a very rapid activation of ERK and JNK after stimulation of PAEC with AIMP1. An activation of these two kinases upon AIMP1 treatment of endothelial cells had already been described (Park *et al.*, 2002c). Park *et al.* treated BAEC with different concentration of AIMP1 for 1 hour and observed that ERK gets activated from low doses (1 nM) to high doses (100 nM) and JNK activation is obtained from doses from 10 nM to 100 nM. In the same article, the authors correlate these observations to the biological data obtained and concluded that AIMP1 at low concentration activated ERK, which resulted in the induction and activation of MMP9 and in the induction of endothelial cell migration; in contrast, AIMP1 at high concentration activated JNK, which mediated apoptosis of endothelial cells. On the basis of these results it is feasible that the kinase involved in the signalling cascade activated by AIMP1 in our experiments and that leads to an inhibitory effect on cell survival and on cell adhesion is JNK and not ERK.

On the other hand a two-dimensional phosphoproteomic approach has been applied to have an overview of the whole phosphoproteome in definite experimental conditions. PAEC were again treated with 200 nM of AIMP1 and the early response was analysed after 10 and 30 minutes. The more significant results were obtained from the 10 minute treatments. After a 10 minute treatment of PAEC with AIMP1, the phosphorylation of elongation factor 1 $\delta$  (EF 1 $\delta$ ), 60S acidic ribosomal protein P2 (60S) and  $\alpha$ -tubulin was found to be up-regulated.

Both EF 1 $\delta$  and 60S have a role in the translation of mRNA into protein. While 60S is one of the strongly acidic proteins associated with the ribosome, elongation factor 1 $\delta$  is a

subunit of the EF-1 mammalian complex which is responsible for the vectorial transfer of charged tRNAs from ARSs to ribosome during protein synthesis. All subunits of the mammalian EF-1 complex ( $\alpha$ ,  $\beta$ ,  $\gamma$  and  $\delta$  subunit) have been shown to undergo phosphorylation *in vivo* and *in vitro* and the  $\delta$  subunit of the EF-1 complex has been reported to interact with KRS, DRS, GRS and VRS within the ARS complex (Sang *et al.*, 2002). Moreover, phosphorylation of  $\alpha$ ,  $\beta$  and  $\delta$  subunits have been shown to lead to stimulation of EF-1 activity and subsequently, increased translational rates (Peters *et al.*, 1995; Venema *et al.*, 1991). Also for the 60S ribosomal protein, phosphorylation has been described previously and this modification increases the interaction of the synthesised polypeptides with the ribosome *in vitro* (MacConnell & Kaplan, 1982; Vidales *et al.*, 1984). Indeed, there is experimental evidence supporting a role for 60S subunits in the control of translation initiation (Sachs & Davis, 1989). Therefore, the phosphorylation of EF-1 $\delta$  and 60S ribosomal protein could lead to enhanced translational rates in AIMP1-treated cells. Possibly, these could represent mechanisms of the physiological translation process involving endogenous AIMP1 as a cofactor in the ARS complex, which are stimulated by the increase of AIMP1 inside the cell.

Tubulin instead, along with a variety of associated proteins, is a constituent of the microtubules, a major component of the cytoskeleton involved in such diverse and dynamic functions as maintaining cell shape, endocytosis, exocytosis, vesicle trafficking, cellular transport, and mitosis (Mandelkow & Mandelkow, 1992). Tubulin exists principally in two forms, as either cytosolic soluble tubulin heterodimers consisting of various  $\alpha$ - and  $\beta$ -tubulin isotypes or as insoluble assembled tubulin polymers (microtubules) (Mandelkow & Mandelkow, 1992). The ability of tubulin to cycle between these two states is one of its most fundamentally important features. Wandosell *et al.* (Wandosell *et al.*, 1987) have showed that, when phosphorylated, tubulin did not assemble into polymers and, thus, was not incorporated in microtubules. In 2000, Faruki *et al.* (Faruki *et al.*, 2000) showed that phosphorylated tubulin was assembled into microtubules only slightly less well than untreated tubulin. But, more recently, Fourest-Lieuvain *et al.* (Fourest-Lieuvain *et al.*, 2006) observed a poor incorporation of phosphorylated tubulin in microtubules and concluded that phospho-tubulin has an impaired polymerization

capacity. Thus, treatment of PAEC with AIMP1 could impair microtubule formation by stimulating  $\alpha$ -tubulin phosphorylation and interfere with processes such as cellular transport, adhesion, regulation of cell shape, polarity and motility. Nevertheless, this result needs to be further investigated and the significance of tubulin phosphorylation is still under debate.

#### **4.6 AIMP1 new interactors in endothelial cells**

One of the aims of this work was to identify new interactors of AIMP1 in endothelial cells. This goal was achieved applying three different techniques. As a first step putative AIMP1-interacting proteins were obtained through affinity purification, followed by SDS-PAGE and identification of the bands of interest by mass spectrometry analysis. After identification of the proteins, the validation of the results has been carried out using pull-down and co-immunoprecipitation assays, followed by SDS-PAGE and Western blot analysis. These two last techniques provided the same information, but were used in parallel to confirm the results. The putative interactors discovered using the affinity purification approach that were confirmed by pull-down and co-immunoprecipitation are: cingulin, filamin-A,  $\alpha$ -tubulin, vinculin, GRP78 and PYG.

Among the new AIMP1 interactors 4 cytoskeletal or cytoskeleton-associated proteins have been discovered: vinculin, cingulin,  $\alpha$ -tubulin and filamin-A.

Among them, vinculin is localized at the cell membrane to cell-cell junctions and cell-substrate junctions (Sechi and Wehland, 2000) and cingulin is localized to tight junctions in confluent cells, while diffusely distributed within the cytoplasm in subconfluent cells (Stevenson *et al.*, 1989);  $\alpha/\beta$  tubulin heterodimers compose the microtubules (Pelling *et al.*, 2007) and filamins are actin-binding proteins that stabilize the three-dimensional actin filament networks and link them to cellular membranes (Zhou *et al.*, 2010). Therefore, the signalling pathway activated by exogenous AIMP1 on endothelial cells could involve these different types of cytoskeletal structures.

In regard to GRP78, this protein represent the endoplasmic-reticulum (ER)-resident member of the HSP70 family. Han *et al.* (Han *et al.*, 2007) have reported that AIMP1 also

interacts with gp96 in mouse pancreas cells, which is the endoplasmic-reticulum (ER)-resident member of the HSP90 family. They also reported that the disruption of the interaction between these two molecules could initiate pathogenic pathways that lead to systemic autoimmune disease.

The results from the AIMP1-interactors discovery experiments, together with the data from the biological assays, immunofluorescence and phosphoproteomic analysis, suggest the involvement of proteins controlling adhesion and cytoskeletal remodelling in the signalling pathway activated by exogenous AIMP1 in PAEC.

#### **4.7 Transcriptional gene regulation upon AIMP1 stimulation of PAEC**

Different studies have been performed on transcriptional gene regulation by AIMP1 stimulation on different types of cells. In this work we have analyzed the expression levels of some of the genes regulated in PAEC treated with AIMP1.

Among the previously analysed genes, we chose genes involved in the angiogenic process, in cell proliferation, survival and adhesion processes and genes codifying for proteins involved in the cell-matrix interaction.

VEGFR1 and VEGFR2 have been observed to be up-regulated in THP-1 cells respectively after 6 and 2 hours of treatment with 100 nM AIMP1 (Ko *et al.*, 2001). Park *et al.* (Park *et al.*, 2002c) reported MMP9 up-regulation in BAEC stimulated for 24 hours with 1nM AIMP1 and MMP2 down-regulation in BAEC stimulated for 24 hours with 10 and 100 nM AIMP1. ICAM1 has been found to be up-regulated both in endothelial cells (HUVEC) (Tandle *et al.*, 2005) and in THP-1 cells (Ko *et al.*, 2001). In the first case, HUVEC were treated with approximately 450 nM EMAP II and up-regulation was observed after 4 hours; in the case of THP-1 cells, up-regulation was observed after a 6 hour treatment of cells with 100 nM AIMP1. In human fibroblasts (HFF) Park *et al.* (Park *et al.*, 2005b) observed up-regulation of collagen (collagen 1a2) when cells were stimulated with 50 nM AIMP1 for 12 hours. CCNG2 (cyclin G2), TNFAIP3 (tumour necrosis factor alpha-induced protein 3), KLF4 (Kruppel-like factor 4) and BIRC3 (baculoviral IAP

repeat-containing 3) were reported to be up-regulated in HUVEC stimulated with 450 nM EMAP II for one (KLF4) or two (CCNG2, TNFAIP3 and BIRC3) hours (Tandle *et al.*, 2005).

In this work the expression levels of the mentioned genes have been evaluated following PAEC stimulation with different concentrations of AIMP1 in time course experiments. While for MMP2 and MMP9 cells were treated with 1, 10 and 100 nM AIMP1 for 1 and 24 hours, for all the other genes cells were treated with 100 nM AIMP1 for 1, 2, 6 and 24 hours. Gene expression levels were determined by performing Real Time PCR analysis in order to compare treated and untreated cells. Relative quantification of the expression level of these genes indicated that, under the tested conditions, AIMP1 treatment regulates the expression of VEGFA, VEGFR2, MMP2 and MMP9. AIMP1 up-regulates VEGFA and VEGFR2 transcripts at a concentration of 100 nM after a two-hour treatment. Instead, transcription of MMP2 is induced after 24 hours treatment and MMP9 expression is induced after 1 and 24-hour treatment.

The result of the up-regulation of VEGFA and VEGFR2 transcription upon 100 nM AIMP1 stimulation, which could be interpreted as a pro-angiogenic signal, is of difficult interpretation. In fact, at that concentration, AIMP1 was reported in literature and shown in this work to inhibit endothelial cell survival, exhibiting an anti-angiogenic effect. It could be hypothesized that a feedback mechanism regulates the VEGF pathway in the tested conditions, but further investigations need to be carried out to clarify this result. Also the result of the up-regulation of MMP2 upon 24 hour treatment with 10 nM is not in line with previous data (Park *et al.*, 2002c).

Instead, the up-regulation of MMP9 in endothelial cells upon low concentrations of AIMP1 treatment is in accordance with the results reported by Park *et al.* (Park *et al.*, 2002c) and could play a key role in the processes of matrix remodelling and endothelial cell migrating during angiogenesis. This result has to be contextualized in the biphasic and dose-dependent role of AIMP1 in angiogenesis, where low concentrations are pro-angiogenic and induce endothelial cell migration (Hou *et al.*, 2006; Park *et al.*, 2002c).

## 5. Conclusions

Despite its role as a cofactor of ARS complex (Quevillon *et al.*, 1997; Park *et al.*, 1999; Kim *et al.*, 2000b; Shalak *et al.*, 2001), AIMP1, when secreted, also acts as a cytokine on different cell types (Ko *et al.*, 2001; Chang *et al.*, 2002; Park *et al.*, 2002a; Park *et al.*, 2002b; Park *et al.*, 2005b). AIMP1 has shown to be a cytokine activating immune cells and endothelial cells, since it is highly secreted from Raw 264.7 cells stimulated by tumour necrosis factor (Park *et al.*, 2002b). AIMP1 has more potent cytokine activity on immune and endothelial cells than its cleaved C-terminal domain, EMAP II (Park *et al.*, 2002b; Park *et al.*, 2002c; Yi *et al.*, 2005) which was firstly described to be the effective cytokine (Kao *et al.*, 1994a; Kao *et al.*, 1994b; Knies *et al.*, 1998; Shalak *et al.*, 2001).

Although the administration of both recombinant EMAP II and AIMP1 has been shown to inhibit tumour growth by inhibition of angiogenesis (Schwarz *et al.*, 1999b; Lee *et al.*, 2006), the mechanism surrounding their angiostatic effect is poorly understood. Angiogenesis, the growth of new blood vessels, is essential for pathological processes such as tumour growth and metastasis (Carmeliet, 2005) and endothelial cells play a key role in all aspects of this cellular event (Jain, 2003). In this work we have analyzed the signalling pathways activated by exogenous AIMP1 on endothelial cells (PAEC) using a wide set of *in vitro* techniques. Among biological assays we confirmed AIMP1 inhibitory effect on PAEC survival with a dose-dependent response.

In this study we demonstrated also that  $\alpha 5\beta 1$  integrin is involved in the inhibitory effect elicited by AIMP1 on PAEC survival: this was supported by the observation that, when blocking  $\alpha 5\beta 1$  integrin with the specific antibody, AIMP1 inhibitory activity on PAEC viability was reverted. This result suggests that AIMP1 could affect survival by inhibiting endothelial cell adhesion. This hypothesis was confirmed by the observation that AIMP1 inhibits PAEC adhesion on fibronectin coating. Thus, in this work we demonstrated that also AIMP1, like EMAP II, has an inhibitory effect on endothelial cell adhesion.

Evidence has been provided that  $\alpha 5\beta 1$  integrin and its ligand fibronectin are coordinately up-regulated in blood vessels in human tumour biopsies and play critical roles in angiogenesis, resulting in tumour growth *in vivo*. Three classes of  $\alpha 5\beta 1$  integrin antagonists (antibody, peptide, and a novel non-peptide antagonist) have been shown to block growth factor-stimulated angiogenesis (Kim *et al.*, 2000a). These results implicate that integrin is the receptor for fibronectin during angiogenesis (Kim *et al.*, 2000a).

To shed light on the mechanisms at the basis of the biological assays results, we decided to investigate the signalling pathways activated by exogenous AIMP1 in endothelial cells.

The results obtained allowed us to hypothesize the assembly of a protein complex on the cytosolic face of the cell membrane composed of cytoskeletal and cytoskeleton-associated proteins, following the uptake of exogenous AIMP1 by PAEC. Our supporting evidence was acquired from different experimental data. Firstly, immunofluorescence experiments showed that AIMP1 distributes in the cells with an asymmetric pattern and that it concentrates at the level of cell protrusions. Secondly, four cytoskeletal proteins were identified among AIMP1-interacting molecules. Thirdly, immunofluorescence experiments showed a co-localization between AIMP1 and cingulin and between AIMP1 and filamin-A when endothelial cells were treated with AIMP1. And, finally,  $\alpha$ -tubulin gets phosphorylated upon a 10 minute treatment of PAEC with exogenous AIMP1.

Among the identified interactors, vinculin is localized at the cell membrane to cell-cell junctions and cell-substrate junctions (Sechi & Wehland, 2000) and cingulin is localized to tight junctions in confluent cells, while diffusely distributed within the cytoplasm in subconfluent cells (Stevenson *et al.*, 1989);  $\alpha/\beta$  tubulin heterodimers compose the microtubules (Sechi & Wehland, 2000; Pelling *et al.*, 2007) and filamins are actin-binding

proteins that stabilize the three-dimensional actin filament networks and link them to cellular membranes (Zhou *et al.*, 2010). Therefore, the signalling pathway activated by exogenous AIMP1 on endothelial cells involves these different types of cytoskeletal structures.

In conclusion, on the basis of our results and literature data, we propose a cellular mechanism in which AIMP1, upon cell uptake, acts on endothelial cells through interaction with at least four cytoskeletal proteins on the cytosolic face of the cell membrane ( $\alpha$ -tubulin, vinculin, cingulin and filamin-A). Interaction and/or activation of these proteins could act regulating the cellular architecture maintenance and remodelling.

## Acknowledgements

I wish to thank Dr. Barbara Canepa and Dr. Sarah Dewilde for having guided me along the way, for sharing their knowledge and scientific expertise with me, for supporting me in all the difficulties and discouraging moments and for their ability to solve all kinds of problems we had to face throughout this “journey”.

I would also like to thank Dr. Alessandra Giuliano Albo and Kaska Lis for performing all the 2-DE experiments and image analysis and Dr. Davide Corpillo for mass spectrometry analysis.

I am very grateful to all those mentioned so far, together with other colleagues at the LIMA - Laura, Stefania, Livia and Raffaella - for being precious colleagues, for maintaining a highly collaborative atmosphere and for making it pleasant to go to work each day. Thank you all for your friendship and help.

My gratitude also goes to my family and friends who have always been there for me.

I would like to thank the Bioindustry Park “Silvano Fumero” for allowing me to develop and focus on this project.

I wish to thank Prof. Alexander Kornelyuk and Dr. Maurizio Mariani for having dedicated time to read and review my thesis.

Finally, I would like to express my thanks to the Professors of the PhD school for having given me the opportunity to be part of such a stimulating scientific environment in these last three years.

## References

- Agrawal,G.K. & Thelen,J.J. (2005) Development of a simplified, economical polyacrylamide gel staining protocol for phosphoproteins. *Proteomics*. **5**, 4684-4688.
- Awasthi,N., Schwarz,M.A., Verma,V., Cappiello,C., & Schwarz,R.E. (2009) Endothelial monocyte activating polypeptide II interferes with VEGF-induced proangiogenic signaling. *Lab Invest* **89**, 38-46.
- Baatout,S. (1997) Endothelial differentiation using Matrigel (review). *Anticancer Res*. **17**, 451-455.
- Barbarese,E., Koppel,D.E., Deutscher,M.P., Smith,C.L., Ainger,K., Morgan,F., & Carson,J.H. (1995) Protein translation components are colocalized in granules in oligodendrocytes. *J.Cell Sci*. **108 ( Pt 8)**, 2781-2790.
- Barnett,G., Jakobsen,A.M., Tas,M., Rice,K., Carmichael,J., & Murray,J.C. (2000) Prostate adenocarcinoma cells release the novel proinflammatory polypeptide EMAP-II in response to stress. *Cancer Res*. **60**, 2850-2857.
- Battersby,S., Boddy,S.C., Critchley,H.O., & Jabbour,H.N. (2002) Expression and localization of endothelial monocyte-activating polypeptide II in the human endometrium across the menstrual cycle: regulation of expression by prostaglandin E(2). *J.Clin.Endocrinol.Metab* **87**, 3928-3935.
- Behrendorf,H.A., van de,C.M., Knies,U.E., Vandenabeele,P., & Clauss,M. (2000) The endothelial monocyte-activating polypeptide II (EMAP II) is a substrate for caspase-7. *FEBS Lett*. **466**, 143-147.
- Berger,A.C., Tang,G., Alexander,H.R., & Libutti,S.K. (2000) Endothelial monocyte-activating polypeptide II, a tumor-derived cytokine that plays an important role in inflammation, apoptosis, and angiogenesis. *J.Immunother*. **23**, 519-527.
- Bottoni,A., Vignali,C., Piccin,D., Tagliati,F., Luchin,A., Zatelli,M.C., & Uberti,E.C. (2007) Proteasomes and RARS modulate AIMP1/EMAP II secretion in human cancer cell lines. *J.Cell Physiol* **212**, 293-297.

- Brabeck,C., Michetti,F., Geloso,M.C., Corvino,V., Gozalan,F., Meyermann,R., & Schluesener,H.J. (2002) Expression of EMAP-II by activated monocytes/microglial cells in different regions of the rat hippocampus after trimethyltin-induced brain damage. *Exp.Neurol.* **177**, 341-346.
- Burbaum,J.J. & Schimmel,P. (1991) Structural relationships and the classification of aminoacyl-tRNA synthetases. *J.Biol.Chem.* **266**, 16965-16968.
- Carmeliet,P. (2005) Angiogenesis in life, disease and medicine. *Nature* **438**, 932-936.
- Chang,S.Y., Park,S.G., Kim,S., & Kang,C.Y. (2002) Interaction of the C-terminal domain of p43 and the alpha subunit of ATP synthase. Its functional implication in endothelial cell proliferation. *J.Biol.Chem.* **277**, 8388-8394.
- Chang,S.Y., Ko,H.J., Heo,T.H., & Kang,C.Y. (2005) Heparan sulfate regulates the antiangiogenic activity of endothelial monocyte-activating polypeptide-II at acidic pH. *Mol.Pharmacol.* **67**, 1534-1543.
- Chomczynski,P. & Sacchi,N. (1987) Single-step method of RNA isolation by acid guanidinium thiocyanate-phenol-chloroform extraction. *Anal.Biochem.* **162**, 156-159.
- Clarijs,R., Schalkwijk,L., Ruiter,D.J., & de Waal,R.M. (2003) EMAP-II expression is associated with macrophage accumulation in primary uveal melanoma. *Invest Ophthalmol.Vis.Sci.* **44**, 1801-1806.
- Cusack,S., Hartlein,M., & Leberman,R. (1991) Sequence, structural and evolutionary relationships between class 2 aminoacyl-tRNA synthetases. *Nucleic Acids Res.* **19**, 3489-3498.
- Daemen,M.A., van', V, Denecker,G., Heemskerk,V.H., Wolfs,T.G., Clauss,M., Vandenabeele,P., & Buurman,W.A. (1999) Inhibition of apoptosis induced by ischemia-reperfusion prevents inflammation. *J.Clin.Invest* **104**, 541-549.
- Dang,C.V., Yang,D.C., & Pollard,T.D. (1983) Association of methionyl-tRNA synthetase with detergent-insoluble components of the rough endoplasmic reticulum. *J.Cell Biol.* **96**, 1138-1147.
- Deineko,V. (2006) Web-ware bioinformatical analysis and structure modelling of N-terminus of human multisynthetase complex auxiliary component protein p43. *Protein Pept.Lett.* **13**, 687-691.

- Draper,D.E. & Reynaldo,L.P. (1999) RNA binding strategies of ribosomal proteins. *Nucleic Acids Res.* **27**, 381-388.
- Eriani,G., Delarue,M., Poch,O., Gangloff,J., & Moras,D. (1990) Partition of tRNA synthetases into two classes based on mutually exclusive sets of sequence motifs. *Nature* **347**, 203-206.
- Fajardo,L.F., Kwan,H.H., Kowalski,J., Prionas,S.D., & Allison,A.C. (1992) Dual role of tumor necrosis factor-alpha in angiogenesis. *Am.J.Pathol.* **140**, 539-544.
- Faruki,S., Geahlen,R.L., & Asai,D.J. (2000) Syk-dependent phosphorylation of microtubules in activated B-lymphocytes2. *J.Cell Sci.* **113 ( Pt 14)**, 2557-2565.
- Ferrario,A., von Tiehl,K.F., Rucker,N., Schwarz,M.A., Gill,P.S., & Gomer,C.J. (2000) Antiangiogenic treatment enhances photodynamic therapy responsiveness in a mouse mammary carcinoma. *Cancer Res.* **60**, 4066-4069.
- Fourest-Lieuvain,A., Peris,L., Gache,V., Garcia-Saez,I., Juillan-Binard,C., Lantez,V., & Job,D. (2006) Microtubule regulation in mitosis: tubulin phosphorylation by the cyclin-dependent kinase Cdk1 2. *Mol.Biol.Cell* **17**, 1041-1050.
- Francin,M., Kaminska,M., Kerjan,P., & Mirande,M. (2002) The N-terminal domain of mammalian Lysyl-tRNA synthetase is a functional tRNA-binding domain. *J.Biol.Chem.* **277**, 1762-1769.
- Frugier,M., Moulinier,L., & Giege,R. (2000) A domain in the N-terminal extension of class IIb eukaryotic aminoacyl-tRNA synthetases is important for tRNA binding. *EMBO J.* **19**, 2371-2380.
- Gnant,M.F., Berger,A.C., Huang,J., Puhlmann,M., Wu,P.C., Merino,M.J., Bartlett,D.L., Alexander,H.R., Jr., & Libutti,S.K. (1999) Sensitization of tumor necrosis factor alpha-resistant human melanoma by tumor-specific in vivo transfer of the gene encoding endothelial monocyte-activating polypeptide II using recombinant vaccinia virus. *Cancer Res.* **59**, 4668-4674.
- Han,J.M., Kim,J.Y., & Kim,S. (2003) Molecular network and functional implications of macromolecular tRNA synthetase complex. *Biochem.Biophys.Res.Commum.* **303**, 985-993.

- Han,J.M., Park,S.G., Lee,Y., & Kim,S. (2006) Structural separation of different extracellular activities in aminoacyl-tRNA synthetase-interacting multi-functional protein, p43/AIMP1 1. *Biochem.Biophys.Res.Commun.* **342**, 113-118.
- Han,J.M., Park,S.G., Liu,B., Park,B.J., Kim,J.Y., Jin,C.H., Song,Y.W., Li,Z., & Kim,S. (2007) Aminoacyl-tRNA synthetase-interacting multifunctional protein 1/p43 controls endoplasmic reticulum retention of heat shock protein gp96: its pathological implications in lupus-like autoimmune diseases. *Am.J.Pathol.* **170**, 2042-2054.
- Hou,Y., Plett,P.A., Ingram,D.A., Rajashekhar,G., Orschell,C.M., Yoder,M.C., March,K.L., & Clauss,M. (2006) Endothelial-monocyte-activating polypeptide II induces migration of endothelial progenitor cells via the chemokine receptor CXCR3. *Exp.Hematol.* **34**, 1125-1132.
- Ibba,M. & Soll,D. (2001) The renaissance of aminoacyl-tRNA synthesis. *EMBO Rep.* **2**, 382-387.
- Ivakhno,S.S. & Kornelyuk,A.I. (2004) Cytokine-like activities of some aminoacyl-tRNA synthetases and auxiliary p43 cofactor of aminoacylation reaction and their role in oncogenesis. *Exp.Oncol.* **26**, 250-255.
- Jacobs,D.I., van Rijssen,M.S., van der,H.R., & Verpoorte,R. (2001) Sequential solubilization of proteins precipitated with trichloroacetic acid in acetone from cultured *Catharanthus roseus* cells yields 52% more spots after two-dimensional electrophoresis. *Proteomics.* **1**, 1345-1350.
- Jaffe,E.A., Nachman,R.L., Becker,C.G., & Minick,C.R. (1973) Culture of human endothelial cells derived from umbilical veins. Identification by morphologic and immunologic criteria. *J.Clin.Invest* **52**, 2745-2756.
- Jain,R.K. (2003) Molecular regulation of vessel maturation. *Nat.Med.* **9**, 685-693.
- Jeffery,C.J. (2003) Multifunctional proteins: examples of gene sharing. *Ann.Med.* **35**, 28-35.
- Jeffery,C.J. (1999) Moonlighting proteins. *Trends Biochem.Sci.* **24**, 8-11.
- Johnson,D.L. & Yang,D.C. (1981) Stoichiometry and composition of an aminoacyl-tRNA synthetase complex from rat liver. *Proc.Natl.Acad.Sci.U.S.A* **78**, 4059-4062.

- Journey, W.S., Janardhan, K.S., Singh, B. (2007) Expression and function of endothelial monocyte-activating polypeptide-II in acute lung inflammation. *Inflamm. Res.* **56**, 1-7.
- Kaminska, M., Shalak, V., & Mirande, M. (2001) The appended C-domain of human methionyl-tRNA synthetase has a tRNA-sequestering function. *Biochemistry* **40**, 14309-14316.
- Kaminska, M., Havrylenko, S., Decottignies, P., Gillet, S., Le, M.P., Negrutskii, B., & Mirande, M. (2009) Dissection of the structural organization of the aminoacyl-tRNA synthetase complex. *J.Biol.Chem.* **284**, 6053-6060.
- Kao, J., Ryan, J., Brett, G., Chen, J., Shen, H., Fan, Y.G., Godman, G., Familletti, P.C., Wang, F., Pan, Y.C., & . (1992) Endothelial monocyte-activating polypeptide II. A novel tumor-derived polypeptide that activates host-response mechanisms. *J.Biol.Chem.* **267**, 20239-20247.
- Kao, J., Fan, Y.G., Haehnel, I., Brett, J., Greenberg, S., Clauss, M., Kayton, M., Houck, K., Kisiel, W., Seljelid, R., & . (1994a) A peptide derived from the amino terminus of endothelial-monocyte-activating polypeptide II modulates mononuclear and polymorphonuclear leukocyte functions, defines an apparently novel cellular interaction site, and induces an acute inflammatory response. *J.Biol.Chem.* **269**, 9774-9782.
- Kao, J., Houck, K., Fan, Y., Haehnel, I., Libutti, S.K., Kayton, M.L., Grikscheit, T., Chabot, J., Nowygrod, R., Greenberg, S., & . (1994b) Characterization of a novel tumor-derived cytokine. Endothelial-monocyte activating polypeptide II. *J.Biol.Chem.* **269**, 25106-25119.
- Keezer, S.M., Ivie, S.E., Krutzsch, H.C., Tandle, A., Libutti, S.K., & Roberts, D.D. (2003) Angiogenesis inhibitors target the endothelial cell cytoskeleton through altered regulation of heat shock protein 27 and cofilin. *Cancer Res.* **63**, 6405-6412.
- Kim, Y., Kim, J.E., Lee, S.D., Lee, T.G., Kim, J.H., Park, J.B., Han, J.M., Jang, S.K., Suh, P.G., & Ryu, S.H. (1999) Phospholipase D1 is located and activated by protein kinase C alpha in the plasma membrane in 3Y1 fibroblast cell. *Biochim.Biophys.Acta* **1436**, 319-330.
- Kim, S., Bell, K., Mousa, S.A., & Varner, J.A. (2000a) Regulation of angiogenesis in vivo by ligation of integrin alpha5beta1 with the central cell-binding domain of fibronectin. *Am.J.Pathol.* **156**, 1345-1362.

- Kim,Y., Shin,J., Li,R., Cheong,C., Kim,K., & Kim,S. (2000b) A novel anti-tumor cytokine contains an RNA binding motif present in aminoacyl-tRNA synthetases. *J.Biol.Chem.* **275**, 27062-27068.
- Kim,J.Y., Kang,Y.S., Lee,J.W., Kim,H.J., Ahn,Y.H., Park,H., Ko,Y.G., & Kim,S. (2002) p38 is essential for the assembly and stability of macromolecular tRNA synthetase complex: implications for its physiological significance. *Proc.Natl.Acad.Sci.U.S.A* **99**, 7912-7916.
- Knies,U.E., Behrendorf,H.A., Mitchell,C.A., Deutsch,U., Risau,W., Drexler,H.C., & Clauss,M. (1998) Regulation of endothelial monocyte-activating polypeptide II release by apoptosis. *Proc.Natl.Acad.Sci.U.S.A* **95**, 12322-12327.
- Ko,Y.G., Park,H., Kim,T., Lee,J.W., Park,S.G., Seol,W., Kim,J.E., Lee,W.H., Kim,S.H., Park,J.E., & Kim,S. (2001) A cofactor of tRNA synthetase, p43, is secreted to up-regulate proinflammatory genes. *J.Biol.Chem.* **276**, 23028-23033.
- Ko,Y.G., Park,H., & Kim,S. (2002) Novel regulatory interactions and activities of mammalian tRNA synthetases. *Proteomics.* **2**, 1304-1310.
- Laemmli,U.K. (1970) Cleavage of structural proteins during the assembly of the head of bacteriophage T4. *Nature* **227**, 680-685.
- Lander,E.S., Linton,L.M., Birren,B., Nusbaum,C., Zody,M.C., Baldwin,J., Devon,K., Dewar,K., Doyle,M., FitzHugh,W., Funke,R., Gage,D., Harris,K., Heaford,A., Howland,J., Kann,L., Lehoczy,J., LeVine,R., McEwan,P., McKernan,K., Meldrim,J., Mesirov,J.P., Miranda,C., Morris,W., Naylor,J., Raymond,C., Rosetti,M., Santos,R., Sheridan,A., Sougnez,C., Stange-Thomann,N., Stojanovic,N., Subramanian,A., Wyman,D., Rogers,J., Sulston,J., Ainscough,R., Beck,S., Bentley,D., Burton,J., Clee,C., Carter,N., Coulson,A., Deadman,R., Deloukas,P., Dunham,A., Dunham,I., Durbin,R., French,L., Grafham,D., Gregory,S., Hubbard,T., Humphray,S., Hunt,A., Jones,M., Lloyd,C., McMurray,A., Matthews,L., Mercer,S., Milne,S., Mullikin,J.C., Mungall,A., Plumb,R., Ross,M., Shownkeen,R., Sims,S., Waterston,R.H., Wilson,R.K., Hillier,L.W., McPherson,J.D., Marra,M.A., Mardis,E.R., Fulton,L.A., Chinwalla,A.T., Pepin,K.H., Gish,W.R., Chissoe,S.L., Wendl,M.C., Delehaunty,K.D., Miner,T.L., Delehaunty,A., Kramer,J.B., Cook,L.L., Fulton,R.S., Johnson,D.L., Minx,P.J., Clifton,S.W., Hawkins,T., Branscomb,E., Predki,P., Richardson,P., Wenning,S., Slezak,T., Doggett,N., Cheng,J.F., Olsen,A., Lucas,S., Elkin,C., Uberbacher,E., Frazier,M., Gibbs,R.A., Muzny,D.M., Scherer,S.E., Bouck,J.B., Sodergren,E.J., Worley,K.C., Rives,C.M., Gorrell,J.H., Metzker,M.L., Naylor,S.L., Kucherlapati,R.S., Nelson,D.L., Weinstock,G.M., Sakaki,Y., Fujiyama,A., Hattori,M., Yada,T.,

- Toyoda,A., Itoh,T., Kawagoe,C., Watanabe,H., Totoki,Y., Taylor,T., Weissenbach,J., Heilig,R., Saurin,W., Artiguenave,F., Brottier,P., Bruls,T., Pelletier,E., Robert,C., Wincker,P., Smith,D.R., Doucette-Stamm,L., Rubenfield,M., Weinstock,K., Lee,H.M., Dubois,J., Rosenthal,A., Platzer,M., Nyakatura,G., Taudien,S., Rump,A., Yang,H., Yu,J., Wang,J., Huang,G., Gu,J., Hood,L., Rowen,L., Madan,A., Qin,S., Davis,R.W., Federspiel,N.A., Abola,A.P., Proctor,M.J., Myers,R.M., Schmutz,J., Dickson,M., Grimwood,J., Cox,D.R., Olson,M.V., Kaul,R., Raymond,C., Shimizu,N., Kawasaki,K., Minoshima,S., Evans,G.A., Athanasiou,M., Schultz,R., Roe,B.A., Chen,F., Pan,H., Ramser,J., Lehrach,H., Reinhardt,R., McCombie,W.R., de la,B.M., Dedhia,N., Blocker,H., Hornischer,K., Nordsiek,G., Agarwala,R., Aravind,L., Bailey,J.A., Bateman,A., Batzoglu,S., Birney,E., Bork,P., Brown,D.G., Burge,C.B., Cerutti,L., Chen,H.C., Church,D., Clamp,M., Copley,R.R., Doerks,T., Eddy,S.R., Eichler,E.E., Furey,T.S., Galagan,J., Gilbert,J.G., Harmon,C., Hayashizaki,Y., Haussler,D., Hermjakob,H., Hokamp,K., Jang,W., Johnson,L.S., Jones,T.A., Kasif,S., Kasprzyk,A., Kennedy,S., Kent,W.J., Kitts,P., Koonin,E.V., Korf,I., Kulp,D., Lancet,D., Lowe,T.M., McLysaght,A., Mikkelsen,T., Moran,J.V., Mulder,N., Pollara,V.J., Ponting,C.P., Schuler,G., Schultz,J., Slater,G., Smit,A.F., Stupka,E., Szustakowski,J., Thierry-Mieg,D., Thierry-Mieg,J., Wagner,L., Wallis,J., Wheeler,R., Williams,A., Wolf,Y.I., Wolfe,K.H., Yang,S.P., Yeh,R.F., Collins,F., Guyer,M.S., Peterson,J., Felsenfeld,A., Wetterstrand,K.A., Patrinos,A., Morgan,M.J., de,J.P., Catanese,J.J., Osoegawa,K., Shizuya,H., Choi,S., & Chen,Y.J. (2001) Initial sequencing and analysis of the human genome. *Nature* **409**, 860-921.
- Lans,T.E., ten Hagen,T.L., van,H.R., Wu,P.C., van Tiel,S.T., Libutti,S.K., Alexander,H.R., & Eggermont,A.M. (2002) Improved antitumor response to isolated limb perfusion with tumor necrosis factor after upregulation of endothelial monocyte-activating polypeptide II in soft tissue sarcoma. *Ann.Surg.Oncol.* **9**, 812-819.
- Lans,T.E., van,H.R., Eggermont,A.M., & ten Hagen,T.L. (2004) Involvement of endothelial monocyte activating polypeptide II in tumor necrosis factor-alpha-based anti-cancer therapy. *Anticancer Res.* **24**, 2243-2248.
- Lee,S.W., Cho,B.H., Park,S.G., & Kim,S. (2004) Aminoacyl-tRNA synthetase complexes: beyond translation. *J.Cell Sci.* **117**, 3725-3734.
- Lee,Y.S., Han,J.M., Kang,T., Park,Y.I., Kim,H.M., & Kim,S. (2006) Antitumor activity of the novel human cytokine AIMP1 in an in vivo tumor model. *Mol.Cells* **21**, 213-217.

- Lee,Y.S., Han,J.M., Son,S.H., Choi,J.W., Jeon,E.J., Bae,S.C., Park,Y.I., & Kim,S. (2008) AIMP1/p43 downregulates TGF-beta signaling via stabilization of smurf2. *Biochem.Biophys.Res.Comm.* **371**, 395-400.
- Liu,S., Tobias,R., McClure,S., Styba,G., Shi,Q., & Jackowski,G. (1997) Removal of endotoxin from recombinant protein preparations 6. *Clin.Biochem.* **30**, 455-463.
- Liu,S.H. & Gottsch,J.D. (1999) Apoptosis induced by a corneal-endothelium-derived cytokine. *Invest Ophthalmol.Vis.Sci.* **40**, 3152-3159.
- Liu,J. & Schwarz,M.A. (2006) Identification of protease-sensitive sites in Human Endothelial-Monocyte Activating Polypeptide II protein. *Exp.Cell Res.* **312**, 2231-2237.
- MacConnell,W.P. & Kaplan,N.O. (1982) The activity of the acidic phosphoproteins from the 80 S rat liver ribosome2. *J.Biol.Chem.* **257**, 5359-5366.
- Mai,G., Wang,Z., Yan,J., Liu,Z., Chen,J., Deng,D., Kang,Y., & Quan,J. (1999) Corneal topographical changes following strabismus surgery. *Yan.Ke.Xue.Bao.* **15**, 174-178.
- Mandelkow,E.M. & Mandelkow,E. (1992) Microtubule oscillations 15. *Cell Motil.Cytoskeleton* **22**, 235-244.
- Marchetti-Deschmann,M., Kemptner,J., Reichel,C., & Allmaier,G. (2009) Comparing standard and microwave assisted staining protocols for SDS-PAGE of glycoproteins followed by subsequent PMF with MALDI MS. *J.Proteomics.* **72**, 628-639.
- Martinis,S.A., Plateau,P., Cavarelli,J., & Florentz,C. (1999) Aminoacyl-tRNA synthetases: a family of expanding functions. Mittelwihr, France, October 10-15, 1999. *EMBO J.* **18**, 4591-4596.
- Marvin,M.R., Libutti,S.K., Kayton,M., Kao,J., Hayward,J., Grikscheit,T., Fan,Y., Brett,J., Weinberg,A., Nowygrod,R., LoGerfo,P., Feind,C., Hansen,K.S., Schwartz,M., Stern,D., & Chabot,J. (1996) A novel tumor-derived mediator that sensitizes cytokine-resistant tumors to tumor necrosis factor. *J.Surg.Res.* **63**, 248-255.
- Matschurat,S., Knies,U.E., Person,V., Fink,L., Stoelcker,B., Ebenebe,C., Behrendorf,H.A., Schaper,J., & Clauss,M. (2003a) Regulation of EMAP II by hypoxia. *Am.J.Pathol.* **162**, 93-103.

- Mirande,M., Kellermann,O., & Waller,J.P. (1982) Macromolecular complexes from sheep and rabbit containing seven aminoacyl-tRNA synthetases. II. Structural characterization of the polypeptide components and immunological identification of the methionyl-tRNA synthetase subunit. *J.Biol.Chem.* **257**, 11049-11055.
- Mirande,M., Le,C.D., Louvard,D., Reggio,H., Pailliez,J.P., & Waller,J.P. (1985) Association of an aminoacyl-tRNA synthetase complex and of phenylalanyl-tRNA synthetase with the cytoskeletal framework fraction from mammalian cells. *Exp.Cell Res.* **156**, 91-102.
- Morales,A.J., Swairjo,M.A., & Schimmel,P. (1999) Structure-specific tRNA-binding protein from the extreme thermophile *Aquifex aeolicus*. *EMBO J.* **18**, 3475-3483.
- Mueller,C.A., Schluesener,H.J., Conrad,S., Meyermann,R., & Schwab,J.M. (2003) Lesional expression of a proinflammatory and antiangiogenic cytokine EMAP II confined to endothelium and microglia/macrophages during secondary damage following experimental traumatic brain injury. *J.Neuroimmunol.* **135**, 1-9.
- Murray,J.C., Heng,Y.M., Symonds,P., Rice,K., Ward,W., Huggins,M., Todd,I., & Robins,R.A. (2004a) Endothelial monocyte-activating polypeptide-II (EMAP-II): a novel inducer of lymphocyte apoptosis. *J.Leukoc.Biol.* **75**, 772-776.
- Murray,J.C., Symonds,P., Ward,W., Huggins,M., Tiga,A., Rice,K., Heng,Y.M., Todd,I., & Robins,R.A. (2004b) Colorectal cancer cells induce lymphocyte apoptosis by an endothelial monocyte-activating polypeptide-II-dependent mechanism. *J.Immunol.* **172**, 274-281.
- Murzin,A.G. (1993) OB(oligonucleotide/oligosaccharide binding)-fold: common structural and functional solution for non-homologous sequences. *EMBO J.* **12**, 861-867.
- Norcum,M.T. (1989) Isolation and electron microscopic characterization of the high molecular mass aminoacyl-tRNA synthetase complex from murine erythroleukemia cells. *J.Biol.Chem.* **264**, 15043-15051.
- Norcum,M.T. & Warrington,J.A. (2000) The cytokine portion of p43 occupies a central position within the eukaryotic multisynthetase complex. *J.Biol.Chem.* **275**, 17921-17924.

- Norcum,M.T. & Boisset,N. (2002) Three-dimensional architecture of the eukaryotic multisynthetase complex determined from negatively stained and cryoelectron micrographs. *FEBS Lett.* **512**, 298-302.
- Nuhrenberg,T.G., Voisard,R., Fahlisch,F., Rudelius,M., Braun,J., Gschwend,J., Kountides,M., Herter,T., Baur,R., Hombach,V., Baeuerle,P.A., & Zohlhofer,D. (2005) Rapamycin attenuates vascular wall inflammation and progenitor cell promoters after angioplasty. *FASEB J.* **19**, 246-248.
- Nuhrenberg,T.G., Langwieser,N., Schwarz,J.B.K., Hou,Y., Frank,P., Sorge,F., Matschurat,S., Seid,S., Kastrati,A., Schomig,A., Clauss,M.A., Zohlhofer,D. (2008) EMAP-II downregulation contributes to the beneficial effects of rapamycin after vascular injury. *Card. Res.* **77**, 580-589.
- Park,S.G., Jung,K.H., Lee,J.S., Jo,Y.J., Motegi,H., Kim,S., & Shiba,K. (1999) Precursor of pro-apoptotic cytokine modulates aminoacylation activity of tRNA synthetase. *J.Biol.Chem.* **274**, 16673-16676.
- Park,H., Park,S.G., Lee,J.W., Kim,T., Kim,G., Ko,Y.G., & Kim,S. (2002a) Monocyte cell adhesion induced by a human aminoacyl-tRNA synthetase-associated factor, p43: identification of the related adhesion molecules and signal pathways. *J.Leukoc.Biol.* **71**, 223-230.
- Park,H., Park,S.G., Kim,J., Ko,Y.G., & Kim,S. (2002b) Signaling pathways for TNF production induced by human aminoacyl-tRNA synthetase-associating factor, p43. *Cytokine* **20**, 148-153.
- Park,S.G., Kang,Y.S., Ahn,Y.H., Lee,S.H., Kim,K.R., Kim,K.W., Koh,G.Y., Ko,Y.G., & Kim,S. (2002c) Dose-dependent biphasic activity of tRNA synthetase-associating factor, p43, in angiogenesis. *J.Biol.Chem.* **277**, 45243-45248.
- Park,S.G., Ewalt,K.L., & Kim,S. (2005a) Functional expansion of aminoacyl-tRNA synthetases and their interacting factors: new perspectives on housekeepers 4. *Trends Biochem.Sci.* **30**, 569-574.
- Park,S.G., Shin,H., Shin,Y.K., Lee,Y., Choi,E.C., Park,B.J., & Kim,S. (2005b) The novel cytokine p43 stimulates dermal fibroblast proliferation and wound repair. *Am.J.Pathol.* **166**, 387-398.
- Park,S.G., Kang,Y.S., Kim,J.Y., Lee,C.S., Ko,Y.G., Lee,W.J., Lee,K.U., Yeom,Y.I., & Kim,S. (2006) Hormonal activity of AIMP1/p43 for glucose homeostasis. *Proc.Natl.Acad.Sci.U.S.A* **103**, 14913-14918.

- Pelling,A.E., Dawson,D.W., Carreon,D.M., Christiansen,J.J., Shen,R.R., Teitell,M.A., & Gimzewski,J.K. (2007) Distinct contributions of microtubule subtypes to cell membrane shape and stability. *Nanomedicine*. **3**, 43-52.
- Peters,H.I., Chang,Y.W., & Traugh,J.A. (1995) Phosphorylation of elongation factor 1 (EF-1) by protein kinase C stimulates GDP/GTP-exchange activity 1. *Eur.J.Biochem*. **234**, 550-556.
- Quevillon,S. & Mirande,M. (1996) The p18 component of the multisynthetase complex shares a protein motif with the beta and gamma subunits of eukaryotic elongation factor 1. *FEBS Lett*. **395**, 63-67.
- Quevillon,S., Agou,F., Robinson,J.C., & Mirande,M. (1997) The p43 component of the mammalian multi-synthetase complex is likely to be the precursor of the endothelial monocyte-activating polypeptide II cytokine. *J.Biol.Chem*. **272**, 32573-32579.
- Quevillon,S., Robinson,J.C., Berthonneau,E., Siatecka,M., & Mirande,M. (1999) Macromolecular assemblage of aminoacyl-tRNA synthetases: identification of protein-protein interactions and characterization of a core protein. *J.Mol.Biol*. **285**, 183-195.
- Quintos-Alagheband,M.L., White,C.W., Schwarz,M.A. (2004) Potential role for antiangiogenic proteins in the evolution of Bronchopulmonary Dysplasia. *Antioxid.Redox.Signal*. **6**, 137-145.
- Renault,L., Kerjan,P., Pasqualato,S., Menetrey,J., Robinson,J.C., Kawaguchi,S., Vassilyev,D.G., Yokoyama,S., Mirande,M., & Cherfils,J. (2001) Structure of the EMAPII domain of human aminoacyl-tRNA synthetase complex reveals evolutionary dimer mimicry. *EMBO J*. **20**, 570-578.
- Rho,S.B., Lee,K.H., Kim,J.W., Shiba,K., Jo,Y.J., & Kim,S. (1996) Interaction between human tRNA synthetases involves repeated sequence elements. *Proc.Natl.Acad.Sci.U.S.A* **93**, 10128-10133.
- Rho,S.B., Lee,J.S., Jeong,E.J., Kim,K.S., Kim,Y.G., & Kim,S. (1998) A multifunctional repeated motif is present in human bifunctional tRNA synthetase. *J.Biol.Chem*. **273**, 11267-11273.
- Robinson,J.C., Kerjan,P., & Mirande,M. (2000) Macromolecular assemblage of aminoacyl-tRNA synthetases: quantitative analysis of protein-protein interactions and mechanism of complex assembly. *J.Mol.Biol*. **304**, 983-994.

- Sachs,A.B. & Davis,R.W. (1989) The poly(A) binding protein is required for poly(A) shortening and 60S ribosomal subunit-dependent translation initiation 2. *Cell* **58**, 857-867.
- Sanders,J., Brandsma,M., Janssen,G.M., Dijk,J., & Moller,W. (1996) Immunofluorescence studies of human fibroblasts demonstrate the presence of the complex of elongation factor-1 beta gamma delta in the endoplasmic reticulum. *J.Cell Sci.* **109 ( Pt 5)**, 1113-1117.
- Sang,L.J., Gyu,P.S., Park,H., Seol,W., Lee,S., & Kim,S. (2002) Interaction network of human aminoacyl-tRNA synthetases and subunits of elongation factor 1 complex. *Biochem.Biophys.Res.Comm.* **291**, 158-164.
- Schluesener,H.J., Seid,K., Zhao,Y., & Meyermann,R. (1997) Localization of endothelial-monocyte-activating polypeptide II (EMAP II), a novel proinflammatory cytokine, to lesions of experimental autoimmune encephalomyelitis, neuritis and uveitis: expression by monocytes and activated microglial cells. *Glia* **20**, 365-372.
- Schwarz,M., Lee,M., Zhang,F., Zhao,J., Jin,Y., Smith,S., Bhuvu,J., Stern,D., Warburton,D., & Starnes,V. (1999a) EMAP II: a modulator of neovascularization in the developing lung. *Am.J.Physiol* **276**, L365-L375.
- Schwarz,M.A., Kandel,J., Brett,J., Li,J., Hayward,J., Schwarz,R.E., Chappey,O., Wautier,J.L., Chabot,J., Lo,G.P., & Stern,D. (1999b) Endothelial-monocyte activating polypeptide II, a novel antitumor cytokine that suppresses primary and metastatic tumor growth and induces apoptosis in growing endothelial cells. *J.Exp.Med.* **190**, 341-354.
- Schwarz,M.A., Zhang,F., Gebb, S., Starnes,V., Warburton,D. (2000) Endothelial-monocyte activating polypeptide II inhibits lung neovascularization and airway epithelial morphogenesis. *Mech. Dev.* **95**, 123-132.
- Schwarz,R.E. & Schwarz,M.A. (2004) In vivo therapy of local tumor progression by targeting vascular endothelium with EMAP-II. *J.Surg.Res.* **120**, 64-72.
- Schwarz,M.A., Zheng,H., Liu,J., Corbett,S., & Schwarz,R.E. (2005) Endothelial-monocyte activating polypeptide II alters fibronectin based endothelial cell adhesion and matrix assembly via alpha5 beta1 integrin. *Exp.Cell Res.* **311**, 229-239.

- Sechi,A.S. & Wehland,J. (2000) The actin cytoskeleton and plasma membrane connection: PtdIns(4,5)P(2) influences cytoskeletal protein activity at the plasma membrane. *J.Cell Sci.* **113 Pt 21**, 3685-3695.
- Shalak,V., Kaminska,M., Mitnacht-Kraus,R., Vandenabeele,P., Clauss,M., & Mirande,M. (2001) The EMAPII cytokine is released from the mammalian multisynthetase complex after cleavage of its p43/proEMAPII component. *J.Biol.Chem.* **276**, 23769-23776.
- Shalak,V., Guigou,L., Kaminska,M., Wautier,M.P., Wautier,J.L., & Mirande,M. (2007) Characterization of p43(ARF), a derivative of the p43 component of multiaminoacyl-tRNA synthetase complex released during apoptosis. *J.Biol.Chem.* **282**, 10935-10943.
- Stevenson,B.R., Heintzelman,M.B., Anderson,J.M., Citi,S., & Mooseker,M.S. (1989) ZO-1 and cingulin: tight junction proteins with distinct identities and localizations 1. *Am.J.Physiol* **257**, C621-C628.
- Stover,C.K., Pham,X.Q., Erwin,A.L., Mizoguchi,S.D., Warrenner,P., Hickey,M.J., Brinkman,F.S., Hufnagle,W.O., Kowalik,D.J., Lagrou,M., Garber,R.L., Goltry,L., Tolentino,E., Westbrook-Wadman,S., Yuan,Y., Brody,L.L., Coulter,S.N., Folger,K.R., Kas,A., Larbig,K., Lim,R., Smith,K., Spencer,D., Wong,G.K., Wu,Z., Paulsen,I.T., Reizer,J., Saier,M.H., Hancock,R.E., Lory,S., & Olson,M.V. (2000) Complete genome sequence of *Pseudomonas aeruginosa* PAO1, an opportunistic pathogen. *Nature* **406**, 959-964.
- Tandle,A.T., Mazzanti,C., Alexander,H.R., Roberts,D.D., & Libutti,S.K. (2005) Endothelial monocyte activating polypeptide-II induced gene expression changes in endothelial cells. *Cytokine* **30**, 347-358.
- Tandle,A.T., Calvani,M., Uranchimeg,B., Zahavi,D., Melillo,G., & Libutti,S.K. (2009) Endothelial monocyte activating polypeptide-II modulates endothelial cell responses by degrading hypoxia-inducible factor-1alpha through interaction with PSMA7, a component of the proteasome. *Exp.Cell Res.* **315**, 1850-1859.
- Tas,M.P. & Murray,J.C. (1996) Endothelial-monocyte-activating polypeptide II. *Int.J.Biochem.Cell Biol.* **28**, 837-841.
- Tsai,B.M., Wang,M., Clauss,M., Sun,P., & Meldrum,D.R. (2004) Endothelial monocyte-activating polypeptide II causes NOS-dependent pulmonary artery vasodilation: a novel effect for a proinflammatory cytokine. *Am.J.Physiol Regul.Integr.Comp Physiol* **287**, R767-R771.

- van Horsen,R., Eggermont,A.M., & ten Hagen,T.L. (2006a) Endothelial monocyte-activating polypeptide-II and its functions in (patho)physiological processes. *Cytokine Growth Factor Rev.* **17**, 339-348.
- van Horsen,R., Rens,J.A., Brunstein,F., Guns,V., van,G.M., Hagen,T.L., & Eggermont,A.M. (2006b) Intratumoural expression of TNF-R1 and EMAP-II in relation to response of patients treated with TNF-based isolated limb perfusion. *Int.J.Cancer* **119**, 1481-1490.
- van Horsen,R., Rens,J.A., Schipper,D., Eggermont,A.M., & ten Hagen,T.L. (2006c) EMAP-II facilitates TNF-R1 apoptotic signalling in endothelial cells and induces TRADD mobilization. *Apoptosis.* **11**, 2137-2145.
- Venema,R.C., Peters,H.I., & Traugh,J.A. (1991) Phosphorylation of valyl-tRNA synthetase and elongation factor 1 in response to phorbol esters is associated with stimulation of both activities 2. *J.Biol.Chem.* **266**, 11993-11998.
- Vidales,F.J., Robles,M.T., & Ballesta,J.P. (1984) Acidic proteins of the large ribosomal subunit in *Saccharomyces cerevisiae*. Effect of phosphorylation 3. *Biochemistry* **23**, 390-396.
- Wakasugi,K. & Schimmel,P. (1999) Two distinct cytokines released from a human aminoacyl-tRNA synthetase. *Science* **284**, 147-151.
- Wandosell,F., Serrano,L., & Avila,J. (1987) Phosphorylation of alpha-tubulin carboxyl-terminal tyrosine prevents its incorporation into microtubules 3. *J.Biol.Chem.* **262**, 8268-8273.
- Wang,X., Shi,B., Wang,S.W., Dong,J.Q., Cui,J.Y., & Han,S.X. (2006) [Effect of heat stress on expression of gp96 in K562 cell line of the chronic myeloid leukemia and its significance]. *Zhongguo Shi Yan.Xue.Ye.Xue.Za Zhi.* **14**, 667-672.
- Warburton,D., Schwarz,M., Tefft,D., Flores-Delgado,G., Anderson,K.D., & Cardoso,W.V. (2000) The molecular basis of lung morphogenesis. *Mech.Dev.* **92**, 55-81.
- Wege,H., Schluesener,H., Meyermann,R., Barac-Latas,V., Suchanek,G., & Lassmann,H. (1998) Coronavirus infection and demyelination. Development of inflammatory lesions in Lewis rats. *Adv.Exp.Med.Biol.* **440**, 437-444.

- Wellings,R.P., Lash,G.E., Murray,J.C., Tas,M., Ward,W., Trew,A.J., & Baker,P.N. (1999) Endothelial monocyte-activating polypeptide-2 is increased in pregnancy but is not further increased in preeclampsia. *J.Soc.Gynecol.Investig.* **6**, 142-146.
- Wolfe,C.L., Warrington,J.A., Davis,S., Green,S., & Norcum,M.T. (2003) Isolation and characterization of human nuclear and cytosolic multisynthetase complexes and the intracellular distribution of p43/EMAPII. *Protein Sci.* **12**, 2282-2290.
- Wu,P.C., Alexander,H.R., Huang,J., Hwu,P., Gnant,M., Berger,A.C., Turner,E., Wilson,O., & Libutti,S.K. (1999) In vivo sensitivity of human melanoma to tumor necrosis factor (TNF)-alpha is determined by tumor production of the novel cytokine endothelial-monocyte activating polypeptide II (EMAPII). *Cancer Res.* **59**, 205-212.
- Yamamoto,M., Fukushima,T., Ueno,Y., Hayashi,S., Kimura,H., Soma,G., & Tomonaga,M. (2000) Clinical significance of the expression of endothelial-monocyte activating polypeptide II (EMAPII) in the treatment of glioblastoma with recombinant mutant human tumor necrosis factor-alpha (TNF-SAM2). *Anticancer Res.* **20**, 4081-4086.
- Yan,X.D., Pan,L.Y., Yuan,Y., Lang,J.H., & Mao,N. (2007) Identification of platinum-resistance associated proteins through proteomic analysis of human ovarian cancer cells and their platinum-resistant sublines. *J.Proteome.Res.* **6**, 772-780.
- Yi,J.S., Lee,J.Y., Chi,S.G., Kim,J.H., Park,S.G., Kim,S., & Ko,Y.G. (2005) Aminoacyl-tRNA synthetase-interacting multi-functional protein, p43, is imported to endothelial cells via lipid rafts. *J.Cell Biochem.* **96**, 1286-1295.
- Zhang,F.R. & Schwarz,M.A. (2002) Pro-EMAP II is not primarily cleaved by caspase-3 and -7. *Am.J.Physiol Lung Cell Mol.Physiol* **282**, L1239-L1244.
- Zhang,Z., Zhang,Z., Artelt,M., Burnet,M., Schluesener,H.J. (2007) Dexamethasone attenuates early expression of three molecules associated with microglia/macrophages activation following rat traumatic brain injury. *Acta Neuropathol.* **113**, 675-682.
- Zheng,M., Schwarz,M.A., Lee,S., Kumaraguru,U., & Rouse,B.T. (2001) Control of stromal keratitis by inhibition of neovascularization. *Am.J.Pathol.* **159**, 1021-1029.

- Zhou,A.X., Hartwig,J.H., & Akyurek,L.M. (2010) Filamins in cell signaling, transcription and organ development. *Trends Cell Biol.* **20**, 113-123.
- Zhu,X., Liu,Y., Yin,Y., Shao,A., Zhang,B., Kim,S., & Zhou,J. (2009) MSC p43 required for axonal development in motor neurons. *Proc.Natl.Acad.Sci.U.S.A* **106**, 15944-15949.
- Zohlhofer,D., Nuhrenberg,T.G., Neumann,F.J., Richter,T., May,A.E., Schmidt,R., Denker,K., Clauss,M.A., Schomig,A., & Baeuerle,P.A. (2004) Rapamycin effects transcriptional programs in smooth muscle cells controlling proliferative and inflammatory properties. *Mol.Pharmacol.* **65**, 880-889.